

NASA CONTRACTOR REPORT



NASA CR-73223

AVAILABLE TO THE PUBLIC

NASA CR-

GPO PRICE \$ _____

CFSTI PRICE(S) \$ _____

Hard copy (HC) _____

Microfiche (MF) _____

653 July 65

RADIATION TRANSPORT FOR BLUNT-BODY FLOWS INCLUDING THE EFFECTS OF LINES AND ABLATION LAYER

by Jin H. Chin

FACILITY FORM 602

N 68-23703	(THRU)
(ACCESSION NUMBER)	
177	(CODE)
(PAGES)	33
CR-73223	(CATEGORY)
(NASA CR OR TMX OR AD NUMBER)	

Prepared by
LOCKHEED MISSILES & SPACE COMPANY
Sunnyvale, California
for Ames Research Center

NASA CR- 73223

RADIATION TRANSPORT FOR BLUNT-BODY FLOWS
INCLUDING THE EFFECTS OF LINES AND ABLATION LAYER

By Jin H. Chin

Distribution of this report is provided in the interest of information exchange. Responsibility for the contents resides in the author or organization that prepared it.

Prepared under Contract No. NAS 2-4219 by
LOCKHEED MISSILES & SPACE COMPANY
Sunnyvale, California

for Ames Research Center

NATIONAL AERONAUTICS AND SPACE ADMINISTRATION

For sale by the Clearinghouse for Federal Scientific and Technical Information:
Springfield, Virginia 22151 - Price \$

FOREWORD

The work described in this report was completed for the National Aeronautics and Space Administration, Ames Research Center, under Contract No. NAS 2-4219, with N. Vojvodich as Technical Monitor.

The author extends his appreciation to L. F. Hearne and K. H. Wilson for their help and discussion during this study.

CONTENTS

FOREWORD	ii
SUMMARY	1
INTRODUCTION	1
1 NOMENCLATURE	3
2 FLOW FIELD ANALYSIS	7
2.1 Governing Equations	7
2.2 Stagnation Flow Field	8
2.2.1 Air Layer	9
2.2.2 Ablation Layer	10
2.3 Streamtube Formulation	13
3 RADIATION TRANSPORT ANALYSIS	15
3.1 Basic Radiative Equations	15
3.2 Equations for a Finite Number of Sublayers	17
3.3 Treatment of Continuum Contributions	19
3.3.1 The Continuum Absorption Coefficient	19
3.3.2 The Multi-Band Model	20
3.4 Treatment of Line Contributions	20
3.4.1 The Line Absorption Coefficient	20
3.4.2 The Line Transmittance and Equivalent Width	22
3.4.3 Absorption Coefficient Notation	24
3.4.4 Line Calculation Limiting Cases	27
4 NUMERICAL METHODS	37
4.1 Division of Continuum Bands and Line Groups	37
4.2 Scheme of Flow Field Iteration	37
4.3 Scheme of Line Calculation	38
5 RESULTS	43
5.1 Effects of Exponential Kernel Approximation	43
5.2 Effects of Continuum Band Models	43
5.3 Effects of Line Model	43
5.4 Effects of Ablation Layers	44
5.5 Effects of the Number of Sublayers	44
5.6 Effects of Environmental Variables	45
5.7 Effects of Perturbation of Radiative Properties	45
5.8 Effects of Precursor Heating	46
5.9 Equivalent Width Results	46
5.10 STRADS Results	47
6 CONCLUDING REMARKS	47

CONTENTS (Continued)

Appendix

A	THERMODYNAMIC PROPERTIES OF AIR AND ABLATION VAPOR	49
B	RADIATIVE PROPERTIES OF AIR AND ABLATION SPECIES	51
B. 1	Absorption Cross Sections of Air Species	51
B. 1. 1	Continuum Absorption Cross Sections	51
B. 1. 2	Line Absorption Cross Sections	51
B. 2	Absorption Cross Sections of Ablation Species	52
C	THE STAGRADS CODE	53
C. 1	STAGRADS Listing	53
C. 2	Input Data Listing	55
C. 3	Output Data Listing, Including Details of Line Data Used	58
	REFERENCES	65
	LIST OF TABLES	67
	LIST OF ILLUSTRATIONS	75
	LISTING OF STAGRADS AND INPUT DATA	99
	OUTPUT DATA LISTING, INCLUDING DETAILS OF LINE DATA USED	163

RADIATION TRANSPORT FOR BLUNT-BODY FLOWS
INCLUDING THE EFFECTS OF LINES AND ABLATION LAYER

By Jin H. Chin
Lockheed Missiles & Space Company

SUMMARY

Efficient numerical methods are developed for fully radiation-coupled inviscid blunt-body flows. The spectral nature of radiation transport is treated in detail, using as many as 21 spectral regions and accounting for air and ablation vapor continua and 75 discrete atomic lines. A concept of line-group equivalent width and average transmittance is introduced in a finite-difference formulation of radiation transport. This concept is used to account for line overlaps and to formulate the numerical procedures.

The application of the numerical methods is described. The effects of environmental variables, of the numerical methods used, and of the uncertainties in radiative properties are discussed. The results demonstrate that the self-absorption and energy loss effects decrease the sensitivity of the heat fluxes to the changes in environmental variables and to the uncertainties in radiative properties.

INTRODUCTION

This report presents the analyses and results of a study of radiation transport for blunt vehicles returning from space missions at superorbital velocities. The study is an extension of the author's previous investigation (refs. 1 and 2). In refs. 1 and 2, the effects of non-grey, self-absorption and energy loss for inviscid blunt-body flows were considered. The air continuum spectral absorption coefficients were represented approximately by a 2-band (level) and a 6-band model. The contributions of discrete atomic line radiation were not taken into account. The solutions of the flow field for the stagnation and nonstagnation regions were formulated separately. A similarity solution was obtained for the stagnation region and a streamtube method was used for the nonstagnation region. The formulation of the present investigation includes the effects of discrete atomic-line radiation and the presence of an inviscid ablation layer adjacent to the wall. Due to time limitations, however, these effects are incorporated in the numerical calculations for the stagnation region only. A newer set of air continuum absorption coefficients is used for both the stagnation and nonstagnation regions.

The purpose of this investigation is to develop economical numerical methods for fully radiation-coupled, inviscid, blunt-body flows, and to assess the effects of environmental variables, of the numerical procedures used, and of the uncertainties in radiative properties.

The flow-field analysis is reviewed in Section 2. The flow field is assumed inviscid with an interface between the ablation products and the shock layer air. The stagnation region air layer and ablation layer are analyzed using similarity transformations, with continuity of pressure across the interface. The streamtube formulation for the nonstagnation region is very briefly described, as only an example result (fig. 23) is given.

The detailed analysis of radiation transport is given in Section 3. The divergence of the radiative flux is calculated by one-dimensional approximations. For the integration of the energy equation, the shock layer and ablation layer are divided into a number of sublayers, each with constant properties. The integrals of the radiative divergence over the individual sublayers are used in the finite-difference energy balance. The various terms in the expression of these integrals are of the same basic functional form. Studies of the mathematical properties of this basic functional form lead to a theory of calculating the continuum and discrete (atomic lines) radiation contributions. A concept of line-group equivalent width and average transmittance is used to calculate the contribution of a group of lines, accounting for line overlaps. Readers not interested in the details of radiation transport calculations may skip most of Section 3.

Section 4 describes the numerical methods, including the division of continuum bands and line groups, the scheme of flow field iteration, and the scheme of line calculations. Some of the equations [e. g., Eqs. (129) - (156)] presented are used in the computer program and may be omitted by readers not interested in the numerical details.

The results of calculations are given in Section 5. Except fig. 23 which shows an example of the heat flux distribution for a blunt vehicle, all results are for the stagnation region obtained using the STAGRADS code.

The air and ablation vapor thermodynamic properties, the radiative properties of air and ablation species, and the description of the STAGRADS code are given in the appendix.

1 NOMENCLATURE

a	constant in exponential kernel approximation $E_3(\xi) \sim (b/a)e^{-b\xi}$, a = 4 is used.
A	$1 + Ky$
$A_{i_1, i_2, m}$	function defined by Eq. (118)
b	constant in exponential kernel approximation $E_3(\xi) \sim (b/a)e^{-b\xi}$, b = 2 is used
b'	$b (\pi e^2 / mc^2)$
$b_{nn'}(\nu)$	line shape factor, Eq. (81)
B	Planck distribution function
c	speed of light
$d_{nn'}$	line-center shift
e	electron charge
E	energy of electronic state above ground state
$E_n(\xi)$	n-th exponential integral
f	band system f-number; or $A^{L+1} \rho v [R_N / (L + 1) u_r]^{1/2}$, Eq. (40)
$f_{nn'}$	absorption f-number for transition $n \rightarrow n'$
F	$\rho v / \rho_s v_s$ or $A^{L+1} \rho v / \rho_w v_w$
g	h/h_s or h/h_w
g_k^f	$f_k g_{n_k}$, a constant for each line
g_n	statistical weight of the n-th state
h	static enthalpy or Planck's quantum constant
H	total enthalpy, or enthalpy ratio (Appendix A)
I	specific intensity
k	Boltzmann's constant
K	body curvature, = $1/R_N$ at stagnation point
l_s, l_y	directional cosines of vector $\vec{\Omega}$, Eq. (54)
L	0 for two-dimensional, 1 for axisymmetric
m	electron mass

\dot{m}_w	wall blowing mass flux
n	number of sublayers; state index
n_k	k -th line lower state index, see Section 3.4.3
N	species particle number density
N_e	electron particle number density
p	static pressure
q	net radiative power gain per unit volume
\vec{q}_r	radiative flux vector
q_{r_s}, q_{r_y}	components of radiative flux in s and y directions
Q	radiative power gain for a finite sublayer; partition function
r	distance from plane or axis of symmetry
r_o	value of r at streamline entry point
R	ratio of equivalent width to line-group width for isolated lines
R_M	maximum radius, fig. 22
R_N	nose radius
R_o	distance from stagnation point to effective axis of symmetry
R^*	ratio of equivalent width to line-group width by integration
s	distance along body from stagnation point
\bar{s}	distance along body from point of symmetry, fig. 22
S	line strength, Eq. (110)
T	absolute temperature
Trans	line-group transmittance
u	velocity parallel to body
u_r	value of ablation layer u at interface, $u_e = u_r (s/R_N)$
v	velocity normal to body
Width	line-group equivalent width
y	normal distance from body surface
z	normal distance from shock wave
Z	compressibility factor
γ_e	line effective half-width
$\bar{\gamma}_k$	k -th line half-width due to 1 electron per unit volume

$\bar{\gamma}_{nn'}$	$\bar{\gamma}$ for $n \rightarrow n'$ transition
$\delta\nu_k$	integration interval for k-th line
Δ	total thickness between shock and wall
ΔH_v	latent heat of vaporization
Δy_i	$y_{i+1} - y_i$
Δz_i	$z_{i+1} - z_i$; $\Delta z_i = \Delta y_i$
$\Delta\nu_m$	integration interval for m-th line group
$\Delta\tau_j$	$\mu_j \Delta z_j$
ξ	transformed normal distance; dummy variable
η	transformed normal distance, Eq. (34)
μ	linear absorption coefficient
ν	frequency
ν_a	average frequency within line group
$\nu_{o, nn'}$	frequency corresponding to unperturbed transition $n \rightarrow n'$
ξ	transformed distance from stagnation point, Eq. (33); dummy variable
ρ	density
ρ_{SL}	sea-level density
σ	cross section; Stefan-Boltzmann constant
τ	optical thickness
ϕ	angle between flight vector and normal
ψ	stream function
Ω	solid angle
Subscripts	
a	air layer
ab	ablation layer; with ablation layer effect
c	continuum contribution
d	discrete contribution
e	at interface between air layer and ablation layer
i	species index; dummy index for sublayer
i_1, i_2	specific sublayers

j dummy sublayer index; dummy index for frequency integration
k dummy index for lines
nn' for transition $n \rightarrow n'$
s immediately behind shock; toward shock
sat at satellite velocity
w at wall conditions
 ν at frequency ν
 ∞ at ambient conditions

2 FLOW FIELD ANALYSIS

2.1 Governing Equations

To simplify the formulation of the problem, the flow field is assumed quasi-steady, inviscid, non-conducting, and in thermodynamic equilibrium. An interface exists between the ablation products and the shock-layer air. The wall is assumed to be at the equilibrium sublimation temperature corresponding to the surface pressure.

In body-oriented coordinates (s, y) shown in fig. 1, the conservation equations for a two-dimensional or axisymmetric, inviscid flow may be written as follows:

continuity

$$\frac{\partial r^L \rho u}{\partial s} + \frac{\partial A r^L \rho v}{\partial y} = 0 \quad (1)$$

s-momentum

$$u \frac{\partial u}{\partial s} + A v \frac{\partial u}{\partial y} + K u v = - \frac{1}{\rho} \frac{\partial p}{\partial s} \quad (2)$$

y-momentum

$$u \frac{\partial v}{\partial s} + A v \frac{\partial v}{\partial y} - K u^2 = - \frac{A}{\rho} \frac{\partial p}{\partial y} \quad (3)$$

energy

$$u \frac{\partial H}{\partial s} + A v \frac{\partial H}{\partial y} = \frac{A}{\rho} q \quad (4)$$

The net radiative power gain per unit volume is related to the divergence of the radiative flux:

$$q = - \operatorname{div} \vec{q}_r = - \left[\frac{\partial q_{ry}}{\partial y} + \frac{\partial q_{rs}}{A \partial s} \right] \quad (5)$$

The equations-of-state of equilibrium air and equilibrium ablation vapor may be expressed in the following form:

$$\rho, T, N_i, \dots = \text{function}(p, h) \quad (6)$$

The boundary conditions are as follows:

At the wall,

$$u = u_w = 0 \quad (7)$$

$$v = v_w = \dot{m}_w / \rho_w = (q_w - \sigma T_w^4) / \rho_w \Delta H_v \quad (8)$$

$$h = h_w = h_w(p_w) \quad (9)$$

The wall is assumed to be black.

At the shock wave,

$$u = u_s = u_\infty [\sin \phi_s \cos(\phi_w - \phi_s) + \epsilon \cos \phi_s \sin(\phi_w - \phi_s)] \quad (10)$$

$$v = v_s = u_\infty [\sin \phi_s \sin(\phi_w - \phi_s) - \epsilon \cos \phi_s \cos(\phi_w - \phi_s)] \quad (11)$$

$$p = p_s = \rho_\infty u_\infty^2 (1 - \epsilon) \cos^2 \phi_s + p_\infty \quad (12)^*$$

$$h = h_s = \left(\frac{1}{2}\right) u_\infty^2 (1 - \epsilon^2) \cos^2 \phi_s + h_\infty \quad (13)^*$$

At the interface,

$$p_{a,e} = p_{ab,e} \quad (14)$$

$$\frac{v_{a,e}}{u_{a,e}} = \frac{v_{ab,e}}{u_{ab,e}} \quad (15)$$

These equations will be approximated for different regions of the flow field.

2.2 Stagnation Flow Field

For the stagnation region, $s/R_N \ll 1$, the conservation equations may be simplified. The kinetic energy change is of a smaller order than the enthalpy change and the pressure variation normal to the wall is small. Equations (3) and (4) may then be approximated by Eqs. (16) and (17), respectively.

$$\frac{\partial p}{\partial y} = 0 \quad \text{or} \quad p = p_s \quad (16)$$

*In superorbital velocities, p_∞ and h_∞ are negligible compared to p_s and h_s , respectively. Precursor heating may increase h_∞ . However, for the velocities of interest in this study, the precursor heating is small, as will be discussed in Section 3.1.

$$u \frac{\partial h}{\partial s} + Av \frac{\partial h}{\partial y} = \frac{A}{\rho} q \quad (17)$$

For this study, the shockwave and the interface are further assumed to be concentric with the body surface so that $\phi_s = \phi_e = \phi_w$.

2.2.1 Air layer. — For the stagnation air layer, Eqs. (10) to (13) reduce to:

$$u_s = u_\infty \frac{s}{R_N} \quad (18)$$

$$v_s = -\epsilon u_\infty \quad (19)$$

$$p_s = \rho_\infty u_\infty^2 (1 - \epsilon) \left(1 - \frac{s^2}{R_N^2} \right) + p_\infty \quad (20)$$

$$h_s = \frac{1}{2} u_\infty^2 (1 - \epsilon^2) + h_\infty \quad (21)$$

For a concentric interface,

$$v_e = 0 \quad (22)$$

For inviscid flow, the interface conditions for u and h cannot be specified; they are part of the solution to be obtained.

Since there are more known boundary conditions at the shockwave, it is more convenient for the air layer solution to use the shockwave as the datum for the normal distance. Using transformations similar to the Lees-Dorodnitsyn transformations for compressible boundary layers and assuming similarity, the following results were obtained in ref. 1*:

$$d\zeta \equiv (L + 1) \frac{\rho}{\rho_s} \frac{dz}{R_N} \quad (23)$$

$$F \equiv - \frac{\rho v}{\rho_\infty u_\infty} = \frac{\rho v}{\rho_s v_s} \quad (24)$$

$$- \frac{dF}{d\zeta} = \frac{u}{u_s} \quad (25)$$

*The analysis of the stagnation flow field for the ablation layer is similar to that for the air layer. Consequently, only the analysis for the ablation layer is presented in detail in the following subsection.

$$g \equiv \frac{h}{h_s} \quad (26)$$

$$F \frac{d^2 F}{d\xi^2} = \frac{1}{(L+1)} \left[\left(\frac{dF}{d\xi} \right)^2 - 2\epsilon (1-\epsilon) \frac{\rho_s}{\rho} \right] \quad (27)$$

$$F \frac{dg}{d\xi} = \left[\frac{R_N}{(L+1) \rho u_\infty} \right] q \quad (28)$$

or

$$F dg = \frac{2}{\rho_\infty u_\infty^3} (q dz) \quad (28a)$$

where z is the distance from the shockwave toward the interface. In Eqs. (23) to (28), the shock layer has been assumed thin compared to the nose radius so that $A \approx 1$.

The boundary conditions are:

At the shockwave

$$\xi = 0, \quad F = -\frac{dF}{d\xi} = g = 1 \quad (29a)$$

at the interface,

$$\xi = \xi_e, \quad F = 0 \quad (29b)$$

where ξ_e is the value of ξ at the interface. The value of ξ_e must be determined from the solution.

The numerical integration of Eqs. (27) and (28a) is described in Section 4.2.

2.2.2 Ablation layer. - For the stagnation ablation layer, Eqs. (16) and (20) indicate:

$$p = p_e = \rho_\infty u_\infty^2 (1-\epsilon) \left(1 - \frac{s^2}{R_N^2} \right) + p_\infty \quad (30)$$

Since the layer edge is a streamline and is concentric with the wall, using $u_e = u_r (s/R_N)$ one obtains:

$$\frac{dp_e}{ds} = -\rho_e u_e \frac{du_e}{ds} = -\rho_e u_r^2 \frac{s}{R_N^2} = -2\rho_\infty u_\infty^2 (1-\epsilon) \frac{s}{R_N^2} \quad (31)$$

Hence,

$$\frac{u_r}{u_\infty} = \left[\frac{2\rho_\infty(1-\epsilon)}{\rho_e} \right]^{1/2} \quad (32)$$

where ρ_e is not known before the solution is obtained.

Equations (1), (2), and (17) may be simplified by introducing the following transformations:

$$\xi = \int_0^s \left(\frac{r}{A} \right)^{2L} u_e ds \quad (33)$$

$$\eta = \frac{u_e}{\sqrt{2\xi}} \left(\frac{r}{A} \right)^L \int_0^y A^L \rho dy \quad (34)$$

$$\frac{\partial \psi}{\partial y} = -\rho u r^L, \quad \frac{\partial \psi}{\partial s} = A \rho v r^L \quad (35)$$

$$f(\xi, \eta) = \frac{\psi}{\sqrt{2\xi}} \quad (36)$$

$$g(\xi, \eta) = \frac{h}{h_w} \quad (37)$$

If similarity is assumed so that all dependent variables are functions of η only, the transformed equations may be shown as follows:

$$f \frac{d^2 f}{d\eta^2} = \frac{1}{(L+1)} \left\{ \left(\frac{df}{d\eta} \right)^2 - 2 \frac{\rho_\infty u_\infty^2}{\rho u_r^2} - \frac{K}{A^{L+1} \rho} \left[\frac{(L+1) R_N}{u_r} \right]^{1/2} f \frac{df}{d\eta} \right\} \quad (38)$$

$$f \frac{dg}{d\eta} = \frac{A R_N}{(L+1) \rho u_r h_w} q \quad (39)$$

The transformation also yields the following relations:

$$f = A^{L+1} \rho v \left[\frac{R_N}{(L+1) u_r} \right]^{1/2} \quad (40)$$

$$\frac{df}{d\eta} = - \left(\frac{u}{u_e} \right) \quad (41)$$

$$\frac{d\eta}{dy} = \left[\frac{(L+1)u_r}{R_N} \right]^{1/2} A^L \rho \quad (42)$$

Further simplification of Eqs. (38) and (39) is possible by introducing the following:

$$F = \frac{f}{\rho_w v_w \left[\frac{R_N}{(L+1)u_r} \right]^{1/2}} = \frac{A^{L+1} \rho v}{\rho_w v_w} \quad (43)$$

$$d\xi = \frac{\left(\frac{2\rho_\infty u_\infty^2}{\rho_w u_r^2} \right)^{1/2}}{\rho_w v_w \left[\frac{R_N}{(L+1)u_r} \right]^{1/2}} d\eta = (L+1) \left(\frac{2\rho_\infty u_\infty^2}{\rho_w v_w^2} \right)^{1/2} \frac{\rho}{\rho_w} A^L \frac{dy}{R_N} \quad (44)$$

Equations (38) and (39) become, respectively,

$$F \frac{d^2 F}{d\xi^2} = \frac{1}{(L+1)} \left\{ \left(\frac{dF}{d\xi} \right)^2 - \frac{\rho_w}{\rho} \left[1 + \frac{1}{A^{L+1}} \left(\frac{\rho_w v_w^2}{2\rho_\infty u_\infty^2} \right)^{1/2} F \frac{dF}{d\xi} \right] \right\} \quad (45)$$

$$F dg = \frac{1}{\rho_w v_w h_w} A^{L+1} q dy \quad (46)$$

For $\Delta_{ab}/R_N \ll 1$, $A \approx 1$.

For conditions with

$$\rho_w v_w^2 / \rho_\infty u_\infty^2 \ll 1$$

one may neglect the last term in Eq. (45).

$$F \frac{d^2 F}{d\zeta^2} = \frac{1}{(L+1)} \left[\left(\frac{dF}{d\zeta} \right)^2 - \frac{\rho_w}{\rho} \right] \quad (47)$$

The boundary conditions are as follows:

at $\zeta = \eta = 0$

$$\frac{dF}{d\zeta} = - \left(\frac{u}{u_e} \right) \left(\frac{\rho_w}{\rho_e} \right)^{1/2} = 0, \quad F = 1, \quad g = 1 \quad (48a)$$

at $\zeta = \zeta_e$ or $\eta = \Delta_{ab}$

$$F = 0, \quad \frac{dF}{d\zeta} = - \left(\frac{\rho_w}{\rho_e} \right)^{1/2}, \quad p = \rho_\infty u_\infty^2 (1 - \epsilon) + p_\infty \quad (48b)$$

Because of the last term in Eq. (47), the momentum equation is coupled to the energy equation. The surface blowing rate and the layer thickness are not known before the solution is obtained.

The numerical integration of Eqs. (46) and (47) is described in Section 4.2.

2.3 Streamtube Formulation

For the nonstagnation region, the streamtube formulation described in ref. 1 is used. For the inviscid air layer, the conservation equations for an infinitesimal streamtube may be written as follows:

continuity

$$\rho u r \frac{dy}{ds} = \rho_\infty u_\infty r_o \frac{dr_o}{ds} \quad (49)$$

momentum

$$\rho u \frac{du}{ds} = - \frac{dp}{ds} \quad (50)$$

energy

$$\rho u \frac{d \left(h + \frac{u^2}{2} \right)}{ds} = q \quad (51)$$

where r_0 is the radial distance at which the streamtube enters the shock. The entry conditions for the streamtube are given by Eqs. (10) to (13). The application of the streamtube method during this study has been limited to air-layer calculations with continuum radiation only. The integration of Eqs. (49) to (51) follows the procedures described in ref. 1 and will not be discussed further in this report. The streamtube method may also be applied to the ablation-layer calculations.

3 RADIATION TRANSPORT ANALYSIS

3.1 Basic Radiative Equations

The net radiative power gain per unit volume by the gas in local thermodynamic equilibrium is given by

$$q(s, y) = \int_{\nu} d\nu \int_{\Omega=4\pi} \mu_{\nu}(s, y) \left[I_{\nu}(s, y, \vec{\Omega}) - B_{\nu}(s, y) \right] d\Omega \quad (52)$$

where I_{ν} is the monochromatic specific intensity (power per unit solid angle per unit area normal to the direction of propagation), B_{ν} the Planck distribution function, and μ_{ν} is the spectral (monochromatic) absorption coefficient accounting for induced emission. The monochromatic specific intensity is governed by the following equation of radiative transfer:

$$\text{div} \left[\vec{\Omega} I_{\nu}(\vec{\Omega}) \right] \equiv \vec{\Omega} \cdot \text{grad} I_{\nu}(\vec{\Omega}) = \mu_{\nu} \left[B_{\nu} - I_{\nu}(\vec{\Omega}) \right] \quad (53)$$

In body-oriented coordinates, Eq. (53) becomes

$$\ell_s \frac{\partial I_{\nu}(\vec{\Omega})}{\partial s} + \ell_y \frac{\partial I_{\nu}(\vec{\Omega})}{\partial y} = \mu_{\nu} \left[B_{\nu} - I_{\nu}(\vec{\Omega}) \right] \quad (54)$$

where ℓ_s and ℓ_y are the directional cosines of the vector $\vec{\Omega}$ with respect to the coordinate axes. The flow field is assumed either two-dimensional or axisymmetric so that the gradient of the specific intensity in the circumferential direction vanishes.

The net radiative flux crossing a unit area with unit normal $\vec{\Omega}'$ is given by

$$q_{r\nu}(\vec{\Omega}') = \int_{\Omega=4\pi} \left[\vec{\Omega} I_{\nu}(\vec{\Omega}) \right] \cdot \vec{\Omega}' d\Omega \quad (55)$$

Then,

$$q_{r\nu, s} = \int_{\Omega=4\pi} \ell_s I_{\nu}(\vec{\Omega}) d\Omega \quad (56a)$$

$$q_{r\nu, y} = \int_{\Omega=4\pi} \ell_y I_{\nu}(\vec{\Omega}) d\Omega \quad (56b)$$

Integrating Eq. (54) over all solid angles and using Eqs. (52), (56a), and (56b), one obtains the monochromatic form of Eq. (5)

$$\frac{\partial q_{r\nu,s}}{A \partial s} + \frac{\partial q_{r\nu,y}}{\partial y} = \text{div } \vec{q}_{r\nu} = -q_{\nu}(s, y) \quad (57)$$

Under conditions that the temperature gradients in the s-direction are small compared to that in the y-direction, one may neglect $\ell_s [\partial I_{\nu}(\bar{\Omega})/A \partial s]$ in Eq. (54) and

$$\left(\frac{\partial q_{r\nu,s}}{A \partial s} \right)$$

in Eq. (57) to obtain the "tangent slab" or one-dimensional approximation for radiation transport.

For the environmental condition of interest in this study ($u_{\infty} < 60,000$ ft/sec, $R_N < 10$ ft) the effect of precursor radiation heating of the ambient air ahead of the bow shock is to increase the wall heat flux by the order of 10 percent or less (refs. 3 and 4). Thus, it does not appear that the neglect of precursor heating in the basic radiative calculations contributes significantly to the uncertainty in magnitude of radiation heating. For this investigation, the precursor heating effect and the shock-wave reflectivity are neglected and the body surface is assumed black.

For one-dimensional radiation transfer, the monochromatic net radiative power gain or the radiative flux divergence is given by refs. 1 and 5.

$$\begin{aligned} - \frac{\partial q_{r\nu,y}}{\partial y} &= q_{\nu}(y) \\ &= -4\pi \mu_{\nu} B_{\nu} + 2\pi \mu_{\nu} B_{w,\nu} E_2 \left(\int_0^y \mu'_{\nu} dy' \right) \\ &\quad + 2\pi \mu_{\nu} \int_0^{\Delta} \mu'_{\nu} B'_{\nu} E_1 \left(\left| \int_{y'}^y \mu''_{\nu} dy'' \right| \right) dy' \end{aligned} \quad (58)$$

where $E_n(\zeta)$ is the n^{th} exponential integral and Δ is the thickness of the "tangent slab."

The succeeding terms on the right-hand side of Eq. (58) can be recognized as (1) radiative loss, (2) absorption of radiation from body surface attenuated by the medium between the body and the local point, and (3) absorption of radiation emitted by medium on both sides of the local point.

In terms of $z = \Delta - y$, the monochromatic optical thickness is given by

$$\tau_\nu(z) = \int_0^z \mu_\nu(z') dz' \quad (59)$$

$$\tau_{\Delta, \nu} = \int_0^\Delta \mu_\nu(z') dz' \quad (60)$$

Equation (58) may then be rewritten as

$$q_\nu(\tau_\nu) = -4\pi \mu_\nu B_\nu + 2\pi \mu_\nu B_{w, \nu} E_2(\tau_{\Delta, \nu} - \tau_\nu) + 2\pi \mu_\nu \int_0^{\tau_{\Delta, \nu}} B_\nu(t) E_1(|\tau_\nu - t|) dt \quad (61)$$

The monochromatic heat fluxes incident to the wall and leaving the shockwave toward the ambient air are given by Eqs. (62) and (63), respectively,

$$q_{w, \nu} = 2\pi \int_0^{\tau_{\Delta, \nu}} B_\nu(t) E_2(\tau_{\Delta, \nu} - t) dt \quad (62)$$

$$q_{s, \nu} = 2\pi \int_0^{\tau_{\Delta, \nu}} B_\nu(t) E_2(t) dt + 2\pi B_{w, \nu} E_3(\tau_{\Delta, \nu}) \quad (63)$$

Integration of Eq. (61) over all frequencies then yields the q required in Eqs. (28), (28a), and (46). Equations (62) and (63) may be integrated over all frequencies to obtain the total heat fluxes.

3.2 Equations for a Finite Number of Sublayers

In order to reduce the computation time required for integration of the conservation and radiative transport equations, the shock layer and ablation layer may be divided into a number of sublayers. Across the width of the sublayer, constant properties are assumed, but radiation traversing through is attenuated by each of the differential widths within the sublayer. Equation (61) may be integrated across the width of the i th sublayer from the shockwave (fig. 2).

$$Q_i(\nu) \equiv \int_{z_i}^{z_{i+1}} q_\nu(z) dz \quad (64)$$

Carrying the integration, one obtains

$$Q_i(\nu) = 2\pi B_w \left[E_3(\tau_{n+1} - \tau_{i+1}) - E_3(\tau_{n+1} - \tau_i) \right] + 2\pi \sum_{j=1}^n B_j \left[E_3(|\tau_i - \tau_{j+1}|) - E_3(|\tau_i - \tau_j|) + E_3(|\tau_{i+1} - \tau_j|) - E_3(|\tau_{i+1} - \tau_{j+1}|) \right] \quad (65)$$

For convenience, the subscript ν has been omitted in Eq. (65) and the equations following. Equations relating monochromatic quantities may be recognized by the presence of at least one term with argument ν . The optical thickness for the sublayers are given by

$$\Delta\tau_i(\nu) = \mu_i \Delta z_i \quad (66a)$$

$$\tau_1(\nu) = 0 \quad (66b)$$

$$\tau_{i+1}(\nu) = \sum_{j=1}^i \Delta\tau_j, \quad i = 1, 2, \dots, n \quad (66c)$$

The monochromatic radiative heat flux to the wall, $q_w(\nu)$, is given by Eq. (67), obtained from Eq. (62).

$$q_w(\nu) = 2\pi \sum_{i=1}^n B_i \left[E_3(\tau_{n+1} - \tau_{i+1}) - E_3(\tau_{n+1} - \tau_i) \right] \quad (67)$$

The monochromatic radiative heat flux leaving the shock front may be similarly derived.

$$q_s(\nu) = 2\pi \sum_{i=1}^n B_i \left[E_3(\tau_i) - E_3(\tau_{i+1}) \right] + 2\pi B_w E_3(\tau_{n+1}) \quad (68)$$

The total energy gain or heat fluxes may be obtained by integration of Eqs. (65), (67), and (68) over all frequencies. The spectral integration for the continuum radiation and the line radiation will be discussed separately in the following subsections.

The third exponential integral, $E_3(\xi)$, may be calculated using numerical correlations and series. However, considerable computation time may be saved by using the "exponential kernel approximation" for the exponential integrals. For instance,

$$E_3(\xi) \sim \frac{b}{a} e^{-b\xi} \quad (69)$$

Matching the values of the approximate function and its slope at zero argument with the exact values $E_3(0)$ and $E_3'(0) = -E_2(0)$, respectively, one obtains $b = 2$ and $a = 4$ so that

$$E_3(\xi) \sim 0.5 e^{-2\xi} \quad (70)$$

The individual terms of Eqs. (65), (67), and (68) are of the general form

$$\begin{aligned} I_{ijk}(\nu) &= B_k E_3(|\tau_i - \tau_j|) \\ &\approx \frac{b}{a} B_k \exp[-b|\tau_i - \tau_j|] \end{aligned} \quad (71)^*$$

One then can study the spectral integration of Eq. (71) as a basic step for performing the spectral integration of the more complicated Eqs. (65), (67), and (68). It will be shown in the Section 3.4.2 that the exponential kernel approximation enables a convenient formulation of line radiation transport.

3.3 Treatment of Continuum Contribution

3.3.1 The continuum absorption coefficient. — The spectral absorption coefficients and the optical thicknesses may be separated into two parts — the continuum (subscript c) and the discrete (subscript d).

$$\mu(\nu) = \mu_c + \mu_d \quad (72)$$

$$\tau(\nu) = \tau_c + \tau_d \quad (73)$$

The discrete part varies with frequency much more rapidly than the continuum part. For the present study, the discrete part corresponds to the contribution due to the atomic lines. The continuum part corresponds to the contribution of molecular band systems, free-free, and photo-absorption processes.

*With $b = 1$ and $a = 1$, Eq. (71) and many of the following equations may be used for radiation transport calculations for a pencil of radiation.

3.3.2 The multi-band model. – For the continuum radiation, the multi-band model is used. The continuum spectral absorption coefficient is assumed constant within the individual spectral bands or intervals. The Planck intensity function is integrated using appropriate series expansions. For instance, consider spectral integration of Eq. (71) over a band with $\nu_1 \leq \nu \leq \nu_2$.

$$\int_{\nu_1}^{\nu_2} I_{ijk}(\nu) d\nu = E_3 \left(\frac{|\tau_i - \tau_j|}{c} \right) \int_{\nu_1}^{\nu_2} B_k(\nu) d\nu$$

$$\approx \frac{b}{a} \exp \left(-b \frac{|\tau_i - \tau_j|}{c} \right) \int_{\nu_1}^{\nu_2} B_k(\nu) d\nu \quad (74)$$

The value of the spectral absorption coefficient for a given band is calculated by appropriate averages. For bands which are expected to be optically thin for most calculations, the partial Planck-mean defined by Eq. (75) may be used.

$$\mu(T, \nu_1, \nu_2) = \frac{\int_{\nu_1}^{\nu_2} \mu(T, \nu) B(T, \nu) d\nu}{\int_{\nu_1}^{\nu_2} B(T, \nu) d\nu} \quad (75)$$

3.4 Treatment of Line Contributions

3.4.1 The line absorption coefficient. – The absorption cross-section of a line (bound-bound) may be written for the transition $n \rightarrow n'$ as follows:

$$\sigma_{nn'}(\nu) = \left(\frac{\pi e^2}{mc^2} \right) f_{nn'} b_{nn'}(\nu) \left(1 - e^{-h\nu_{nn'}/kT} \right) \quad (76)$$

where

e, m = electron charge and mass, respectively
 c = velocity of light

- k = Boltzmann's constant
 $f_{nn'}$ = absorption f-number for transition $n \rightarrow n'$
 $\nu_{nn'}$ = line center frequency for transition $n \rightarrow n'$
 $b_{nn'}(\nu)$ = line shape factor normalized according to

$$\int_0^{\infty} b_{nn'}(\nu) d\nu = 1 \quad (77)$$

The factor $(1 - e^{-h\nu_{nn'}/kT})$ accounts for induced emission.

To obtain the spectral absorption coefficient, the cross section is multiplied by the occupation number, N_n , of state n (the number density of a given species in state n). For a monatomic gas in local thermodynamic equilibrium, the occupation number is given by the Boltzmann formula

$$N_n = \frac{g_n}{Q} N e^{-(E_n/kT)} \quad (78)$$

where

- g_n = statistical weight of the n^{th} state
 Q = electronic partition function of monatomic species
 E_n = energy of n^{th} electronic state above ground state
 N = total number of particles of the given species per unit volume

The partition function is given by

$$Q = \sum_n g_n e^{-(E_n/kT)} \quad (79)$$

The energy levels, partition functions, and statistical weights for nitrogen and oxygen atoms and ions are given in ref. 6.

From Eqs. (76) and (78), the bound-bound absorption coefficient for transition $n \rightarrow n'$ is then given by

$$\mu_{nn'} = \left(\frac{\pi e^2}{mc^2} \right) f_{nn'} \frac{g_n}{Q} N e^{-E_n/kT} b_{nn'}(\nu) \left[1 - \exp\left(\frac{-h\nu_{nn'}}{kT} \right) \right] \quad (80)$$

For electron-impact broadening, the lines follow a Lorentz shape with the half-width proportional to the electron particle density:

$$b_{nn'}(\nu) = \frac{1}{\pi} \frac{\gamma_{nn'}}{\left[\nu - (\nu_{o, nn'} - d_{nn'}) \right]^2 + \gamma_{nn'}^2} \quad (81)$$

$$\gamma_{nn'} = \bar{\gamma}_{nn'} Ne \quad (82)$$

where

$\nu_{o, nn'}$ = frequency corresponding to unperturbed transition $n \rightarrow n'$

$d_{nn'}$ = line-center shift

$\bar{\gamma}_{nn'}$ = half-width due to 1 electron per unit volume for $n \rightarrow n'$

Ne = electron particle number density

The normalized half-width $\bar{\gamma}_{nn'}$, as calculated by R. Johnston, for carbon, nitrogen, and oxygen atoms and ions are tabulated in ref. 7.

Excited electronic states having the same core configuration, principal and orbital quantum numbers but with different spin multiplicity and total orbital angular momentum for L-S coupling have nearly the same E_n . Therefore, it is convenient to combine these states into a single group so that only the occupation number of this group of states need be calculated. However, the f-numbers of the individual transitions must be multiplied by the ratio of the statistical weight of the individual lower state to that of the group of states. In other words, one may consider in Eq. (80) that g_n is the statistical weight of a group of lower states of similar energies and $f_{nn'}$ is an effective f-number which is equal to the f-number of the particular transition multiplied by a statistical-weight ratio.

The total bound-bound absorption coefficient is the sum of all $\mu_{nn'}$ due to different lower-state groups of different species.

3.4.2 The line transmittance and equivalent width. — Consider the spectral integration of Eq. (71) over a finite frequency interval $\Delta\nu$ across which the Planck intensity function and the continuum contribution may be approximated by constant values. Then,

$$I_{ijk} \equiv \int_{\Delta\nu} I_{ijk}(\nu) d\nu \approx \frac{b}{a} \int_{\Delta\nu} B_k e^{-b|\tau_i - \tau_j|_c} e^{-b|\tau_i - \tau_j|_d} d\nu \quad (83)$$

$$\approx \frac{b}{a} B_k(\nu_a) \exp\left[-b|\tau_i - \tau_j|_{c, \nu_a}\right] \int_{\Delta\nu} \exp\left[-b|\tau_i - \tau_j|_d\right] d\nu$$

where ν_a is an average frequency (e. g., center frequency) within $\Delta\nu$.

Define the average transmittance as follows:

$$\text{Trans}_{ij} \equiv \frac{1}{\Delta\nu} \int_{\Delta\nu} e^{-b|\tau_i - \tau_j|} d\nu \quad (84)$$

Then,

$$I_{ijk} \approx \frac{b}{a} B_k(\nu_a) e^{-b|\tau_i - \tau_j|} c, \nu_a \Delta\nu \text{Trans}_{ij} \quad (85)$$

Alternately, one can write Eq. (83) as follows:

$$\begin{aligned} I_{ijk} &\approx \frac{b}{a} \int_{\Delta\nu} B_k e^{-b|\tau_i - \tau_j|} c d\nu - \frac{b}{a} \int_{\Delta\nu} B_k e^{-b|\tau_i - \tau_j|} c \left(1 - e^{-b|\tau_i - \tau_j|} d\right) d\nu \\ &\approx I_{c,ijk} - \frac{b}{a} B_k(\nu_a) e^{-b|\tau_i - \tau_j|} c, \nu_a \int_{\Delta\nu} \left(1 - e^{-b|\tau_i - \tau_j|} d\right) d\nu \end{aligned} \quad (86)$$

where

$$I_{c,ijk} = \frac{b}{a} \int_{\Delta\nu} B_k e^{-b|\tau_i - \tau_j|} c d\nu \quad (87)$$

is the continuum contribution.

Define the equivalent width over $\Delta\nu$ as follows:

$$\text{Width}_{ij} = \int_{\Delta\nu} \left(1 - e^{-b|\tau_i - \tau_j|} d\right) d\nu \quad (88)$$

Then, Eq. (86) may be rewritten as

$$I_{ijk} \approx I_{c_{ijk}} - \frac{b}{a} B_k(\nu_a) e^{-b|\tau_i - \tau_j|} c, \nu_a \text{Width}_{ij} \quad (89)$$

The use of Eqs. (87) and (88) permits different spectral divisions for the calculation of the two terms on the right-hand side of Eq. (89).

From Eqs. (84) and (88)

$$\text{Width}_{ij} = \Delta\nu(1 - \text{Trans}_{ij}) \quad (90)$$

The study of line transport then reduces to the calculation of Trans_{ij} or Width_{ij} .

3.4.3 Absorption coefficient notation. - In order to avoid using too many indices to describe the variables, the following system of notation will be used:

i = dummy index for sublayers

i_1, i_2 = specific sublayers

k = dummy index for lines (except in product kT)

m = dummy index for line frequency regions

n_k = k th line lower state index (The species index is eliminated and the value of n_k specifies the species. The term N_{n_k} will be used to denote the total particle number density for the species specified by n_k .)

Thus,

$$\mu_i(\nu) = \left(\frac{\pi e^2}{mc^2} \right) \sum_k f_k \frac{g_{n_k}}{Q_{i, n_k}} N_{i, n_k} e^{-E_{n_k}/kT_i} \left(1 - e^{-h\nu_k/kT_i} \right) b_{i, k}(\nu) \quad (91)$$

represents the spectral absorption coefficient of the i^{th} sublayer at ν . For many situations, the line-center frequency ν_k in $[1 - \exp(-h\nu_k/kT)]$ may be approximated by ν_m , an average frequency for the m^{th} frequency region. It should be noted that lines outside the m^{th} frequency region may contribute to the value of $\mu_i(\nu)$ at ν within the m^{th} frequency region.

In terms of the new notation, one has the following:

$$b_{i, k}(\nu) = \frac{1}{\pi} \frac{\gamma_{i, k}}{\left[\nu - (\nu_k - d_{i, k}) \right]^2 + \gamma_{i, k}^2} \quad (92)$$

$$\text{Trans}_{i_1, i_2, m} = \frac{1}{\Delta\nu_m} \int_{\Delta\nu_m} \exp \left[-b \sum_i^{i_1, i_2} \mu_i(\nu) \Delta z_i \right] d\nu \quad (93)$$

$$\text{Width}_{i_1, i_2, m} = \Delta\nu_m (1 - \text{Trans}_{i_1, i_2, m}) = \int_{\Delta\nu_m} \left\{ 1 - \exp \left[-b \sum_i^{i_1, i_2} \mu_i(\nu) \Delta z_i \right] \right\} d\nu \quad (94)$$

The sum in Eq. (93) represents the following operation:

$$\sum_i^{i_1, i_2} \xi_i = \begin{cases} 0 & , i_2 = i_1 \\ \sum_{i=i_1}^{i_2-1} \xi_i & , i_2 > i_1 \\ \sum_{i=i_2}^{i_1-1} \xi_i & , i_2 < i_1 \end{cases} \quad (95)$$

In order to simplify the calculations, the effects of line shift will be neglected. For the conditions of interest, it is reasonable to consider only lines due to neutral nitrogen atoms with an effective density equal to the sum of the actual NI and OI values.* With this approximation, N_{i, n_k} may be replaced by N_i and Q_{i, n_k} by Q_i . The numerical computation is thus considerably simplified. One may now write

*One may also neglect the contribution of the OI vacuum ultraviolet lines.

$$\text{Width}_{i_1, i_2, m} = \int_{\Delta\nu_m} \left(1 - \exp \left\{ -b' \sum_i^{i_1, i_2} \frac{N_i}{Q_i} \left[1 - \exp \left(-\frac{h\nu_m}{kT_i} \right) \right] \right. \right. \\ \left. \left. \Delta z_i \sum_k g f_k \exp \left(-\frac{E_{n_k}}{kT_i} \right) \frac{1}{\pi} \frac{\gamma_{i, k}}{(\nu - \nu_k)^2 + \gamma_{i, k}^2} \right\} \right) d\nu \quad (96)$$

where

$$b' = b(\pi e^2/mc^2)$$

$$g f_k = f_k g_{n_k}, \text{ a constant for each line}$$

The expression for the average transmittance now becomes:

$$\text{Trans}_{i_1, i_2, m} = \frac{1}{\Delta\nu_m} \int_{\Delta\nu_m} \prod_i^{i_1, i_2} \exp \left\{ -b' \frac{N_i}{Q_i} \left[1 - \exp \left(-\frac{h\nu_m}{kT_i} \right) \right] \Delta z_i \right. \\ \left. \sum_k g f_k \exp \left(-\frac{E_{n_k}}{kT_i} \right) \frac{1}{\pi} \frac{\gamma_{i, k}}{(\nu - \nu_k)^2 + \gamma_{i, k}^2} \right\} d\nu \quad (97)$$

where

$$\prod_i^{\bar{i}_1, \bar{i}_2} \xi_i = \begin{cases} 1 & , \bar{i}_2 = \bar{i}_1 \\ \prod_{i_1}^{\bar{i}_2-1} \xi_i & , \bar{i}_2 > \bar{i}_1 \\ \prod_{i_2}^{\bar{i}_1-1} \xi_i & , \bar{i}_2 < \bar{i}_1 \end{cases} \quad (98)$$

In the conditions of interest, it is reasonable to assume that $\bar{\gamma}_{nn'} = \bar{\gamma}_{i,k}$ is a slow-varying function of temperature. Then, the following approximation may be used:

$$\gamma_{i,k} \approx \bar{\gamma}_k Ne_i \quad (99)$$

3.4.4 Line calculation limiting cases. - The study of line transport now reduces to the calculation of $Width_{i_1, i_2, m}$ or $Trans_{i_1, i_2, m}$ according to Eqs. (96) and (97). In general, the integral in Eqs. (96) or (97) can not be expressed in terms of simple combinations of analytic functions. Although numerical integrations can always be used to evaluate these integrals, the computation time required may become excessive. One should then look for appropriate approximations applicable to different asymptotic situations. For situations where numerical integrations must be used, the numerical schemes should be selected with a consideration for the minimization of computation time.

The approximations for different asymptotic situations are discussed below:

(1) Thin-line approximation. -

For $\xi \ll 1$, $e^{-\xi} \approx 1 - \xi$. Now,

$$\begin{aligned}
b' & \sum_i^{i_1, i_2} \frac{N_i}{Q_i} \left[1 - \exp\left(-\frac{h\nu_m}{kT_i}\right) \right] \Delta z_i \sum_k g f_k \exp\left(-\frac{E_{nk}}{kT_i}\right) \frac{1}{\pi} \frac{\gamma_{i,k}}{(\nu - \nu_k)^2 + \gamma_{i,k}^2} \\
& \approx b' \sum_i^{i_1, i_2} \frac{N_i}{Q_i} \left[1 - \exp\left(-\frac{h\nu_m}{kT_i}\right) \right] \Delta z_i \sum_k g f_k \exp\left(-\frac{E_{nk}}{kT_i}\right) \frac{1}{\pi} \frac{\gamma_{i,k}}{0 + \gamma_{i,k}^2} \equiv \tau_{i_1, i_2, m}
\end{aligned} \tag{100}$$

where the identity defines $\tau_{i_1, i_2, m}$, an effective optical thickness evaluated at the line centers. Then, for $\tau_{i_1, i_2, m} \ll 1$:

Width i_1, i_2, m

$$\begin{aligned}
& \approx \int_{\Delta\nu_m} b' \sum_i^{i_1, i_2} \frac{N_i}{Q_i} \left[1 - \exp\left(-\frac{h\nu_m}{kT_i}\right) \right] \Delta z_i \sum_k g f_k \exp\left(-\frac{E_{nk}}{kT_i}\right) \frac{1}{\pi} \frac{\gamma_{i,k}}{(\nu - \nu_k)^2 + \gamma_{i,k}^2} d\nu \\
& = b' \sum_i^{i_1, i_2} \frac{N_i}{Q_i} \left[1 - \exp\left(-\frac{h\nu_m}{kT_i}\right) \right] \Delta z_i \sum_k g f_k \exp\left(-\frac{E_{nk}}{kT_i}\right) \int_{\Delta\nu_m} \frac{1}{\pi} \frac{\gamma_{i,k}}{(\nu - \nu_k)^2 + \gamma_{i,k}^2} d\nu \\
& = b' \sum_i^{i_1, i_2} \frac{N_i}{Q_i} \left[1 - \exp\left(-\frac{h\nu_m}{kT_i}\right) \right] \Delta z_i \sum_k g f_k \exp\left(-\frac{E_{nk}}{kT_i}\right) G(\nu_{u_m}, \nu_{l_m}, \nu_k, \gamma_{i,k}) \tag{101}
\end{aligned}$$

where

$$G(\nu_{u_m}, \nu_{l_m}, \nu_k, \gamma_{i,k}) = \frac{1}{\pi} \left[\tan^{-1} \left(\frac{\nu_{u_m} - \nu_k}{\gamma_{i,k}} \right) - \tan^{-1} \left(\frac{\nu_{l_m} - \nu_k}{\gamma_{i,k}} \right) \right] \tag{102}$$

with ν_{u_m} and ν_{l_m} as the upper and lower limits, respectively, of the m^{th} frequency interval.

When the contributing lines are well within the frequency region (not near the two boundaries), Eq. (102) may be approximated by:

$$G(\nu_m, \nu_k, \gamma_{i,k}) = 1 \quad (103)$$

With the above approximation, the equivalent width then becomes the sum of the so-called strengths* of the contributing lines.

Equation (101) is valid for both isolated and overlapped lines, provided $\tau_{i_1, i_2, m} \ll 1$.

(2) Isolated-line approximation

When $\Delta\nu_m$ is large compared with $\gamma_{i,k}$ and the contributing lines within the frequency region may be considered isolated, the integral in Eq. (96) may be approximated by the sum of integrals for the individual line. Thus,

$$\text{Width}_{i_1, i_2, m} \approx \sum_k \int_{\delta\nu_k} \left(1 - \exp \left\{ -b' \sum_i^{i_1, i_2} \frac{N_i}{Q_i} \left[1 - \exp \left(-\frac{h\nu_m}{kT_i} \right) \right] \Delta z_i \right. \right. \\ \left. \left. g f_k \exp \left(-\frac{E_{nk}}{kT_i} \right) \frac{1}{\pi} \frac{\gamma_{i,k}}{(\nu - \nu_k)^2 + \gamma_{i,k}^2} \right\} \right) d\nu \quad (104)$$

where $\delta\nu_k$ is the integration interval for the k^{th} line.

The integral in Eq. (104) for a single value of the index k represents the equivalent width of a single line for a nonisothermal path. The use of an effective half-width (ref. 8) may enable representation of the equivalent width in terms of the Ladenburg-Reiche function (ref. 9).

Consider the following integral:

$$I = \int_{-\infty}^{\infty} \left[1 - \exp \left(-\frac{1}{\pi} \sum_i \frac{S_i \gamma_i}{\xi^2 + \gamma_i^2} \right) \right] d\xi \\ \approx \int_{-\infty}^{\infty} \left[1 - \exp \left(-\frac{1}{\pi} \frac{1}{\xi^2 + \gamma_e^2} \sum_i S_i \gamma_i \right) \right] d\xi \quad (105)$$

*The strength of a single line over an isothermal path (L) may be defined as $(N_i/Q_i) [1 - \exp(-h\nu_k/kT_i)] L g f_k \exp(-E_{nk}/kT_i)$

where γ_e is an effective half-width. (The determination of γ_e will be discussed later.)

Equation (105) may be integrated to yield:

$$I \approx 2\pi \gamma_e f \left(\frac{\sum_i S_i \gamma_i}{2\pi \gamma_e^2} \right) \quad (106)$$

where

$$f(\xi) = \xi e^{-\xi} [I_0(\xi) + I_1(\xi)] \quad (107)$$

is the Ladenburg-Reiche function with $I_0(\xi)$ and $I_1(\xi)$ being the modified Bessel functions.

Two asymptotic expressions of $f(\xi)$ exist:

$$f(\xi) \approx \begin{cases} \xi & , \quad \xi \ll 1 \\ \sqrt{\frac{2\xi}{\pi}} & , \quad \xi \gg 1 \end{cases} \quad (108)$$

at $\xi = \frac{2}{\pi}$, the two asymptotic expressions become equal.

Since the lines are considered isolated, the interval of integration δ_k may be extended to $(-\infty, \infty)$. Therefore, one may rewrite Eq. (104) as follows:

$$\text{Width}_{i_1, i_2, m} \approx \sum_k 2\pi \gamma_{e,k} f \left(\frac{\sum_i^{i_1, i_2} S_{i,k,m} \gamma_{i,k}}{2\pi \gamma_{e,k}^2} \right) \quad (109)$$

where

$$S_{i,k,m} = b' \frac{N_i}{Q_i} \left(1 - e^{-\frac{h\nu_m}{kT_i}} \right)^{\Delta z_i} g f_k e^{-\frac{E_{n_k}}{kT_i}} \quad (110)$$

Now, consider the determination of γ_e . Comparing Eqs. (101) and (109) and using the first of Eq. (108) for isolated thin lines, one obtains:

$$\gamma_{e_k} = \frac{\sum_i^{i_1, i_2} S_{i, k, m} \gamma_{i, k}}{\sum_i^{i_1, i_2} S_{i, k, m}} \quad (111)$$

which is mean weighted according to the line strengths of the individual sub-layers.

Using the second of Eq. (108) for isolated strong lines, one obtains the following equation:

$$\begin{aligned} \text{Width}_{i_1, i_2, m} &\approx \sum_k 2\pi \gamma_{e_k} \left[\frac{\sum_i^{i_1, i_2} S_{i, k, m} \gamma_{i, k}}{2\pi \gamma_{e_k}} \right]^{1/2} \\ &= \sum_k 2 \left(\sum_i^{i_1, i_2} S_{i, k, m} \gamma_{i, k} \right)^{1/2}, \quad \left(\begin{array}{l} \text{isolated strong line} \\ \text{square-root approximation} \end{array} \right) \end{aligned} \quad (112)$$

The effective half-width does not appear in Eq. (112). Therefore, it is reasonable to assume that the effective half-width defined by Eq. (111) may be used, as an approximation, in Eq. (109) for situations between the thin and strong limits for isolated lines.*

For numerical calculation of the Ladenburg-Reiche function, the following approximations are useful:

$$f(\xi) \approx \begin{cases} \xi & \xi \leq (0.685)^4 \\ 0.685 \xi^{3/4} & (0.685)^4 < \xi \leq \frac{4}{\pi^2} \frac{1}{(0.685)^4} \\ \sqrt{\frac{2}{\pi}} \xi^{1/2} & \xi > \frac{4}{\pi^2} \frac{1}{(0.685)^4} \end{cases} \quad (113)$$

*This may be compared with the Curtis-Godson approximation (ref. 10).

(3) Effective isothermal region. Extending the idea of the effective half-width to non-isolated lines, one may rewrite Eq. (96) as follows:

$$\text{Width}_{i_1, i_2, m} \approx \int_{\Delta\nu_m} \left\{ 1 - \exp \left[-b' \sum_i^{i_1, i_2} \frac{N_i}{Q_i} \left(1 - e^{-\frac{h\nu_m}{kT_i}} \right) \Delta z_i \right. \right. \\ \left. \left. \sum_k g_k^f e^{-\frac{E_{n_k}}{kT_i}} \frac{1}{\pi} \frac{\nu_{i,k}}{(\nu - \nu_k)^2 + \gamma_{e_k}^2} \right] \right\} d\nu \quad (114)$$

where γ_{e_k} is an effective half-width of the k^{th} line.

Under certain situations, a single lower state or a small number of lower states of nearly the same electronic energy contribute to the m^{th} frequency region. One may then introduce the following approximations:

$$E_{n_k} \approx E_m \quad (115)$$

$$\gamma_{i,k} \approx \bar{\gamma}_k N_{e_i} \quad (116)$$

Equation (114) may then be written as follows:

$$\text{Width}_{i_1, i_2, m} \approx \int_{\Delta\nu_m} \left\{ 1 - \exp \left[-b' \sum_i^{i_1, i_2} \frac{N_i}{Q_i} \left(1 - e^{-\frac{h\nu_m}{kT_i}} \right) \Delta z_i e^{-\frac{E_m}{kT_i}} N_{e_i} \right. \right. \\ \left. \left. \sum_k g_k^f \frac{1}{\pi} \frac{\bar{\gamma}_k}{(\nu - \nu_k)^2 + \gamma_{e_k}^2} \right] \right\} d\nu \quad (117)$$

The two summations in Eq. (117) may be performed separately, thus saving a considerable amount of numerical calculations. Let

$$A_{i_1, i_2, m} = \sum_i^{i_1, i_2} \frac{N_i}{Q_i} \left[1 - \exp\left(-\frac{h\nu_m}{kT_i}\right) \right] \Delta z_i \exp\left(-\frac{E_m}{kT_i}\right) N e_i \quad (118)$$

Then, Eq. (117) becomes

$$\text{Width}_{i_1, i_2, m} \approx \int_{\Delta\nu_m} \left\{ 1 - \exp\left[-A_{i_1, i_2, m} \sum_k b' g_{f_k} \frac{1}{\pi} \frac{\bar{\gamma}_k}{(\nu - \nu_k)^2 + \gamma_{e_k}^2}\right] \right\} d\nu \quad (119)$$

The fact that $A_{i_1, i_2, m}$ is a sum, independent of the dummy sublayer index i , implies that the equivalent width given by Eq. (119) may be considered to be that due to an effective isothermal region.

Equation (119) may be further simplified, if the thin-line or the isolated strong-line approximation is used.

From Eq. (100),

$$\begin{aligned} \tau_{i_1, i_2, m} &= b' \sum_i^{i_1, i_2} \frac{N_i}{Q_i} \left[1 - \exp\left(-\frac{h\nu_m}{kT_i}\right) \right] \Delta z_i \sum_k g_{f_k} \exp\left(-\frac{E_{nk}}{kT_i}\right) \frac{1}{\pi} \frac{1}{\gamma_{i, k}} \\ &\approx b' \sum_i^{i_1, i_2} \frac{N_i}{Q_i} \left[1 - \exp\left(-\frac{h\nu_m}{kT_i}\right) \right] \Delta z_i \exp\left(-\frac{E_m}{kT_i}\right) \sum_k g_{f_k} \frac{1}{\pi \gamma_{i, k}} \end{aligned} \quad (120)$$

Then, for $\tau_{i_1, i_2, m} \ll 1$, Eq. (101) yields with $G = 1$:

$$\text{Width}_{i_1, i_2, m} \approx \sum_i^{i_1, i_2} \frac{N_i}{Q_i} \left[1 - \exp\left(-\frac{h\nu_m}{kT_i}\right) \right] \Delta z_i \exp\left(-\frac{E_m}{kT_i}\right) \sum_k b' g_{f_k} \quad (121)$$

Now, consider Eq. (119) for isolated thin lines, one has in analogy to Eq. (109).

$$\begin{aligned} \text{Width}_{i_1, i_2, m} &\simeq \sum_k 2\pi \gamma'_{e_k} \left[\frac{A_{i_1, i_2, m} b' g_{f_k} \bar{\gamma}_k}{2\pi \gamma'_{e_k}{}^2} \right] \\ &= A_{i_1, i_2, m} \sum_k b' g_{f_k} \frac{\bar{\gamma}_k}{\gamma'_{e_k}} \end{aligned} \quad (122)$$

Subtracting Eq. (121) from Eq. (122), one obtains the following

$$\sum_k b' g_{f_k} \left\{ A_{i_1, i_2, m} \frac{\bar{\gamma}_k}{\gamma'_{e_k}} - \sum_i^{i_1, i_2} \frac{N_i}{Q_i} \left[1 - \exp\left(-\frac{h\nu_m}{kT_i}\right) \right] \Delta z_i \exp\left(-\frac{E_m}{kT_i}\right) \right\} = 0 \quad (123)$$

For arbitrary variation of g_{f_k} and of the number of k -terms, an expression of the effective half-width satisfying Eq. (123) is given below:

$$\gamma'_{e_k} = \frac{\left\{ \sum_i^{i_1, i_2} \frac{N_i}{Q_i} \left[1 - \exp\left(-\frac{h\nu_m}{kT_i}\right) \right] \Delta z_i \exp\left(-\frac{E_m}{kT_i}\right) N e_i \right\}}{\left\{ \sum_i^{i_1, i_2} \frac{N_i}{Q_i} \left[1 - \exp\left(-\frac{h\nu_m}{kT_i}\right) \right] \Delta z_i \exp\left(-\frac{E_m}{kT_i}\right) \right\}} \bar{\gamma}_k \quad (124)$$

Equation (124) may also be derived directly from Eq. (111), using Eqs. (115) and (116).

The equivalent width for isolated strong lines for the effective isothermal region, according to the square-root approximation, may be obtained from Eq. (112).

$$\text{Width}_{i_1, i_2, m} \approx \sum_k 2 \left(\left\{ \sum_i^{i_1, i_2} \frac{N_i}{Q_i} \left[1 - \exp\left(-\frac{h\nu_m}{kT_i}\right) \right] \Delta z_i \exp\left(-\frac{E_m}{kT_i}\right) N e_i \right\} \right)^{1/2} \quad (b' g_k^f \bar{\gamma}_k)$$

$$= 2 A_{i_1, i_2, m}^{1/2} \sum_k (b' g_k^f \bar{\gamma}_k)^{1/2} \quad (125)$$

The effective half-width does not appear in Eq. (125). From the above consideration, it is assumed that the effective half-width defined by Eq. (111) (or Eq. (124) as a special case) may be used as an approximation along the whole "curve of growth."

(4) Criteria for line isolation. From the above discussions, it is apparent that the calculations are much simplified if the isolated-line approximation may be made. With the Lorentz line shape, the wings of the lines extend to $+\infty$ and $-\infty$. Therefore, the lines always overlap to a certain degree. One needs then to qualify the description "isolated lines" and to establish suitable criteria for line isolation for numerical calculations.

Let

Z = quantity calculated using the isolated-line approximations

Z^* = quantity calculated by numerical integration without the isolated-line approximations

Then, if

$$\left| \frac{Z - Z^*}{Z} \right| \leq \epsilon \ll 1, \quad (126)$$

the isolated-line approximations may be used.

Now,

$$\text{Trans}_{i_1, i_2, m} - \text{Trans}_{i_1, i_2, m}^* = \frac{1}{\Delta\nu_m} \left(\text{Width}_{i_1, i_2, m} - \text{Width}_{i_1, i_2, m}^* \right) \quad (127)$$

The following criterion is more stringent than Eq. (126):

$$\left| \frac{\text{Trans}_{i_1, i_2, m} - \text{Trans}_{i_1, i_2, m}^*}{\text{Smaller of} \left(\text{Trans}_{i_1, i_2, m}, \frac{\text{Width}_{i_1, i_2, m}}{\Delta\nu_m} \right)} \right| \leq \epsilon \ll 1 \quad (128)$$

Unfortunately, the usefulness of the isolated-line approximations is lost if $\text{Trans}_{i_1, i_2, m}^*$ or $(\text{Width}_{i_1, i_2, m} / \Delta\nu_m)$ must be calculated for application in Eq. (128). Therefore, other more convenient approaches should be used.

Consider the calculation of the equivalent width of two overlapping lines, as shown in fig. 3a. The values of the integrand in Eq. (96), calculated by summing the two isolated-line contributions exceed that based on two overlapping lines. For the profiles in fig. 3a

$$R \equiv \frac{1}{\Delta\nu_m} \sum_k \text{Width}_{k, m} \sim 0.3^\dagger$$

$$R^* \equiv \frac{1}{\Delta\nu_m} \text{Width}_m^*$$

$$Z_R \equiv \frac{R - R^*}{R^*} \sim 0.1$$

In fig. 3b, the line-center separation is three times that in fig. 3a and the value of Z_R is much smaller than 0.1 for the same value of R .

Qualitatively, the value of R may indicate the degree of overlapping. As the value of R increases, the value of R^* approaches unity, as illustrated in fig. 4. At small values of R , the values of Z_R are small so that the lines may be considered isolated. For a given group of lines (hence a particular pattern of line spacing) within $\Delta\nu_m$, it may be possible to obtain an approximate relation $R^* = F(R)$ by correlating the numerical results of some typical distributions of temperature and species concentration (with or without using the approximation of effective isothermal region). This approximate relation may then be used in radiation-coupled flow field calculations. In view of the uncertainties in f -number and half-width values, the above approach appears reasonable.

[†]The value of R is inversely proportional to $\Delta\nu_m$.

4. NUMERICAL METHODS

The division of the continuum bands and line groups used in the computer code STAGRADS (STAGnation point, RADIation-coupled, with external Source*) is briefly described in Section 4.1. Details of the spectral divisions are given in Appendixes B and C. The schemes of flow field iteration and of line calculations are discussed in Sections 4.2 and 4.3, respectively.

4.1 Division of Continuum Bands and Line Groups

For the continuum air radiation, eight different models are provided before the lines are incorporated. These models consist of from two to nine spectral bands (see Table 1). The first option (LINEØP = 1) of radiation transport calculations accounts for only the air continuum contributions using one of the eight models. For calculations with lines, two options are provided. In one option (LINEØP = 2), the air continuum contribution is first calculated using one of the eight models of band divisions. The continuum contribution is then corrected for the presence of the lines [see Eqs. (86) to (89)]. In another option (LINEØP = 3), the spectral division of the continuum bands is made coincident with that of the line groups and the total contribution is calculated according to Eq. (85).

A total of 21 line groups are used (see Appendix C). Three of the groups contain only a single line per group. Three of the groups contain no lines at all so that the last option (LINEØP = 3) of transport calculations may be used.

For calculations with ablation layer, only the continuum contributions of the ablation species are included in order to reduce the requirement of computer storage and time. To account for the variation of the ablation species absorption coefficients over a wide spectrum, the division of the continuum bands for these species is made coincident with that of the line groups. For calculations with ablation layer, the last option (LINEØP = 3) is used so that the contributions of the air atomic lines are included.

4.2 Scheme of Flow Field Iteration

The integration of the conservation equations is for the air layer from the shock-wave toward the interface and for the ablation layer from the body surface toward the interface. For the integration of the radiative terms and the energy Eqs. (28a) and (46), the air layer and the ablation layer are divided into a number of sublayers. The air layer is divided in equal increments of the actual distance, but the ablation layer is divided in equal increments of the transformed distance [see Eq. (44)]. At

*In ref. 1, the radiation transport formulation includes the presence of external radiation sources. For this study, no external radiation sources are considered.

present, a maximum of ten air sublayers and ten ablation sublayers is allowed in the computer code in order to reduce the requirement of computer storage and time.

The integration of the momentum Eqs. (27) and (47) requires much less computer time and storage. Consequently, their integration may be performed with finer increments than that for the energy equations. The density ratios in Eqs. (27) and (47) are calculated by interpolations from values obtained using the energy equations.

The flow field calculation begins with the integration of the air layer momentum equation, using an assumed distribution of $\rho_S/\rho \approx h/h_S$. The integration is stopped when Eq. (29b) is satisfied at the interface, thus determining the air layer thickness. The air layer is then divided into a number of sublayers and the energy Eq. (28a) integrated. Across a sublayer, an average value of the nondimensional normal velocity F is used, and the net radiative energy gain is given by the spectrally integrated Q [see Eq. (65)]. Iteration is made to obtain a consistent set of velocity and enthalpy distributions.

For calculations with ablation layer, an initial enthalpy distribution, linear in the transformed normal distance between the wall enthalpy and an enthalpy at the interface estimated from the air layer results, is assumed. The density distribution is calculated using the equations of state of the ablation vapor. The initial blowing rate is estimated using the air layer results, a surface heat balance, and an estimate of the vapor enthalpy rise. The momentum and energy equations are integrated in the same manner as for the air layer. The air layer temperature distribution is maintained unchanged during ablation layer calculations. Iteration on the wall heat flux is also made to obtain a consistent set of wall heat flux, blowing rate, and velocity and enthalpy distributions.

The effect of the presence of the ablation layer on the air layer enthalpy distribution is then checked. If necessary, the air layer calculation is repeated while the ablation temperature distribution is maintained unchanged. Further repetitions of ablation layer and air layer calculation are then made, if required, to obtain a consistent set of wall heat flux, blowing rate, and velocity and enthalpy distributions for both layers.

At present, the criteria for convergence used in STAGRADS are: enthalpy distribution, 1 percent and heat flux to the wall, 2 percent. The convergence of the blowing rate is governed by that of the wall heat flux. The convergence of the velocity distribution is governed by that of the enthalpy distribution.

4.3 Scheme of Line Calculation

When numerical integrations are required to evaluate $Width_{i1,i2,m}$ or $Trans_{i1,i2,m}$, the selection of the computation schemes should be carefully made to minimize the computer time. For example, the calculation of exponential functions requires much more time than for performing multiplications. Therefore, it may be more economical to calculate

$$\exp \left(- \sum_i^{i_1, i_2} \xi_i \right)$$

according to

$$\prod_i^{i_1, i_2} \exp(\xi_i)$$

if there are many variations of i_1 and i_2 . Computation time may also be reduced by using common factors and by avoiding calculating the same variables many times (with increasing computer storage requirement, however).

Consider the numerical integration of the integral in Eqs. (96) or (97). The integrand is to be evaluated for many values of ν , say ν_j , within $\Delta\nu_m$. Let j be the dummy index for ν . In terms of the system of index notation selected, the important variables are summarized as follows: (Note $\Delta y_i = \Delta z_i$)

$$Bgf_k = b'gf_k \quad (129)$$

$$\text{Dyn}q_i = \frac{N_i}{Q_i} \Delta y_i \quad (130)$$

$$\text{Dyn}qe_i = \frac{N_i}{Q_i} \Delta y_i Ne_i = \text{Dyn}q_i Ne_i \quad (131)$$

$$\text{Dyn}q_{i,m} = \frac{N_i}{Q_i} \Delta y_i \left[1 - \exp \left(- \frac{h\nu_m}{kT_i} \right) \right] = \text{Dyn}q_i \left[1 - \exp \left(- \frac{h\nu_m}{kT_i} \right) \right] \quad (132)$$

$$\text{Dyn}qe_{i,m} = \frac{N_i}{Q_i} \Delta y_i \left[1 - \exp \left(- \frac{h\nu_m}{kT_i} \right) \right] Ne_i = \text{Dyn}q_{i,m} Ne_i \quad (133)$$

$$S_{i,k,m} = \frac{N_i}{Q_i} \Delta y_i \left[1 - \exp \left(- \frac{h\nu_m}{kT_i} \right) \right] \exp \left(- \frac{E_{nk}}{kT_i} \right) b'gf_k = \text{Dyn}q_{i,m} \exp \left(- \frac{E_{nk}}{kT_i} \right) Bgf_k \quad (134)$$

$$S_{i,m} = \sum_k S_{i,k,m} = \text{Dyn}q_{i,m} \sum_k \exp \left(- \frac{E_{nk}}{kT_i} \right) Bgf_k \quad (135)$$

$$S_{i_1, i_2, k, m} = \sum_i^{i_1, i_2} S_{i, k, m} = \text{Bgf}_k \sum_i^{i_1, i_2} \text{Dynq}_{i, m} \exp\left(-\frac{E_{n_k}}{kT_i}\right) \quad (136)$$

$$S_{i_1, i_2, m} = \sum_i^{i_1, i_2} S_{i, m} = \sum_k S_{i_1, i_2, k, m} \quad (137)$$

$$\gamma_{i, k} = N e_i \bar{\gamma}_k \quad (138)$$

$$\tau_{i, k, m, j} = \frac{S_{i, k, m}}{\pi} \frac{\gamma_{i, k}}{(\nu_j - \nu_k)^2 + \gamma_{i, k}^2} \quad (139)$$

$$\tau_{i, m, j} = \sum_k \tau_{i, k, m, j} \quad (140)$$

$$\tau_{i, k, m} = \frac{S_{i, k, m}}{\pi} \frac{1}{\gamma_{i, k}} \quad (141)$$

$$\tau_{i, m} = \sum_k \tau_{i, k, m} \quad (142)$$

$$\tau_{i_1, i_2, k, m} = \sum_i^{i_1, i_2} \tau_{i, k, m} \quad (143)$$

$$\tau_{i_1, i_2, m} = \sum_k \tau_{i_1, i_2, k, m} = \sum_i^{i_1, i_2} \tau_{i, m} \quad (144)$$

$$SY_{i, k, m} = S_{i, k, m} \gamma_{i, k} \quad (145)$$

$$SY_{i, m} = \sum_k SY_{i, k, m} \quad (146)$$

$$SY_{i_1, i_2, k, m} = \sum_i^{i_1, i_2} SY_{i, k, m} \quad (147)$$

$$SY_{i_1, i_2, m} = \sum_k SY_{i_1, i_2, k, m} \quad (148)$$

$$ye_{i_1, i_2, k, m} = \frac{SY_{i_1, i_2, k, m}}{S_{i_1, i_2, k, m}} \quad (149)$$

$$\xi_{i_1, i_2, k, m} = \frac{SY_{i_1, i_2, k, m}}{2\pi ye_{i_1, i_2, k, m}^2} \quad (150)$$

$$Em\tau_{i, k, m, j} = \exp(-\tau_{i, k, m, j}) \quad (151)$$

$$Em\tau_{i, m, j} = \exp(-\tau_{i, m, j}) \quad (152)$$

$$Em\tau_{i_1, i_2, m, j} = \prod_i^{i_1, i_2} Em\tau_{i, m, j} \quad (153)$$

$$\text{Width}_{i_1, i_2, k, m} = 2\pi ye_{i_1, i_2, k, m} f(\xi_{i_1, i_2, k, m}) \quad (154)$$

$$\text{Width}_{i_1, i_2, m} = \sum_k 2\pi ye_{i_1, i_2, k, m} f(\xi_{i_1, i_2, k, m}) = \sum_k \text{Width}_{i_1, i_2, k, m} \quad (155)$$

[For isolated lines; $f(\xi)$ is given by Eq. (113).]

$$\text{Width}_{i_1, i_2, m}^* = \sum_j (1 - Em\tau_{i_1, i_2, m, j}) \delta\nu_j \quad (156)$$

(according to appropriate numerical integration scheme)

$$\frac{1}{\Delta\nu_m} \text{Width}_{i_1, i_2, m}^* = F\left(\frac{1}{\Delta\nu_m} \text{Width}_{i_1, i_2, m}, \text{LINE SPACING PATTERN}\right) \quad (157)$$

(approximate, empirical-numerical correlation).

The numerical integration of the integral in Eq. (96) then corresponds to the application of Eq. (156), with a suitable scheme of evaluating $Em\tau_{i_1, i_2, m, j}$ according to Eq. (153).

In the numerical scheme of line calculations for each line group, the equivalent width is first calculated assuming that the lines are isolated. If this value exceeds 1 percent of the spectral width for the line group, Eq. (156) is then used to calculate the equivalent width with line overlaps. The correlation discussed in connection with fig. 4 may be used for radiation-coupled flow field calculations. However, the computer time for typical flow field cases is found to be of the order of only one minute (UNIVAC 1108). Consequently, efforts in obtaining equivalent-width correlations appear unessential (though desirable) at present.

The numerical calculation of Eq. (156) [or integration of Eq. (96)] is based on a variable interval Simpson's Rule, modified in such a way as to yield results two orders higher in accuracy than the basic Simpson's Rule. Depending upon the pattern of line spacings, the degree of overlap, and the accuracy criterion imposed, the number of evaluations of the integrand [of Eq. (96) or $(1 - Em\tau_{i_1, i_2, m, j})$] for a line group may vary over a wide range, say from 20 to 800 for a single equivalent width.

5. RESULTS

Results of numerical calculations are presented in this section. Almost all of the results presented are obtained using STAGRADS. Only an example of the heat flux distributions obtained using STRADS is given. Additional results from STRADS may be found in refs. 11 and 12. A reference case ($u_\infty = 15.24$ km/sec, $\rho_\infty/\rho_{SL} = 1.66 \times 10^{-4}$, $R_N = 256$ cm) is selected for uncertainty studies.

5.1 Effects of Exponential Kernel Approximation

In ref. 1, the exponential integrals used in the radiation transport calculations were calculated using series representation and numerical correlations. In Section 3.2, the exponential kernel approximation, $E_3(\xi) \approx 0.5 \exp(-2\xi)$, is introduced. This approximation enables the formulation of the concept of line transmittance and equivalent width, as discussed in Section 3.4.2. The effects of the exponential kernel approximation on the shock layer enthalpy distribution, the radiative flux to the wall and to the shock, and the air layer thickness are shown in fig. 5, for a representative environmental condition (the reference case). The air continuum contributions alone are considered, using band Model No. 4 (5 bands) and 10 sublayers. The close agreement of the enthalpy, heat fluxes, and air layer thickness can be seen. The enthalpies calculated with actual $E_3(\xi)$ are slightly higher than that with approximate $E_3(\xi)$. However, the optical thicknesses of the four of the five bands with actual $E_3(\xi)$ are slightly lower than that with approximate $E_3(\xi)$. The net results are slightly higher heat fluxes with the exponential kernel approximation. The approximation $E_3(\xi) \approx 0.5 \exp(-2\xi)$ is used in all results presented below.

5.2 Effects of Continuum Band Models

The effects of air continuum band models on the radiative flux to the wall can be seen in Table 1. Only air continuum contributions are considered. The results indicate that the two-band model does not account fully for the self-absorption effect in the vacuum ultraviolet. Band Model 4 (Planck-mean for $0.5 \leq \nu \leq 10.95$ eV plus 4 vacuum UV bands) provides results sufficiently close to that obtained with more complicated band models and is adopted for "nominal calculations." Figure 6 shows further comparison of results obtained using Models 1 and 4, including line contributions.

5.3 Effects of Line Model

Two options (LINEOP = 2 or 3) of line calculations are discussed in Sections 3.4.2 and 4.1. When air layer calculations alone are considered, either of the two options may be used. When the effects of ablation layer are examined, the option LINEOP = 3 is used. Figure 7 shows the nondimensional enthalpy distributions, heat fluxes, and air layer thicknesses for the two line calculation options.

The results are for the same environmental condition (the reference case) as for figs. 5 and 6. The two line options yield nearly the same results.

5.4 Effects of Ablation Layers

The presence of a relatively high density ablation vapor adjacent to the body surface further attenuates the radiative flux to the wall. In an inviscid analysis, the chemical reaction between the air species and the wall is not considered. The wall is assumed to be at the equilibrium sublimation conditions corresponding to the surface pressure. The surface material considered in this study is 70/30 carbon phenolic (see Appendix A for its thermodynamic properties). A 21-band model of continuum absorption coefficients, with the same spectral divisions as that for the air line groups, is used (see Appendix B.2).

For the reference case, the air layer temperatures are increased slightly near the interface when the effects of the ablation layer are included, as shown in fig. 8. The heat flux to the shock is increased slightly (3 percent) whereas that to the wall is reduced greatly (41 percent). The results are for the nominal f numbers for the molecular band systems given in Table B-2, unless indicated otherwise. Figure 9 shows the temperature and tangential velocity distributions across the air and ablation layers. It is seen that the ablation vapor is heated slowly at first near the wall and very rapidly near the interface. The tangential velocity distribution is replotted in terms of a transformed "mass" distance in fig. 10. The ablation layer is seen to carry about the same mass as the air layer, although it is physically thin compared to the air layer.

The particle number densities in the air and ablation layers are given in fig. 11.* The continuum optical thicknesses are given in fig. 12. The ablation layer is optically thicker than the air layer over all frequencies shown.

Figure 13 shows the spectral heat fluxes. Actually, the heat fluxes should be a series of steps, being constant over a line group frequency region as shown for the optical thickness in fig. 12. In order to show the effects of ablation layer in the same figure, the spectral heat fluxes are "assigned" to a selected point of each line group and straight lines are drawn between adjacent points. The results indicate that the ablation layer effectively blocks all radiation fluxes with frequencies greater than 10.95 eV, due to the photo absorption of C ground and excited states, C⁺ excited states, and H Lyman (see Table B-1).

5.5 Effects of the Number of Sublayers

In order to test the accuracy of the finite-difference method of integrating the radiation transport and energy equations, the reference case is recalculated with fewer sublayers, from 10 + 10 (10 subdivisions in both the air and ablation layers) to 6 + 6. The results are compared in fig. 14. It is seen that the effects on the heat fluxes and total layer thickness are small. The surface reradiation is of the same order as the heat flux to the wall, causing a significant deviation in the non-dimensional surface blowing rate.

*Only species used in radiative property calculations are plotted (see Appendix B).

For the study of the effects of environmental variables, the combination of 6 air sublayers and 6 ablation sublayers will be considered adequate.

5.6 Effects of Environmental Variables

The effects of nose radius variation on the radiative fluxes, for constant velocity and altitude, are shown in fig. 15. Increasing the nose radius from 1 to 8.4 ft (30.48 to 256 cm) only increases the heat flux to the wall by 68 percent without ablation layer effects and 24 percent with ablation layer effects. Increasing the nose radius increases the heat loss to the ambient air more rapidly.

Further results for different environmental variables are given in Table 2 and figs. 16, 17, and 18. At the highest altitude (250 kft) considered, the surface reradiation exceeds the heat flux to the wall. The assumption that the surface is at the equilibrium sublimation temperature is not physically meaningful. However, the results may still be presented with the understanding that zero ablation is considered. The number of calculated points are insufficient to construct figs. 16, 17, and 18 accurately. Some of the points are obtained by "interpolation" of data points in other figures.

The results indicate that the heat flux to the wall is changed according to the following:

- (1) It increases as the velocity increases; the ablation layer tends to decrease the velocity effect.
- (2) It increases only slowly as the nose radius increases; the ablation layer reduces the nose-radius effect further.
- (3) It decreases due to the presence of the ablation layer, more for lower altitudes, larger nose radii, and higher velocity.

In general, it can be stated that the ablation layer becomes more efficient in reducing the zero-ablation radiative flux to the wall as the latter increases. The analogy between the ablation layer effectiveness in reducing radiative heat flux to the wall and the convective blowing effectiveness is noted.

5.7 Effects of Perturbation of Radiative Properties

The effects of uncertainties of the radiative properties are illustrated in figs. 19 and 20. In fig. 19, curve 3 corresponds to the reference case when nominal (N) values of the radiative properties are used. Curves 1, 2, 4, and 5 represent results without the ablation layer. Curves 1 and 2 are results of calculation (LINEØP = 1) with air continuum contributions only, with nominal cross sections for curve 1 and $2 \times$ the first-band cross sections ($\nu < 10.95$ eV) for curve 2. The effects of air lines may then be seen by comparing curves 1 and 3 and the corresponding heat fluxes. Doubling the first-band cross sections alone is not sufficient to "match" the line effects.

For curve 4, the line half widths used are twice the nominal value, while for curve 5 the line f-numbers are doubled. The effects are to increase both the heat fluxes to the wall and to the shock, but by less than 10 percent.

For curve 6, the line half-widths, line f-numbers, and the ablation species molecular band system f-numbers are twice the nominal values. Again the heat flux increase is relatively small, being less than 17 percent.

The effects of increasing the ablation species molecular band system f-numbers alone by a factor of two may be seen in fig. 20. The heat flux to the wall is only slightly reduced. Attempts were made to study the effects of increasing the f-numbers by a factor of the order of 10. However, because of the rapid temperature rise near the wall, convergence difficulties were encountered in iteration of the ablation layer enthalpy distribution. Approximate energy conservation calculations for the enthalpy rise for a one-dimensional ablation vapor flow indicates, however, the enthalpy rise is nearly the maximum. Consequently, increasing the f-numbers further may not change the heat flux to the wall appreciably, although the enthalpy distribution may change significantly.

5.8 Effects of Precursor Heating

No detailed analysis of the precursor heating effects is performed in this study. However, using the results of spectral heat fluxes to the shock obtained from STAGRADS and the results of refs. 3, 4, and 13, a first order estimate of the preheating effect on the radiative flux to the wall may be made. For instance, using fig. 11 of ref. 13 and assuming all radiation leaving the shock with $\nu > 12.15$ eV* (see Table 2) is absorbed by the cold air near the shockwave, for $u_\infty = 15.24$ km/sec and $\rho_\infty/\rho_{SL} = 1.66 \times 10^{-4}$, the increase in radiative flux to the wall may be estimated to be in the order of 5 percent for the nose radii considered in Table 2. For velocities higher than 60 kft/sec the preheating effects may become more significant, however.

5.9 Equivalent Width Results

Figure 21 illustrates the results of equivalent widths of the line groups, for isothermal air layers of different thickness. The temperature and density correspond to that immediately behind the normal shock for the reference case. As discussed in Section 4.3, the equivalent width is first calculated assuming that the lines are isolated. If this value exceeds 1 percent of the spectral width of the line group, the equivalent width is recalculated by numerical calculation of Eq. (156) to account for line overlaps. As the layer thickness increases, the equivalent widths of line groups with strong line overlaps approach the group width asymptotically, for instance line groups 19 and 15 in fig. 21. When the ratio of equivalent width to line-group width is much less than unity, the slope of the line may indicate whether the lines are thin or within the strong-line, square-root regime (see Eq. (113)). For instance, the lines within group 1 are thin whereas that within group 13 are within the square-root regime, for most of the values of Δ in fig. 21.

*Cold N₂ has a multitude of narrow molecular bands starting at 12.4 eV, but strong absorption may not begin until the N₂ photo-ionization continua are reached at about 15.5 eV (ref. 14).

The results of fig. 21 indicate that line overlaps must be taken into account for blunt-body radiation transport calculations.

5.10 STRADS Results

Downstream of the stagnation region, the stream-tube formulation is used to calculate the flow field and radiative fluxes. In this study, the computer code STRADS developed in ref. 1 is modified to incorporate the air continuum band models used in STAGRADS. The effects of ablation layer are not included. The air line contributions are "simulated" approximately by multiplying the first-band cross sections with an appropriate factor.

The configuration considered is a blunt vehicle flying at a 33 deg angle-of-attack, as shown in fig. 22. The formulation of STRADS is based on two-dimensional and axisymmetric configurations. In order to simulate the actual attitude, the effective axis of symmetry is displaced at a distance R_0 from the stagnation point, as shown in fig. 22.

The radiation heating distributions, normalized with respect to the stagnation radiative flux to the wall calculated by STAGRADS, are given in fig. 23. The dimensional symbols are defined in fig. 22. Varying the value of the first-band cross section multipliers from 2 to 4 produces no significant changes in the normalized heating distributions. The radiation heating distribution is seen to exhibit a strong velocity dependency. Further results from STRADS may be found in refs. 11 and 12.

6. CONCLUDING REMARKS

An efficient numerical procedure for fully radiation-coupled blunt-body flows has been formulated in this study. The effects of air continuum, atomic line, and ablation layer radiations are taken into account for determining the stagnation point velocity and temperature fields, the heat fluxes to the wall and to the shock, and the surface blowing rate. The efficiency of the numerical methods is due to the finite-difference integration of the radiation-transport terms and the energy equation, to the formulation of the concept of line-group equivalent width and average transmittance, and to the procedure of calculating the equivalent width with line overlaps.

Using the computer code developed, the effects of environmental variables, of the numerical methods used, and of the uncertainties in radiative properties have been delineated. The results indicate the following conclusions:

- (1) The exponential kernel approximation of the exponential integral yields results for enthalpy distributions and heat fluxes very nearly the same as that with actual exponential integrals.
- (2) The two-band model of air continuum radiation underpredicts the self-absorption effects in the vacuum ultraviolet. Increasing the vacuum UV band numbers from 1 to 4 (Model 4) provides results sufficiently close to that obtained with more complicated band models.

- (3) The two options of line calculations, $LINEOP = 2$ or 3 , yield nearly the same results.
- (4) The ablation layer is very effective in reducing the heat flux to the wall and thus the surface ablation rate. It practically blocks all radiative fluxes with frequency greater than 10.95 eV. The ablation layer becomes more efficient in reducing the zero-ablation radiative flux to the wall as the latter increases.
- (5) Reducing the number of sublayers from $10 + 10$ to $6 + 6$ still yields results adequate for the study of the effects of environmental variables.
- (6) The self-absorption and energy loss effects decrease the sensitivity of the heat fluxes to the changes in environmental variables and to the uncertainties in radiative properties. An order of magnitude change of the nose radius (from 1 to 10 ft) only increases the heat flux to the wall by 30 percent. Considering the change of convective heat rates with nose radius, blunt configurations may prove to be more effective than slender configurations in reducing the total wall heat fluxes.
- (7) For velocities less than 18 km/sec (~ 60 kft/sec), the effect of precursor heating on the radiative flux to the wall is small.

In future work, the following studies are recommended:

- (1) The formulation of radiation transport may be extended to include the precursor radiation and the spectral emissivity of the body surface.
- (2) The contributions of additional radiative systems, such as the lines due to nitrogen ions, and oxygen and carbon atoms and ions, may be included.
- (3) The formulation of the flow field may be extended to include the precursor heating effect and the viscous effect (including conduction and diffusion).
- (4) The radiation transport formulation developed may be used for calculations around the body.
- (5) The accuracy of the one-dimensional radiation transport may be investigated, particularly when the temperature gradient in the direction parallel to the body is large.
- (6) The numerical procedures used in STAGRADS may be further improved to increase the accuracy and to reduce the computation time.

APPENDIX A

THERMODYNAMIC PROPERTIES OF AIR AND ABLATION VAPOR

For a given composition of elementary species, two state variables are sufficient to specify the thermodynamic properties of a gaseous mixture in thermodynamic equilibrium. The state properties may be put in a tabular form so that property calculations may be made by table look-up and interpolation. Alternately, curve fits of one state variable versus a second at several levels of a third may be used. The latter method is particularly convenient when many calculations are made at a fixed level of a certain state variable. For instance, for a blunt body in hypersonic flow, the shock layer normal pressure gradient may be neglected. Curve fits or correlations of temperature and other state properties versus enthalpy at several constant levels of pressure will be very convenient for calculations along a body normal. Correlations of this kind for air may be found in refs. 15, 16, and 17.

For air calculations in the present study, correlations of refs. 15 to 17 may be used. However, for the purpose of reducing the computer time required, new correlations with a more suitable set of units are generated. The division of enthalpy ranges is also selected in such a manner that interpolations of the coefficients in the correlations between adjacent pressure levels may be more conveniently made.

The units selected for correlation purposes are:

- P , pressure in atm
- T , temperature in eV , 1 eV = 11605. 7° K
- H , enthalpy ratio, $h/h_{\text{satellite}}$, $h_{\text{satellite}} = 12,484 \text{ Btu/lb}_m$
- PV/V_{SL} , in atm, V_{SL} = sea-level (1 atm, 288.16° K) air specific volume

The correlation formula coefficients for air are given in Table A-1.

With the values of the compressibility factor available, the concentrations of air species may be readily calculated if Hansen's (ref. 18) simplified model of air chemistry is used. However, in this study, the particle densities (their logarithm) of neutral nitrogen and oxygen atoms and electrons are calculated by double interpolation with respect to temperature and the logarithm of density using the results of Gilmore (ref. 19) and Moeckel and Weston (ref. 20).

The surface material considered in ablation layer calculations is 70/30 carbon-phenolic. The 70/30 carbon-phenolic is assumed to be at the equilibrium sublimation conditions corresponding to the surface pressure. The sublimation latent heat is 4,270; 4,220; 3,900 cal/gm at 0.1, 1, and 10 atm, respectively. If the material sensible heat is included in the energy balance, the effective heat of sublimation will be higher.

The thermodynamic properties (temperature, enthalpy, density, species particle concentrations, and pressures) of 70/30 carbon-phenolic vapor in thermodynamic equilibrium were calculated by a free-energy minimization program, and are put in a table form for double interpolation with respect to pressure and enthalpy. Between two consecutive table values, the temperature and the logarithm of specific volume and of species concentrations are assumed to be linear in enthalpy and in the logarithm of pressure.

APPENDIX B

RADIATIVE PROPERTIES OF AIR AND ABLATION SPECIES

The absorption coefficient of a given species is the product of its particle number density and absorption cross sections. For a given mixture of species, the absorption coefficient is the sum of these products. The cross sections of air species and ablation vapor species are discussed below.

B.1 Absorption Cross Sections of Air Species

B.1.1 Continuum absorption cross sections. — The effective cross sections of neutral nitrogen (NI) and neutral oxygen (OI) given in Tables 4-3 and 4-5 of ref. 7 are used. These cross sections include the bound-free and free-free photon absorption contributions and are per particle of NI or OI. For the conditions of interest, the relative contribution due to NII is small. The incorporation of absorption contributions due to NII and N^- continuum has not been made.

For the eight continuum band models described in Section 4.1, partial Planck mean [see Eq. (75)] cross sections are used for bands with frequency less than 10.95 eV. The NI cross sections increase in steps for frequency above 10.95 eV and average values are used for each of the steps. The OI cross sections do not change appreciably between 4.0 and 13.61 eV but increase in steps above 13.61 eV. For OI, partial Planck means are used up to 13.61 eV and average values are used for each of the steps above 13.61 eV. The selection of the band boundaries is based on the locations of the step changes in cross sections. The band boundaries for the eight models are given in Table 1. For frequencies above 10.95 eV, the cross sections for the highest-frequency band correspond to that of the lowest-frequency step within the band. For example, in Model 1, the average cross sections between 10.95 and 12.15 eV are used for the second band with boundaries at 10.95 and 30.0 eV.

For calculations with lines and ablation layer, the frequency regions are relatively narrow. The value of the cross section at a specified point within the frequency region is used. The logarithms of the cross sections are assumed to be linear in frequency and temperature between tabulated values.

B.1.2 Line absorption cross sections. — Only the contribution of NI lines are included in the present STAGRADS code. The effective NI particle density for line calculations is taken as the sum of the actual NI and OI particle densities. A total of 75 NI lines are considered. Some of the lines are "effective" lines formed by treating two or more closely situated lines as single lines. The f numbers and the half-width (at $T = 10,000^\circ \text{K}$) of the NI lines given in Tables 4-9 and 4-15, respectively, of ref. 7 are used. The line shifts are neglected and the half-widths are considered independent of temperature [see Eq. (99)]. See Appendix C.3 for details of line data used.

B.2 Absorption Cross Sections of Ablation Species

Only the continuum contributions of ablation species are included in the present STAGRADS code. The radiative systems considered include the Swan, Fox-Herzberg, Deslandres-D'Azambuja, Freymark, and Mulliken band systems of C_2 , the CO_4^+ system, and the continuum processes due to the C^+ free-free contribution and the photo-absorption of CO, H Balmer, H Lyman, C ground and excited states, and C^+ excited states.

As discussed in Section 4.1, the division of the continuum bands for the ablation species is made coincident with that of the line groups.

The spectral ranges of the 21 bands and the average cross sections of the absorption processes are given in Table B-1. The cross section σ_0 of the molecular band systems were obtained by wavelength averaging the results obtained by John Weisner (ref. 21) and by normalizing to unity f-number. The temperature dependence is determined from the cross-section values at two temperatures ($3,000^\circ K$ and $9,000^\circ K$ or $10,000^\circ K$) and is very approximate. The cross-sections of the continuum processes are given by the same simple correlation, with f taken as a unity. No perturbation of the continuum cross-sections is considered in this study. The f-numbers of the band systems are given in Table B-2.

The C_2 Swan systems are the only band contributors considered within the first five bands. Preliminary results of calculation indicated that the optical thickness for these bands ($> 0.62\mu$) was too low. As the absorption in the IR is generally strong due to the presence of the polyatomic molecules adjacent to the wall and due to systems not included (e.g., C_2 Phillips and Ballik-Ramsey Band systems and H Paschen and Brackett continua), the C_2 Swan contribution within Band 1 is raised by a factor of 10 to compensate for the neglected absorbing systems.

APPENDIX C

THE STAGRADS CODE

The listing of the STAGRADS code, for calculation in UNIVAC 1108 at LMSC, is given after the figures near the end of the report. The input data required for the reference case ($u_\infty = 15.24$ km/sec, $\rho_\infty/\rho_{SL} = 0.166 \times 10^{-3}$, $R_N = 256$ cm) are then listed. Brief explanations are given for the code and the input. The program is very complex. The purpose of presenting the listing is for the benefit of those who have the desire to modify the program and to make use of some of the subroutines for other related problems.

Representative output data, including details of the line data used, are also given at the end of the report with brief explanations.

C.1 STAGRADS Listing (See page 99.)

The listing of STAGRADS given is in FORTRAN IV. STAGRADS consists of a main program and a number of subroutines and functions. In the order of appearance in the listing, they will be explained briefly below.

C.1.1 Main Program. The main program serves the following functions:

- (1) Read all input data.
- (2) Write a majority of the output results.
- (3) Integrate the energy equation and iterate the enthalpy distribution for the air layer.
- (4) Call the appropriate subprograms (i.e., Subroutine VEL for integration of the momentum equation to obtain the velocity distribution).

The built-in data TC (I, J) are used only in Subroutine ABSORP. They are repeated here for the purpose of checking (see listing near statement no. 72).

C.1.2 Subroutine STAGAB, STAGAB (STAGrads ABlation) is for calculation of stagnation ablation layer. It serves the following functions:

- (1) Integrate the energy equation and iterate the enthalpy distribution, wall heat flux and surface blowing rate for the ablation layer.
- (2) Write output of ablation layer results.
- (3) Call the appropriate subprograms (i.e., Subroutine VEL for calculation of the velocity distribution).

C.1.3 Subroutine NGGBSP. NGGBSP (Non-Grey Gas) is used for radiation transport calculations involving finite bands of the air continuum contributions. As listed, the exponential kernel approximation is used for $E_3(\xi)$. However, the actual $E_3(\xi)$ may be used if only the air continua are considered.

C.1.4 Subroutine CRLINE. CRLINE (CoRrection for LINE) is used for radiation transport calculations when the contributions of the air lines and ablation species continua are included. It is used for either of the two line-calculation options discussed in Section 4.1.

C.1.5 Subroutine ABSORC. ABSORC (ABSORption for Continua) calculates the air continuum absorption coefficients (NI and OI) for a specified frequency within the individual line groups.

C.1.6 Subroutine LINE. LINE calculates the equivalent widths or transmittance for the line groups. It writes out the calculated results if requested by appropriate controls.

C.1.7 Function FLR. FLR calculates the Ladenburg-Reiche function according to the approximations given by Eq. (113).

C.1.8 Subroutine INTEG. INTEG (INTEGration) performs integration to obtain the equivalent width. It is based on a modified Simpson's rule. It writes out the smallest integration step and other information if requested by the control.

C.1.9 Subroutine INTRND. INTRND (INTEgRaND) calculates the integrands required for equivalent width calculations.

C.1.10 Subroutine DOUBL. DOUBL (DOUBLe interpolation) is used to calculate particle concentrations of NI, OI and e by double interpolation with respect to temperature and the logarithm of specific volume.

C.1.11 Subroutine PROPT. PROPT (PROPerTy) calculates air temperature, PV product, and compressibility factor for given pressure and enthalpy, using the correlation formulas given in Table A-1.

C.1.12 Subroutine ABSORP. ABSORP (ABSORption) calculates the air continuum absorption coefficients (NI and OI) for the individual bands for the eight band models.

C.1.13 Subroutine SPABCO. SPABCO (SPectral ABSorption COefficient) calculates the ablation species continuum absorption coefficients for the 21 spectral regions.

C.1.14 Subroutine PROT. PROT (PROPerTy) calculates for the ablation vapor the specific volume, temperature, and particle densities of C_2 , C, CO, H, and C^+ by double interpolation with respect to enthalpy and the logarithm of pressure. The property tables are input in the main program.

C.1.15 Subroutine SESB. SESB (State Equation for Surface Blowing) calculates the surface enthalpy for 70/30 carbon phenolic in sublimation equilibrium at the surface pressure. The surface specific volume and temperature calculated in SESB are actually not used in STAGAB; they are recalculated by PROT for consistency with the vapor properties.

C.1.16 Subroutine PLANCK. PLANCK calculates the fraction of black-body powers within two frequency limits and for a given temperature.

C.1.17 Function EXPF. EXPF limits the absolute value of the argument for EXP to 85 to avoid numerical overflow.

C.1.18 Subroutine VEL. VEL (VELOCITY) integrates the momentum equation for the air layer and ablation layer.

C.1.19 Subroutine TBLP4. TBLP4 is used for interpolation of variables such as specific volume ratio, transformed distances and velocities in VEL.

C.1.20 Subroutine MODL1, MODL2, ... MODL8. These subroutines specify the frequency limits for the 8 air continuum band models. They also select the proper cross section indices for calculations in ABSORP.

C.1.21 Function E2F. (listed after input data) E2F calculates the second exponential integral by series and numerical correlations. It may be used in conjunction with E3F in NGGBSP and CRLINE, when the actual exponential integral instead of the exponential kernel approximation is employed.

C.2 Input Data Listing (See page 155.)

The input data for an example case (the reference case) are listed immediately following the STAGRADS listing. All input data are read in within the main program.

The input line and line group data are first read. The 10 read statements after the comment "Input Line and Line-Group Data" read in the values of the following variables:

NHV	Total number of line groups
NLST	Total number of lower states
GEE(I)	Statistical weight of I-th lower state
EPS(I)	Electronic energy of I-th lower state, eV
FHVM(I)	Lower frequency limit of I-th line group, eV
FHVP(I)	Upper frequency limit of I-th line group, eV
FHV(I)	A selected (e.g., central) frequency within I-th line group, eV
ISOE(I)	> 0 if the approximation of effective isothermal region may be used for the I-th line group; otherwise ≤ 0 .
NUMINT(I)	> 0 if numerical integration is to be used (when required) to calculate the equivalent width of the I-th line group; otherwise ≤ 0 .
NU(I)	Number of lines in I-th line group

NLINE	Total number of lines, calculated by summing all NU
ND(I)	Lower state index for I-th line
HVL(I)	Center frequency of I-th line, eV
FF(I)	Effective f-number of I-th line (f-number of the particular transition multiplied by a statistical-weight ratio, see Section 3.4.1)
GAMBA(I)	Half-width (eV) of I-th line for 1 electron/cm ³ .

Ncxt, some of the 4 input tables are read, between Statements 8 and 99 in the listing. Each of the 4 tables is headed by a leader card.

<u>Table 01</u>	(Leader Card with value of NC = 0 1; near statement 10)
L	0 for two-dimensional and 1 for axisymmetric
CASE	Case identification
PA	Ambient pressure, atm
RHOA	$\rho_{\infty} / \rho_{SL}$
UA	u_{∞} , km/sec
RN	R_N , cm
NS	≈ 10 , number of air sublayers
ES	ρ_{∞} / ρ_s
HA	h_{∞} / h_{sat}
TW	T_W , eV (if < 0.02 , reset to 0.02; recalculated as equilibrium surface temperature if ablation layer effects are considered)
MODEL	Air continuum band model number, = 1, 2, ..., 8
LINEOP	$\left\{ \begin{array}{l} 1, \text{ only air continua with one of the eight band models} \\ 2, \text{ calculate air continua with one of the eight band models and then} \\ \text{correct for air lines} \\ 3, \text{ 21 spectral regions with air continua and lines, with or without} \\ \text{ablation continua} \end{array} \right.$
FCONTN	Multiplying factor for air continuum cross sections ($\nu < 10.95$ eV) for the 8 band models
FDHAB	Multiplying factor for surface material latent heat of vaporization
NRITE1	> 0 print nondimensional enthalpy distributions during iteration; $\bar{=} 0$ no print
NRITE2	> 0 print equivalent-width information, final result only; $\bar{=} 0$ no print
NRITE3	> 0 print equivalent-width information during iteration; $\bar{=} 0$ no print
NRITE4	> 0 print equivalent-width integration information during iteration; $= 0$ final result only; < 0 no print

NRITE5 > 0 print line strength of sublayer, etc. during iteration; = 0 final re-
 sult only; < 0 no print
 NRITE6 > 0 print line strength of air-layer regions, etc. during iteration; = 0
 final result only; < 0 no print
 NRITE7 > 0 print nondimensional enthalpy distributions, QWT, etc., when either
 (but not both) the air or ablation layer iteration converges; ≤ 0 no
 print
 CMAG 0.0001 times absolute value of the average value of integrand
 ERR Integration accuracy control constant

With $err = 0.1$ and 0.01 , the result is said to be accurate to 4-6 places and 5-7 places, respectively. Decreasing the value of err will increase the computing time required.

From the results of equivalent-width calculations for a variety of conditions, a value of $err = 0.1$ is found adequate for most situations. Under certain situations when the lines are very narrow and with a small degree of overlapping, it is found that a value of err in the order of 0.01 is required for line groups 4 and 5 in order to obtain accurate results in equivalent widths by numerical integration. However, a value of err in the order of 0.1 is adequate for flow field and total heat flux calculations.

FRAC First integration step size divided by total integration interval
 NSAB ≤ 10 , number of ablation sublayers

Table 01 must be input for each run of flow field calculations. For flow field calculations without the ablation layer, Table 01 ends with a card with -1 (value of NC) in the first two columns. For flow fields calculations with ablation layer, Tables 03 and 04 are also required; the "-1" card is then put at the end of Table 04.

For flow field calculations, each case must end with a "-1" card. For subsequent cases of the same computer run, Tables 03 and 04 may be omitted if they are identical with the corresponding ones in the preceding case.

Table 02 (Leader card with value of NC = 02; near Statement 80)

Table 02 is input for equivalent width calculations with given layer thickness, number of sublayers, and distributions of temperature and specific volume. No "-1" card is required to end each case.

N Total number of sublayers
 DELTA Total thickness of layer, cm
 T(I) Temperature of I-th sublayer, eV
 V(I) ρ_{SL}/ρ of I-th sublayer

CMAG, ERR, FRAC }
 NRITE1 → NRITE6 } see Table 01

Table 03 (Leader card with value of NC = 03; near Statement 7010)

Table 03 inputs the thermodynamic properties of the ablation layer vapor.

IP	Total number of pressure values in table (3 allowed in present program)
IT	Total number of temperature values in table (20 allowed in present program)
PRTAB(I)	The i-th pressure value, in $\log_{10}(p, \text{atm})$
TTAB(I, J)	J-th temperature value for I-pressure value, °K
ENTAB(I, J)	Enthalpy for I-th pressure and J-th temperature, cal/gm
RHOTAB(I, J)	Density for I-th pressure and J-th temperature, gm/cm ³
C2TAB(I, J)	Particles/cm ³ for I-th pressure and J-th temperature, for C ₂
C1TAB(I, J)	For C ₁
COTAB(I, J)	For CO
HTAB(I, J)	For H
CPTAB(I, J)	For C ⁺
EMTAB(I, J)	For e

Table 04 (Leader card with value of NC = 04; near Statement 7020)

Table 04 inputs the f-numbers and continuum cross section multipliers for ablation layer radiating systems.

ICOSR	Total number of input COSR values
COSR(I)	f-numbers for band systems. For continua, COSR = 1.0 if the standard values of the cross sections are used. The order of COSR(I) is given in Table C-1.

C.3 Output Data Listing, Including Details of Line Data Used (See page 163.)

The data for the 21 line groups are first listed. The headings of the data are:

HV	Frequency within a line group for calculating Planck intensity function and continuum cross section, eV
HV+	Upper frequency limit of line group, eV
HV-	Lower frequency limit of line group, eV
N	Number of lines within line group

TABLE C-1
COSR(I) VALUES

I	Absorption Processes	Remarks
1	C ₂ Swan	Use f value
2	C ₂ F-H	Use f value
3	C ₂ D-D	Use f value
4	C ₂ Frey	Use f value
5	C ₂ Mull	Use f value
6	Unassigned	Use 0 value
7	Unassigned	Use 0 value
8	Unassigned	Use 0 value
9	CO 4 +	Use f value
10	CO Photo	Use 1 for standard value
11	Unassigned	Use 0 value
12	Unassigned	Use 0 value
13	Unassigned	Use 0 value
14	H Balmer	Use 1 for standard value
15	H Lyman	Use 1 for standard value
16	Unassigned	Use 0 value
17	Unassigned	Use 0 value
18	C Photo	Use 1 for standard value
19	Unassigned	Use 0 value
20	Unassigned	Use 0 value
21	C ⁺ Photo	Use 1 for standard value
22	Unassigned	Use 0 value
23	C ⁺ + e ⇌ C + hν , (C ⁺ free-free)	Use 1 for standard value

LINE Line index
 NLST Lower state index
 HV(I) Line center frequency, eV
 F(I) Effective f-number of line, same as FF(I) in Section C.2
 GAM(1) Line half-width for 1 electron/cm³, eV/(e/cm³)

- BFG(I) $b'gf$, Eq.(129) eV-cm²/particle
 ISOE > 0 , if effective isothermal region may be assumed; $\bar{=}$ 0 otherwise
 NUMINT > 0 , if equivalent width is calculated by integration when its value according to isolated lines exceeds 1 percent of line-group width; $\bar{=}$ 0 if calculated according to isolated lines only
 GEE(I) Statistical weight of I-th lower state
 EPS(I) Electron energy of I-th lower state, eV

The next group of output data is the air continuum cross sections TC(I, J) used in ABSORP. In ABSORP, TC(1 → 14, 1) are temperatures in eV and TC(1 → 14, 2 → 27) are values of $38 + \log_{10}$ (cross-section, cm²). These values have been converted to °K and cm², respectively, in the main program before being printed out. Each index J (2 → 27) is for a particular frequency interval (either a partial Planck mean or a representative average).

J:	2	3	4	5	6	7	8	9
Species:	NI	NI	NI	NI	NI	NI	NI	NI
ν_1 , eV:	0.5	2.0	4.0	6.0	9.50	10.95	12.15	13.61
ν_u , eV:	2.0	4.0	6.0	9.5	10.95	12.15	13.61	14.50

10	11	12	13	14	15	16	17	18
NI	OI	OI	OI	OI	NI	OI	NI	OI
14.50	0.5	2.0	4.0	13.61	0.50	0.50	2.00	2.00
30.00	2.0	4.0	10.95 (13.61)	30.00	10.95	10.95	10.95	10.95

19	20	21	22	23	24	25	26	27
NI	NI	NI	NI	NI	OI	OI	OI	OI
0.5	1.0	2.0	3.0	4.00	0.5	1.0	2.0	3.0
1.0	2.0	3.0	4.0	10.95	1.0	2.0	3.0	4.0

The next group of output consists of data of particle per air atom for equilibrium air. Following a column of 14 temperatures (3,000 → 24,000°K), the particles per air atom for NI, OI, and e (3 column as a group for one density) for $\log_{10}(\rho_{SL}/\rho) = 1.97634, 2.97634, \text{ and } 3.97634$ are given. The values of SPTABO (I, J, K) with the main program are in $-\log_{10}$ (particles/air atom). These values have been converted to particles/air atom before being printed out.

The next group of output corresponds to Table 01 of input. The units of the variables and the definitions of the symbols are given there.

If Table 03 is input, the data will be printed out. The data printed for the reference case are for three pressures ($\log_{10} p$, atm = -1.0, 0.0, 1.0). Columns 1 to 9 are respectively temperature ($^{\circ}\text{K}$), enthalpy (cal/gm), density (gm/cm^3), and particles/ cm^3 for C_2 , C_1 , CO, H, C^+ , and e.

If Table 04 is input, the values of COSR(I) are printed out. See Table C-1 for identification of the index.

The next group of output repeats the information for the line groups including the selected frequency and the lower and upper line indices.

The symbols appearing in the output are defined below:

NCOUNT	Number of iterations for enthalpy distribution, one counter for the air layer and another counter for the ablation layer
DELTA	Layer thickness for air or ablation layer, cm
PO	Air and ablation layer pressure, atm
HO	h_s/h_{sat}
TO	T_s , eV
QWT	Total heat flux to wall, watts/ cm^2
QSHOKT	Total heat flux to shock, watts/ cm^2
I	Sublayer index from shock
YC	z/Δ for air layer; y/Δ_{ab} for ablation layer (measured from center of sublayers)
UC	Normalized tangential velocity
VC	Normalized normal velocity
HC	h/h_s for air layer; h/h_w for ablation layer
T	Temperature, eV
V	ρ_{SL}/ρ
Z	Compressibility
HV	Selected (e.g., central) frequency of line group, eV
HV+	Upper limit frequency of line group, eV
HV-	Lower limit frequency of line group, eV
NLINE	Number of lines in line group, eV
TAUC	Continuum optical thickness for air layer
TAUCT	Continuum optical thickness from shock to wall
LINEOP	Line-calculation option (See Section 4.1)
EMD	$\rho_w v_w / \rho_{\infty} u_{\infty}$

NQWT	Number of iterations for heat flux to the wall for each ablation-layer calculation
NCONH	Counter for enthalpy distribution iteration for each assumed wall heat flux
QWTA1 } QWTA2 }	Previously assumed wall heat flux, watts/cm ²
QWTC1 } QWTC2 }	Previously calculated wall heat flux, watts/cm ²
QWT1	New assumed wall heat flux, watts/cm ²
HW	h_w/h_{sat}
TW	T_w , eV
VW	ρ_{SL}/ρ_w
VCW	v_w/u_∞
UR	u_r/u_∞ calculated based on interface streamline momentum consideration
RMOM	$\rho_w v_w^2 / \rho_\infty u_\infty^2$
URMAS	u_r/u_∞ calculated based on mass balance for a finite number of sublayers
IAB	Ablation sublayer index from wall
NC1, NC2, NCO NH, NC ⁺	Particle/cm ³ for C ₁ , C ₂ , CO, H, and C ⁺ , respectively
M	Line group index
IP1, I	Upper and lower index for region with indices IP1 and I
ISO . WIDTH	Equivalent width assuming isolated lines, eV
ACT . WIDTH	Equivalent width with overlap, eV
DNU* TRN	$\Delta\nu \cdot TRANS$, eV
ISO-ACT WIDTH	ISO . WIDTH - ACT . WIDTH, eV
WIDTH (IP1, I)	Equivalent width, eV
DELTAB	Δ_{ab} , ablation layer thickness, cm
DELTAT	Δ , thickness between shock and wall, cm
US	u_s
ZETA	$\int_0^z \frac{\rho}{\rho_s} \frac{dz}{\Delta}$
NCNTR1	Counter for number of air layer enthalpy iteration convergence

NCNTR2	Counter for number of ablation layer calculation convergence
NCNTR3	Counter for number of either (but not both) air layer or ablation layer convergence
FNUL(KK)	Lower frequency limit of KK-th air continuum band, eV
FNUH(KK) (FNUU)	Upper frequency limit of KK-th air continuum band, eV
FNU	Central frequency of air continuum band, eV
AB	1.0, signifies with self-absorption
QW(KK)	Continuum heat flux to wall for KK-th band, watts/cm ²
QWTC	Total continuum heat flux to wall, watts/cm ²
QDEL(KK)	Continuum heat flux to shock for KK-th band, watts/cm ²
QDELT	Total continuum heat flux to shock, watts/cm ²
SQW(KK)	Spectral continuum flux to wall for KK-th band, watts/cm ² eV
SQDEL(KK)	Spectral continuum flux to shock for KK-th band, watts/cm ² eV
TAU(I, KK)	Continuum optical thickness for KK-th band from I-th boundary to shock (I = 1)
K, KM	Line index and line index within line group, respectively
JD	Lower-state index
I	Sublayers index from shock
IP1, J	Boundary upper and lower indices
GAM(I)	Line half-width, eV
SS(I)	Line strength, Eq. (110), eV
SST(I + 1)	$\sum_{J=1}^I SS(J)$, eV
SGAM(I, KM)	SS(I) * GAM(I), (eV) ²
SGAMT(I + 1)	$\sum_{J=1}^I SGAM(J, KM)$, (eV) ²
TAUD(I)	Line-center optical thickness, SS(I)/ π GAM(I)
TAUDT(I + 1)	$\sum_{J=1}^I TAUD(J)$
SS12	Line strength between boundaries IP1 and J, eV

SGAM12	Value of SGAM between boundaries IP1 and J, $(\text{eV})^2$
GAME12	Effective half-width, $\text{SGAM12}/\text{SS12}$, eV
ZETA12	Argument of the Ladenburg-Reiche function, Eqs. (106) and (107)
WID12K	K-th line contribution to isolated line equivalent width for region between boundaries IP1 and J, eV
WID12(IP1 , J)	Equivalent width according to isolated lines for region between boundaries IP1 and J, eV
TAU12	Line-center optical thickness for region between boundaries IP1 and J
NCOUNT, NREJE	Counter for advancing to next integration interval or for rejecting existing integration step size, respectively. In Subroutine INTEG. Approximate number of evaluations of integrand for each region between two boundaries = $(\text{NCOUNT} + \text{NREJE}) \times 4$
DNU	Line group spectral width, eV
DXX(I)	Some integration step sizes, eV
Normalized Smallest Step	= DXX/DNU

REFERENCES

1. Chin, Jin H.; Inviscid Radiating Flow Around Bodies, Including the Effect of Energy Loss and Non-Grey Self-Absorption, Lockheed Missiles & Space Company, Report LMSC-668005, October 1965.
2. Chin, Jin H.; Effects of Non-Grey Self-Absorption and Energy Loss for Blunt Body Flows, Presented at the Symposium on Interdisciplinary Aspects of Radiative Energy Transfer, February 24-26, 1966, Philadelphia, Pennsylvania, (to be published in J. Quant. Spectrosc. Radiat. Transfer, January, 1968).
3. Wilson, K.H.; Private Communication, June, 1967.
4. Coleman, W.D., Lefferdo, J.M., Hearne, L.F., and Gallagher, L.W.; A Study of the Effects of Uncertainties on the Performance of Thermal Protection Systems for Vehicles Entering the Earth's Atmosphere at Hyperbolic Speeds, Lockheed Missiles & Space Company, Sunnyvale, California, (Monthly Progress Report for the Period 1 June 1967-30 June 1967, Contract NAS 2-4219).
5. Sparrow, E.M. and Cess, R. D.; Radiation Heat Transfer, Brooks/Cole Publishing Company, Belmont, California, 1966, Chapter 7.
6. Gilmore, F.R.; Energy Levels, Partition Functions and Fractional Electronic Populations for Nitrogen and Oxygen Atoms and Ions to 25,000°K, RAND RM-3748-PR, August 1963.
7. Wilson, K.H., and Nicolet, W.E.; Spectral Absorption Coefficients of Carbon, Nitrogen, and Oxygen Atoms, LMSC 4-17-66-5, November, 1965.
8. Simmons, F.S.; Radiances and Equivalent Widths of Lorentz Lines for Nonisothermal Paths, J. Quant. Spectrosc. Radiat. Transfer vol. 7, 111-121, 1967.
9. Penner, S.S.; Quantitative Molecular Spectroscopy and Gas Emissivities, Addison-Wesley, 1959, pp. 42-45.
10. Goody, R.M.; Atmospheric Radiation Vol. I Theoretical Basis, Oxford Clarendon Press 1964, pp. 237-239.
11. Hearne, L.F., Coleman, W.D., Lefferdo, J.M., Gallagher, L.W., and Chin, J.H.; A Study of the Effects of Environmental and Ablator Performance Uncertainties on Heat Shielding Requirements for Hyperbolic Entry Vehicles, NASA CR-Lockheed Missiles & Space Company, Sunnyvale, Calif., Dec 1967.
12. Hearne, L.F., Coleman, W.D., Lefferdo, J.M., Gallagher, L.W., and Chin, J.H.; A Study of the Effects of Environmental and Ablator Performance Uncertainties on Heat Shielding Requirements for Hyperbolic Entry Vehicles, NASA CR-Lockheed Missiles & Space Company, Sunnyvale, Calif., Dec 1967 - Data Volume.

13. Yoshikawa, Kenneth K.; Analysis of Radiative Heat Transfer for Large Objects at Meteoric Speeds, NASA TN D-4051, June, 1967.
14. Huffman, R.E., Tanaka, R.E. and Larrabee, J.C.; Absorption Coefficients of Nitrogen in the 1000-580A Wavelength Region, J. Chem. Phys. vol. 39, 4, 1963.
15. Viegas, J.R. and Howe, J.T.; Thermodynamic and Transport Property Correlation Formulas for Equilibrium Air From 1,000°K to 15,000°K, NASA TN D-1429, October, 1962.
16. Lockheed Missiles & Space Company, Final Report, Study of Heat Shielding Requirements for Manned Mars Landing and Return Missions, LMSC Report 4-74-64-1, December 1964, Contract NAS 2-1798, p. 3-30.
17. Howe, J.T. and Sheaffer, Y.S.; Effects of Uncertainties in the Thermal Conductivity of Air on Convective Heat Transfer for Stagnation Temperature up to 30,000°K, NASA TN D-2678, February, 1965.
18. Hansen, C. F.; Approximations for the Thermodynamic and Transport Properties of High Temperature Air, NASA TR R-50, 1959.
19. Gilmore, F.R.; Equilibrium Composition and Thermodynamic Properties of Air to 24,000°K, Rand Corporation Memorandum RM-1543, August, 1955.
20. Moeckel, W.E. and Weston, Kenneth C.; Composition and Thermodynamic Properties of Air in Chemical Equilibrium, NACA TN 4265, April, 1958.
21. Weisner, John D.; Private Communication, April, 1966.

LIST OF TABLES

Table		Page
1	Effect of Continuum Band Model on Stagnation Radiative Flux	68
2	Effect of Environmental Variables	69
A-1	Correlation Formula Coefficients, Air	70
B-1	Spectral Range and Average Cross Sections for 70/30 Carbon-Phenolic "21 Band" Model	72
B-2	Ablation Species Band System f-Numbers	73
C-1	COSR(I) Values	59

TABLE 1

EFFECT OF CONTINUUM BAND MODEL ON STAGNATION RADIATIVE FLUX

(Calculation Performed Before Line Contributions are Incorporated)

$$u_\infty = 15.24 \text{ km/sec ; } \rho_\infty / \rho_{SL} = 1.79 \times 10^{-4} ; R_N = 323 \text{ cm ; 12 Air Sublayers}$$

Model No.	No. of Bands	Spectral Range in eV											Wall Radiative Flux watts/cm ²
		1	2	3	4	5	6	7	8	9	10	11	
1	2	0.5-1.0	1.0-2.0	2.0-3.0	3.0-4.0	4.0-6.0	6.0-9.5	9.5-10.95	10.95-12.15	12.15-13.61	13.61-14.5	14.5-30.0	2,603
2	3	1	1	1	1	1	1	1	1	1	1	1	2,563
3	4	1	1	1	1	1	1	1	1	1	1	1	2,475
4*	5	1	1	1	1	1	1	1	1	1	1	1	2,433
5	4	1	1	1	1	1	1	1	1	1	1	1	2,563
6	9	1	1	1	1	1	1	1	1	1	1	1	2,414
7	9	1	1	1	1	1	1	1	1	1	1	1	2,434
8	5	1	1	1	1	1	1	1	1	1	1	1	2,560

*Band model 4 is adopted for "nominal calculation."

TABLE 2
EFFECTS OF ENVIRONMENTAL VARIABLES

R _N	u _∞ km/sec	ρ _∞ /ρ _{SL}	q _s	q _{s, ab}	q _w	q _{w, ab}	σT _w ⁴	$\frac{(\rho_w V_w)}{(\rho_\infty u_\infty)}$	$\frac{(\rho_w V_w)}{(\rho_\infty u_\infty)}$	Δ _a cm	Δ _{ab} cm	P _s atm	T _s eV	Precursor Heating Effect % of q _s (or q _{s, ab})		
														ν > 14.5	ν > 12.15	ν > 10.95
30.48	12.20	1.66(-4)	1,488		385		1,127	0	0	1.295	0	0.282	1.045	3.0	12.0	17.2
	15.24	1.66(-4)	3,452	3,529	1,806	1,324	1,236	0.103	0.017	1.142	0.082	0.447	1.245	8.8	29.6	42.1
	17.38	1.66(-4)	6,070	6,449	3,513	1,626	1,304	0.352	0.054	1.048	0.218	0.575	1.416	11.7	37.7	53.0
	15.24	3.26(-5)	1,537		170		1,435*	0	0	1.130	0	0.087	1.122	1.7	5.7	7.7
	15.24	5.94(-4)	14,227	14,278	8,086	3,602	1,606	0.336	0.102	1.155	0.327	1.573	1.352	9.2	31.3	47.8
122	15.24	1.66(-4)	5,360	5,565	2,591	1,479	1,236	0.245	0.046	4.250	0.671	0.447	1.245	7.8	29.0	44.0
256	12.20	3.26(-5)	1,404		106		1,361*	0	0	9.910	0	0.056	0.955	0.8	3.8	5.2
	12.20	5.94(-4)	6,375	6,625	3,482	2,396	1,458	0.130	0.062	10.450	1.338	1.006	1.120	2.0	10.4	21.5
	15.24	1.66(-4)	6,518	6,569	3,030	1,642	1,236	0.324	0.076	8.501	1.999	0.447	1.245	6.8	26.4	41.8
	17.38	3.26(-5)	2,288		921		928	0	0	7.447	0	0.113	1.274	10.1	31.4	41.8
	17.38	5.94(-4)	50,650	52,919	22,826	6,120	1,696	0.966	0.201	7.247	6.083	2.048	1.545	7.3	22.8	36.9

*Value too high due to pressure below input ablation property table pressure values and no extrapolation allowed.

q_s, q_w radiative flux toward shock and wall, respectively, without ablation layer effect.

q_{s, ab}, q_{w, ab} with ablation layer effect. T 1 eV = 11605.7°K

Carbon-phenolic surface, 6 air sublayers + 6 ablation sublayers.

TABLE A-1
CORRELATION FORMULA COEFFICIENTS, AIR

Property y	H _{lower}	H _{upper}	P (atm)	a ₀	a ₁	a ₂	a ₃	a ₄	a ₅	a ₆	Accuracy (%)
T, ev	0	0.0785	.01-10	1.1835678-1	6.5812617-1	9.3439634-1	-3.053483	2.4147548	-5.8669396-1		6.4
	0.0785	1.50	0.01	1.0487607-1	9.5327098-1	3.2467991-3	-1.5121987	1.3027109	-3.0545366-1		6.4
			0.1	9.6979514-2	1.1433893	-3.5657184-1	1.0029650	-1.0029650	-2.450222-1		6.2
			1.0	1.1613734-1	1.0843619	1.1034320-1	-1.6526663	1.3729724	-3.3199664-1		3.9
	1.50	5.50	0.01	-1.5819349	3.3455871	-1.86234081	5.2266941-1	-7.2395315-2	3.9710259-3		1.0
	5.50		0.1	-1.9378666	3.8547943	-2.0904567	5.7519457-1	-7.8194046-2	4.2031910-3		1.0
	5.50	9.9	0.10	-1.8226109	3.4993767	-1.7229472	4.3981665-1	-5.5808967-2	2.8371443-3		1.0
	5.50	7.43	1.0	-1.2891001	2.5154559	-1.0005790	2.1112489-1	-2.2369219-2	9.6330532-4		1.3
	5.50	6.78	10.0	1.9205406	-5.1167326	2.2507384	-3.7221565-1	2.7302427-2	-7.470516-4		2.2
			0.01	1.9295706+2	-1.3236946+2	3.5826685+1	-4.7588249	3.1128795-1	-8.0365421-3		1.0
			0.10	2.8774962+1	-1.3395786+1	2.1445183	-1.1088207-1				1.0
			1.0	-7.3068604-2	9.3749066-1	-1.9204991-1	1.5081737-2				1.0
T (alternate)	0.0361	0.36	0.01	-9.5098987-3	2.7498727	7.6381683-1	-1.2213621+2	5.5486666+2	-7.1270856+2		1.3
	5.50	9.9	0.10	3.5647251-2	2.4819323-1	4.7476579+1	-5.0754271+2	2.1990801+3	-4.2729834+3	3.0866908+3	1.0
	5.50	7.43	1.0	-1.9368604-3	2.3758528	3.8650062	-9.1807305+1	3.2603521+2	-3.4814242+2		1.3
	5.50	6.78	10.0	1.7905563-2	1.15133458	1.4744230+1	-1.3762337+2	4.0607364+2	-3.9827694+2		1.0
	0.36	1.50	0.01	-9.1095707-1	1.0041215+1	-3.1187126+1	5.0529627+1	-4.4270302+1	1.9837832+1		1.0
			0.10	-1.1822706-1	2.8525348	-5.5224045	5.6209047	-2.9035087	6.1978861-1		1.0
			1.0	6.5851264-2	1.5634838	-1.7494294	8.5083235-1	-1.1486050-1			1.0
			10.0	-9.2105463-2	2.4273938	-3.0304437	1.7403332	-3.4802097-1			1.0
PV/V _{SL} (atm)	5.50	11.0	0.01	3.5245559+2	-2.8068595+2	9.1419875+1	-1.5572599+1	1.4670453	-7.2599443-2	1.4764338-3	1.4
	0.0785	1.50	0.10	4.1466486	3.1607714+1	7.0980384+1	1.7031562+2	1.2768093+2	-2.9994045+1		5.7
			0.10	3.4124600	4.5715635+1	2.2226337+1	-8.3560087+1	6.3467061+1	-1.3608968+1		5.4
			1.0	3.1948184	5.0919529+1	1.6382194+1	-7.3823582+1	5.7745495+1	-1.2956107+1		4.0
			10.0	3.7750871	4.8311173+1	3.6479840+1	-9.8644062+1	7.2579584+1	-1.6722375+1		2.6
	1.50	5.50	0.01	-1.2724814+2	2.5536017+2	-1.3807613+2	4.0678168+1	-5.8880258	3.3852882-1		1.0
			0.10	-1.4284936+2	2.7319929+2	-1.4179943+2	4.0480512+1	-5.6722231	3.1539598-1		1.0
			1.0	-1.3549011+2	2.488272+2	-1.1659636+2	3.1199285+1	-4.1153845	2.173742-1		1.0
			10.0	-7.3263048+1	1.3473469+2	-3.6334966+1	6.1591101	-4.2335399-1	9.2513935-3		1.3
	5.50	11.0	0.01	-6.3540412+2	-1.7310820+2	1.8382531+2	-3.6014227+1	2.8527773	-8.1544340-2		1.9
	5.50	9.9	0.10	2.5708608+4	-1.7743649+4	4.8244025+3	-6.4277878+2	4.2158865+1	-1.0911416		1.0
	5.50	7.43	1.0	3.6719114+3	-1.7467849+3	2.8519962+2	-1.4827085+1				1.0
	5.50	6.78	10.0	1.1714926+2	1.7900484+1	-2.9186689	7.5179851-1				1.0
PV/V _{SL} (alternate)	0.0361	0.36	0.01	-2.9150224-1	1.8632507	-4.0867975+3	-4.0867975+3	1.9336595+4	-2.5392596+4		1.1
			0.10	-3.923492-1	1.1212841+2	-9.4952171+1	-2.5456987+3	1.2088268+4	-1.5053815+4		1.5
			1.0	-7.9702854-2	9.8552205+1	4.7099724+1	-2.5586988+3	9.8867488+3	-1.1004637+4		1.1
			10.0	5.5855155-1	7.0821747+1	3.9679145+2	-4.0339294+3	1.2486950+4	-1.25649937+4		1.0
	0.36	1.5	0.01	1.932261	2.5195433+1	5.9373260+1	-1.3021310+2	9.3944820+1	-2.0986612+1		1.6
			0.10	1.3690118	7.0948172+1	-5.9618294+1	2.5066220+1				1.0
			1.0	-2.1078820	6.9536693+1	-5.0323748+1	2.0157349+1				1.0
			10.0	-4.1878757	1.0303833+2	-9.9332450+1	5.6323946+1				1.0
	5.5	11.0	0.01	4.6079518+4	-3.6897522+4	1.2067170+4	-2.0617303+3	1.9472386+2	-9.6571314	1.9676061-1	1.3

TABLE A-1 (Continued)

Property y	H_{lower}	H_{upper}	P (atm)	a_0	a_1	a_2	a_3	a_4	a_5	Accuracy (%)
Z	0	0.0785	.01-10		$Z = 1.0$					
	0.0785	1.50	0.01	0.90204210	1.3765963	-1.5847662	1.5546703	-0.51615931		1.3
			0.10	0.89964231	1.3061862	-1.4626525	1.4298675	-0.46987220		1.3
			1.0	0.90237909	1.1686618	-1.1537565	1.1151654	-0.36066937		1.7
			10.0	0.88730931	1.1296640	-1.0581270	0.98701218	-0.29414222		1.3
	1.50	5.50	0.01	1.2736413	0.50509824	-0.54156490-2				1.1
			0.10	1.3301822	0.44379041	0.97737477-3				1.0
			1.0	1.3685294	0.39338470	0.48567735-2				1.0
			10.0	1.4055444	0.33971451	0.82709458-2				1.0
	5.50	11.0	0.01	2.8602478	0.16921459	.25806779-2				1.0
	5.50	9.9	0.1	2.8614600	0.15494900	.32019459-2				1.0
	5.50	7.43	1.0	-1.3604584	1.047895	-0.6454679-1				1.0
	5.50	6.78	10.0	-0.84086440	1.1224999	-0.66709173-1				1.0

$$y = a_0 + a_1 x + a_2 x^2 + a_3 x^3 + \dots$$

$x = H = h/h_{satellite}$, $h_{satellite} = 12484$ Btu/lbm, V_{SL} for air at 1 atm & 288.16°K

Data Sources:

- (1) Hansen, C.F. NACA TR R-50 for $1,000 \leq T^{\circ}K \leq 12,000$
- (2) LMSC Report 4-74-64-1, for $12,000 \leq T^{\circ}K \leq 25,000$

TABLE B-1

SPECTRAL RANGES AND AVERAGE CROSS SECTIONS FOR 70/30
CARBON-PHENOLIC "21 BAND" MODEL

Band No.	Frequency (eV)		System	σ_0	B	Remarks
	Lower	Upper				
1	0.50	0.80	C ₂ Swan C ⁺ f - f	1.86(-16)	1.2	$\mu = 2.43(-36)(C^+)^2 T^{-1/2}$
2	0.80	0.965				
3	0.965	1.20				
4	1.20	1.395				
5	1.395	1.60				
6	1.60	2.35	C ₂ Swan	1.14(-16)	0	
7	2.35	3.25	C ₂ F-H	3.94(-18)	0.29	
			C ₂ D-D	3.26(-18)	0.65	
8	3.25	4.10	C ₂ Swan	3.19(-18)	0.27	
			C ₂ F-H	2.44(-17)	0	
			C ₂ D-D	1.31(-17)	0.79	
			C ₂ Frey	2.41(-16)	1.52	
			H Balmer	3.38(-17)	10.2	
9	4.10	6.20	Band No. 8 plus			
			C ₂ D-D	4.5(-19)	1.17	
			C ₂ Frey	3.98(-16)	0.72	
			C ₂ Mull	1.5 (-17)	0	
			CO 4+	3.52(-17)	1.6	
			H Balmer	1.19(-17)	10.2	
10	6.20	8.00	CO 4+	6.23(-17)	0	
11	8.00	8.60	H Balmer C Photo	5.55(-18) 2.0(-19)	10.2 7.46	
12	8.60	9.00	CO 4+	6.75(-17)	0	
13	9.00	9.70	H Balmer C Photo	3.09(-18) 1.3(-18)	10.2 2.67	
14	9.70	10.95	CO 4+	6.35(-18)	0.46	
			H Balmer	2.1(-18)	10.2	
			C Photo	2.05(-17)	1.26	
15	10.95	12.15	H Balmer	1.32(-18)	10.2	
16	12.15	12.70	C Photo	2.05(-17)	1.26	
17	12.70	13.35	-	1.8(-17)	0	
18	13.35	13.85	CO Photo	1.0(-17)	0	
			H Lyman	4.85(-18)	0	
			C Photo	2.05(-17)	1.26	
19	13.85	14.50	-	1.8(-17)	0	
20	14.50	16.50	C ⁺ Photo	-	-	
21	16.50	20.00				$\sigma = 3.4 \times 10^{-20} T^{-1} e^{-5.4/T}$

NOTE: σ , cm²; μ , cm⁻¹; T, eV; (-16) = 10⁻¹⁶; $\sigma = f\sigma_0 e^{-B/T}$

TABLE B-2

ABLATION SPECIES BAND SYSTEM f NUMBERS

System	f-Number
C ₂ Swan	0.0059
C ₂ Fox-Herzberg	0.02
C ₂ Deslandres- D'Azambuja	0.006
C ₂ Freymark	0.002
C ₂ Mulliken	0.02
CO 4+	0.017

LIST OF ILLUSTRATIONS

Figure		Page
1	Geometry of Inviscid Flow Field	76
2	Geometry for a Finite Number of Sublayers	77
3	Calculation for Two Overlapping Lines	78
4	Qualitative Variation of R^* and R	79
5	Effects of Exponential Kernel Approximation	80
6	Effects of Air Continuum Band Models	81
7	Effects of Line-Calculation Options	82
8	Effects of Ablation Layer	83
9	Temperature and Tangential Velocity Distribution, in Physical Normal Distance	84
10	Tangential Velocity Distribution in Transformed Mass Normal Distance	85
11	Particle Density Distributions	86
12	Continuum Optical Thickness	87
13	Spectral Heat Flux to Wall and Shock	88
14	Effects of Number of Sublayers	89
15	Effects of Nose Radius, Constant Velocity and Altitude	90
16	Effects of Velocity, Constant Nose Radius	91
17	Effects of Nose Radius, Constant Altitude	92
18	Effects of Nose Radius, Constant Velocity	93
19	Effects of Perturbation of Radiative Properties	94
20	Effects on Ablation Layer Enthalpy Distribution and Heat Flux to Wall by Perturbing Ablation Molecular Species f-Numbers	95
21	Equivalent Widths for Isothermal Layers of Different Thicknesses	96
22	Blunt Vehicle Configuration for STRADS Calculations	97
23	Effect of Velocity on Radiation Heating Distribution, Blunt Vehicle	98

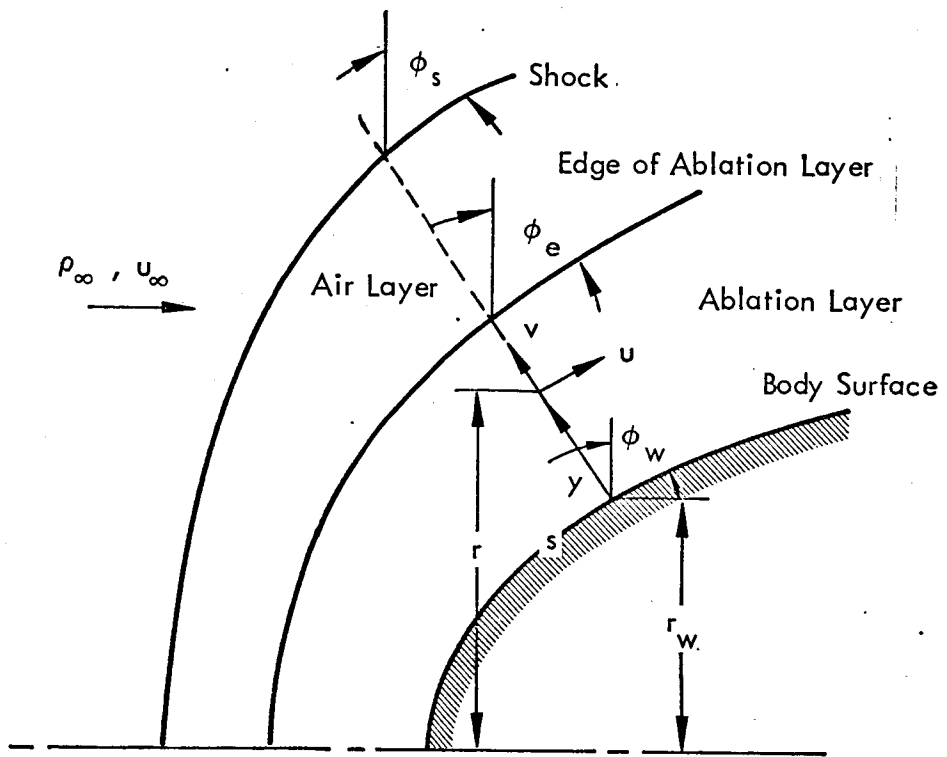


Fig. 1 Geometry of Inviscid Flow Field

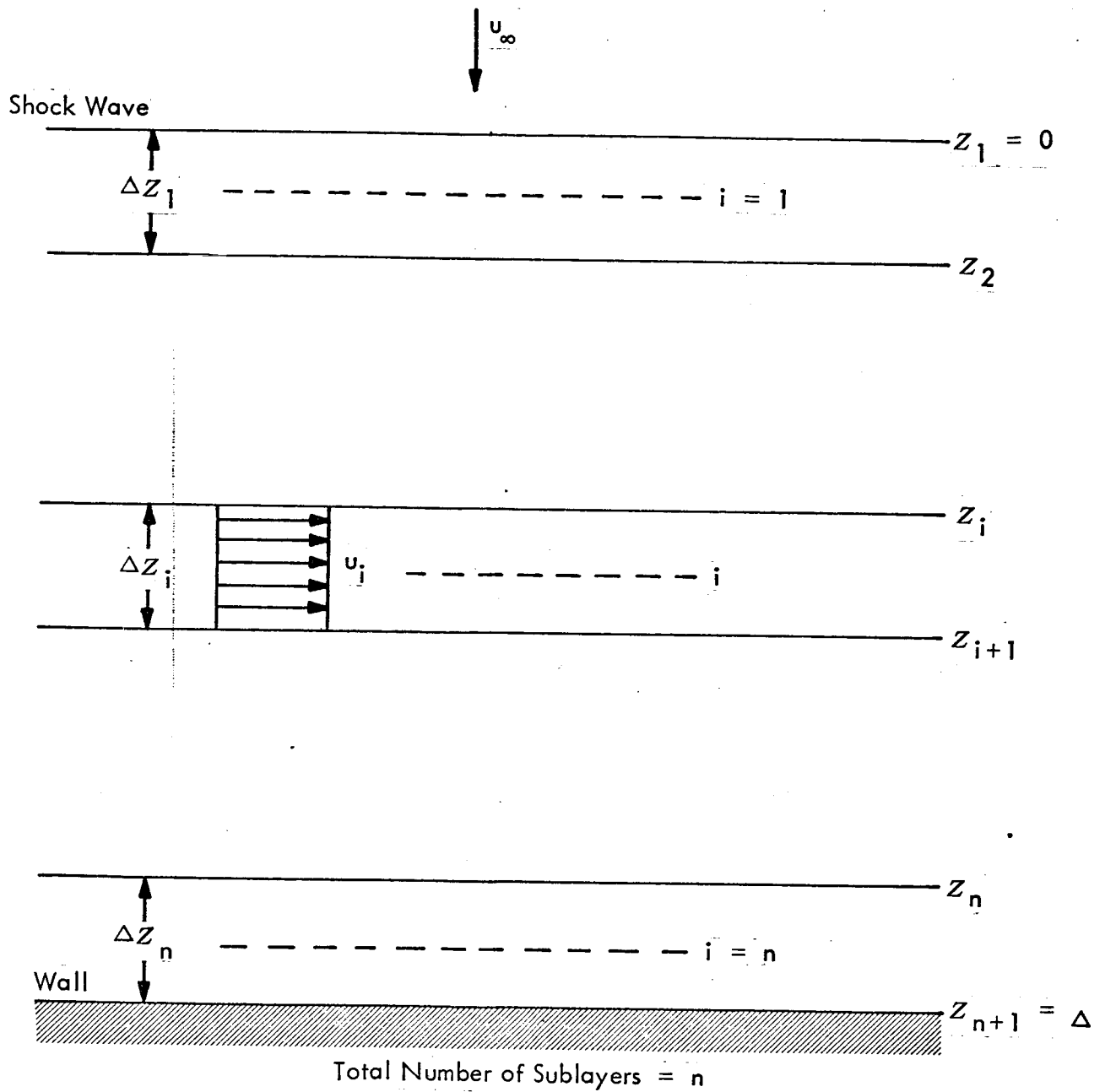


Fig. 2 Geometry for a Finite Number of Sublayers

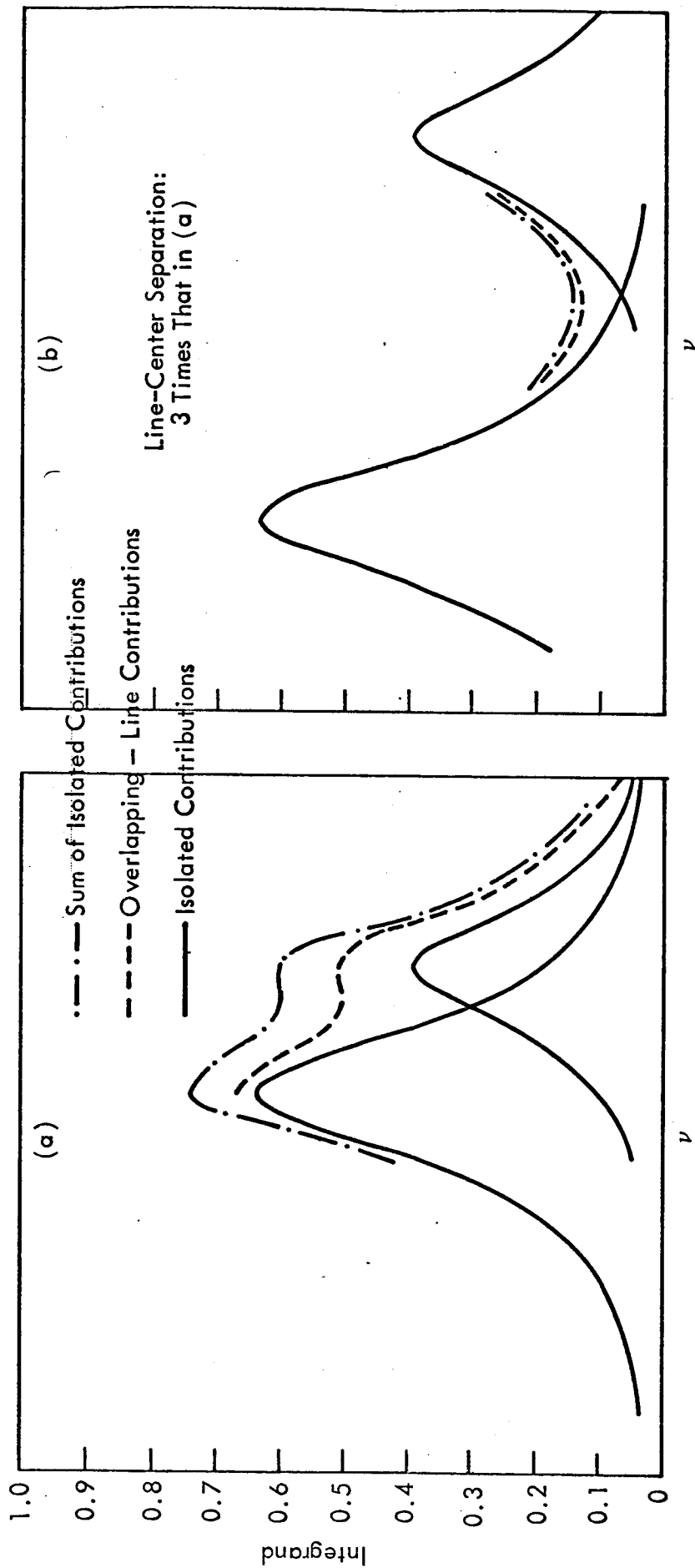


Fig. 3 Calculation for Two Overlapping Lines

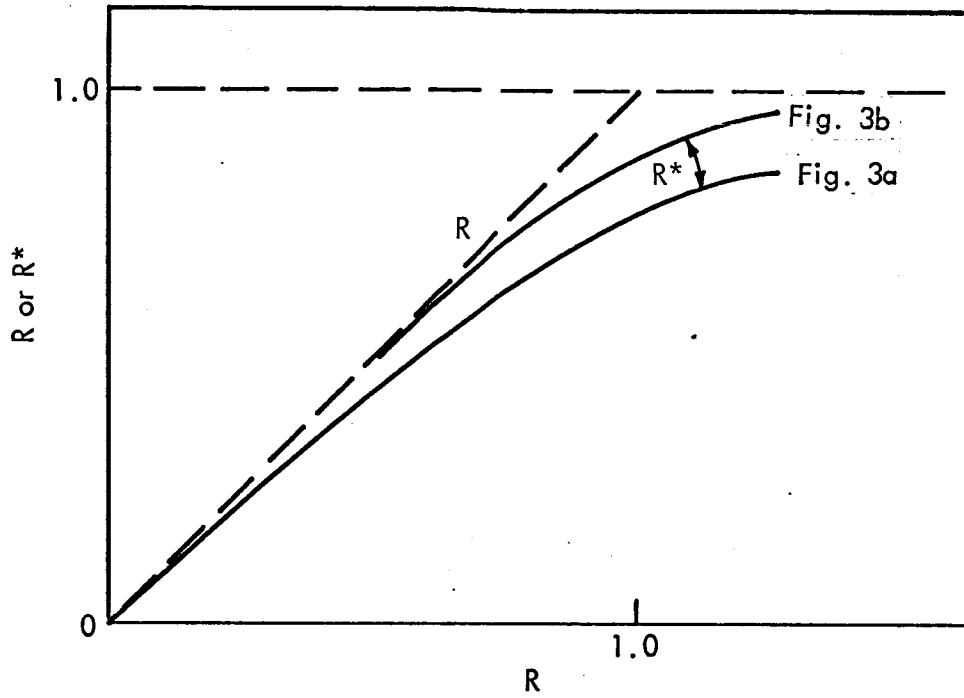


Fig. 4 Qualitative Variation of R^* and R

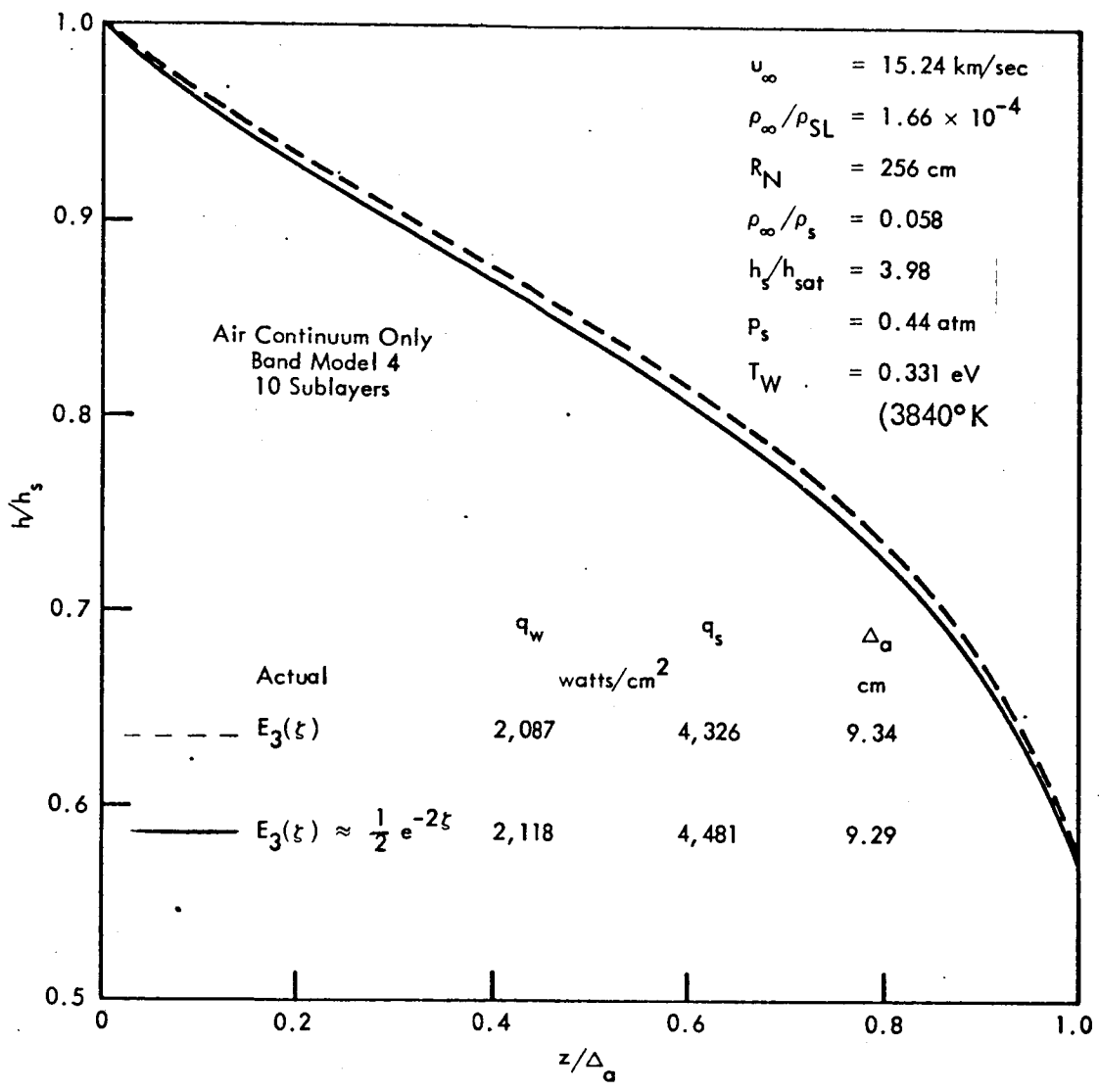


Fig. 5 Effects of Exponential Kernel Approximation

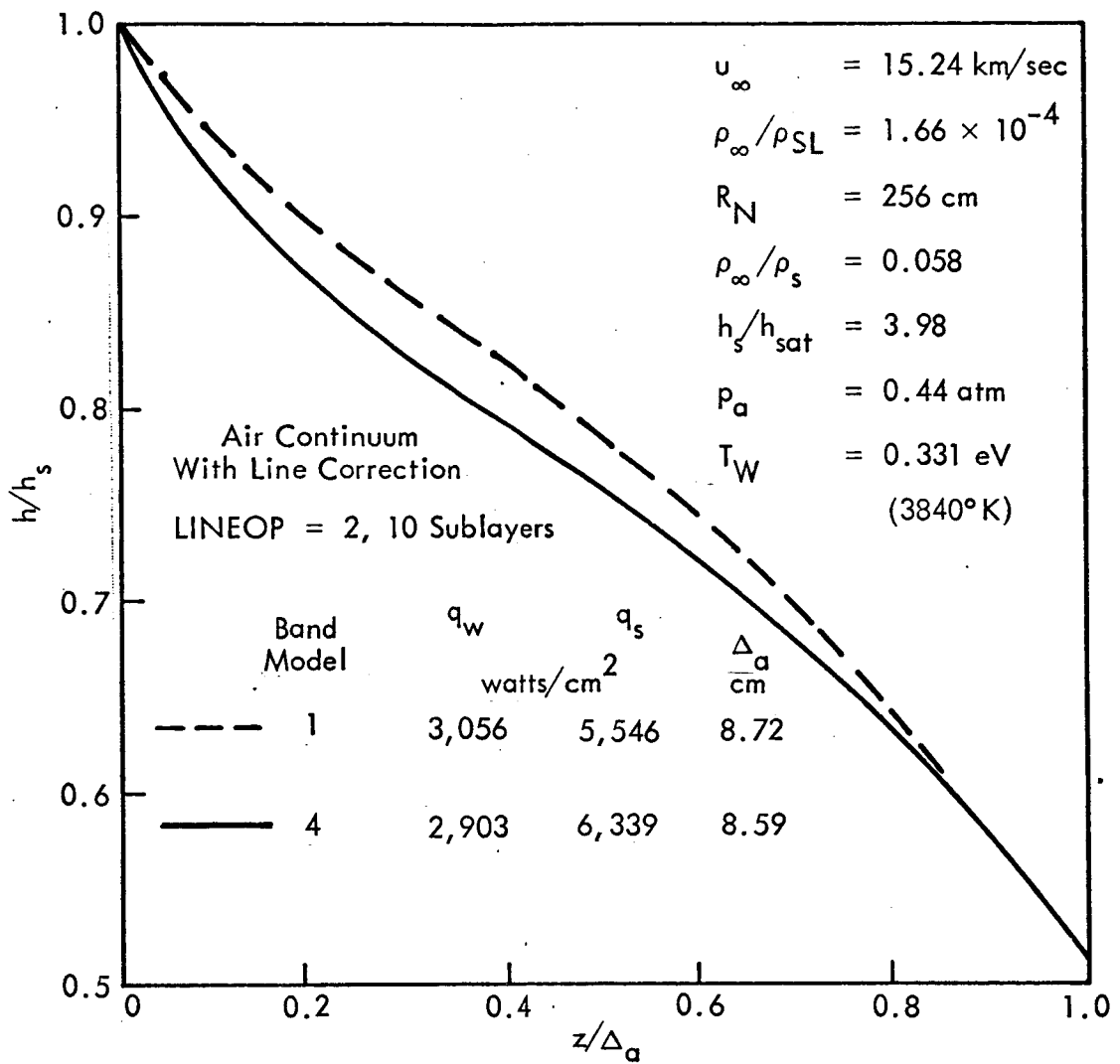


Fig. 6 Effects of Air Continuum Band Models

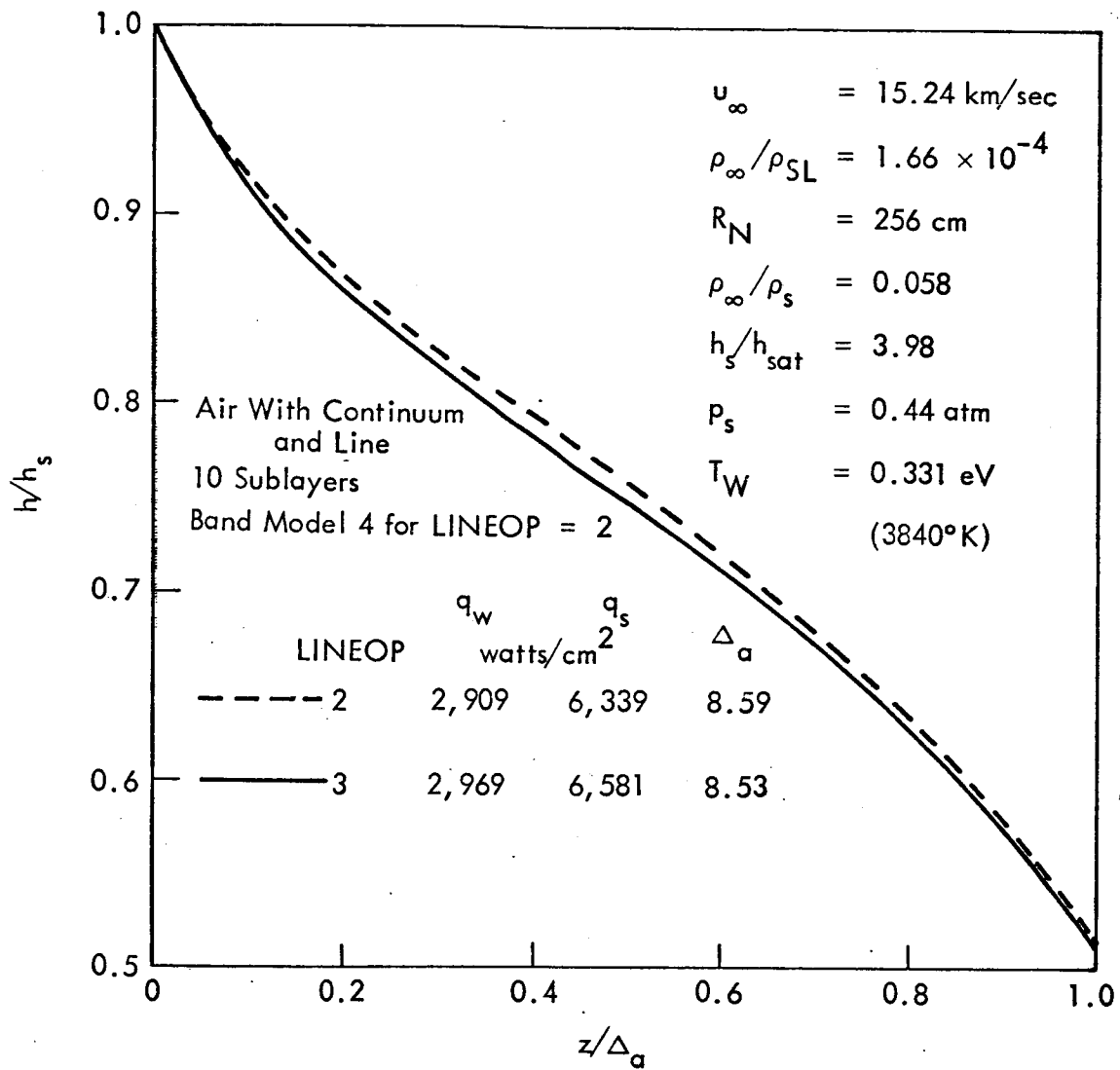


Fig. 7 Effects of Line-Calculation Options

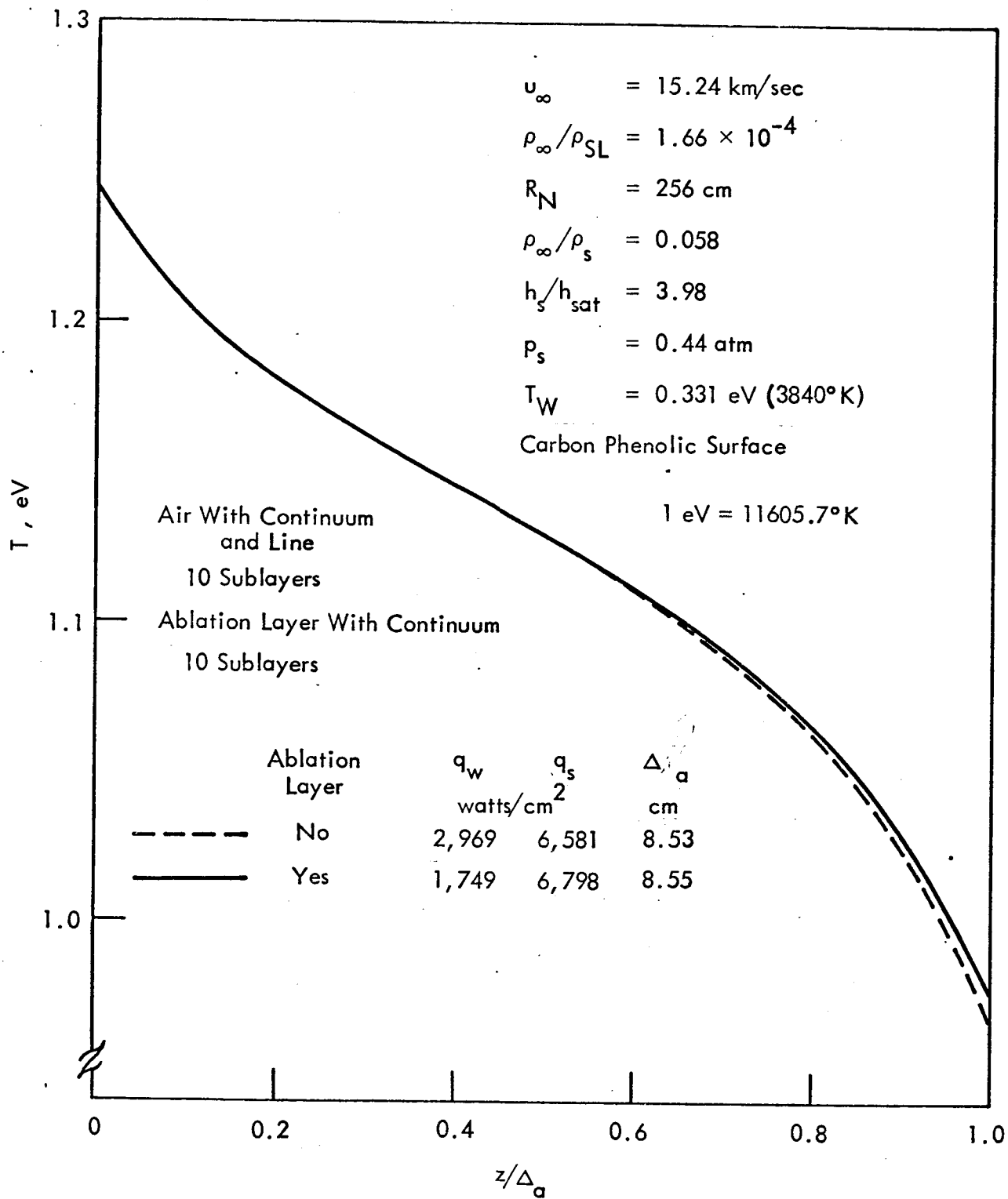


Fig. 8 Effects of Ablation Layer

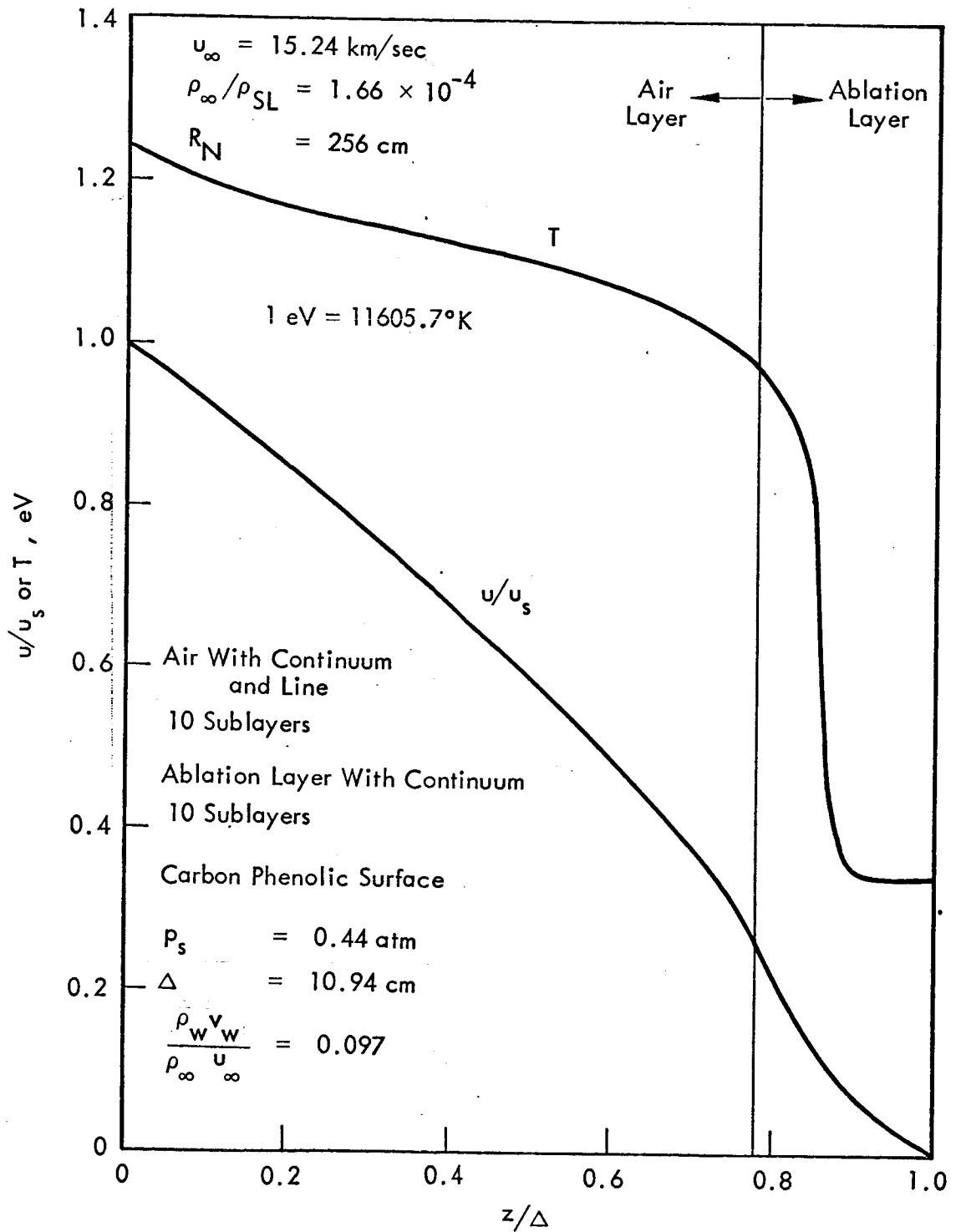


Fig. 9 Temperature and Tangential Velocity Distribution in Physical Normal Distance

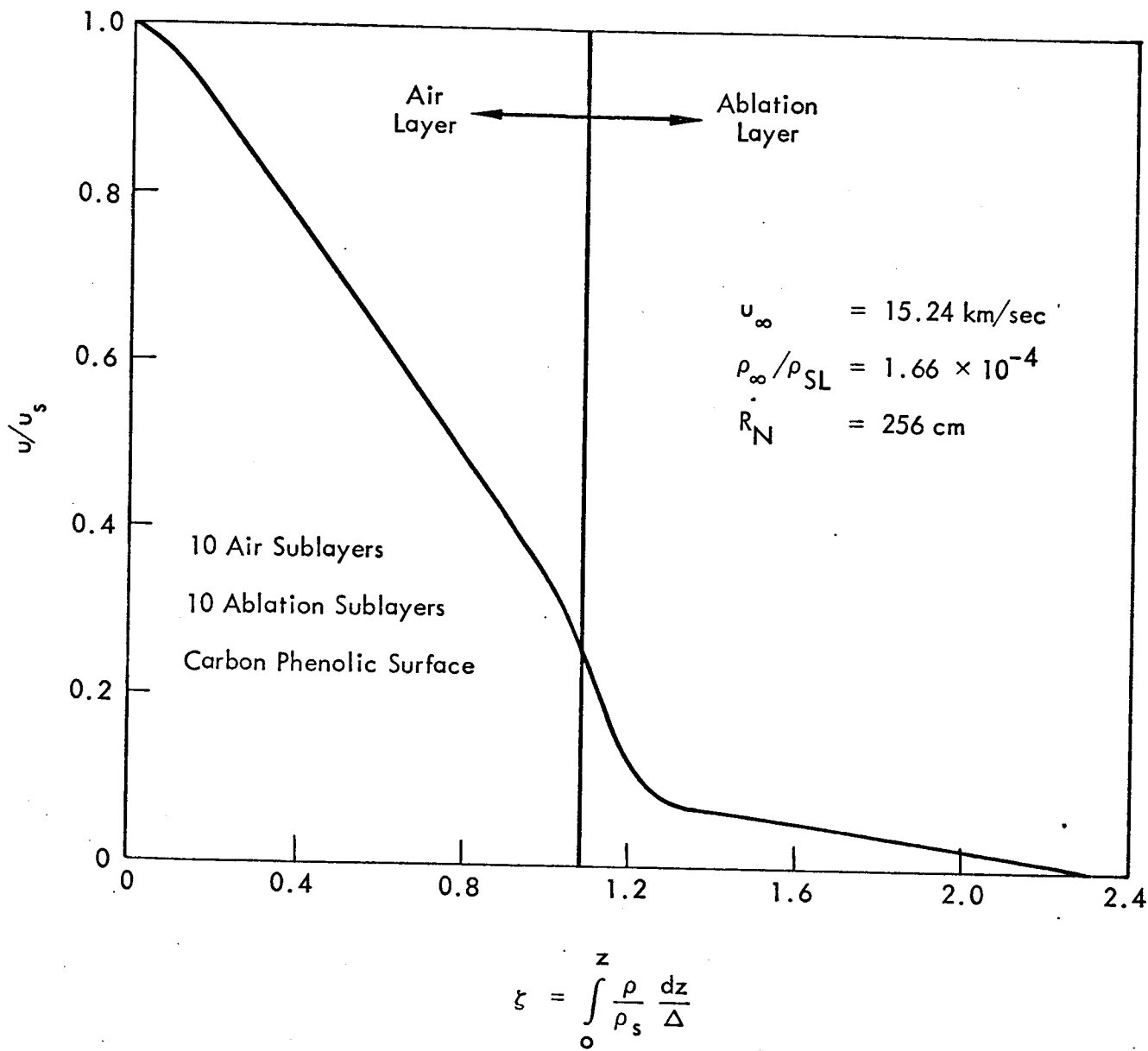


Fig. 10 Tangential Velocity Distribution in Transformed Mass Normal Distance

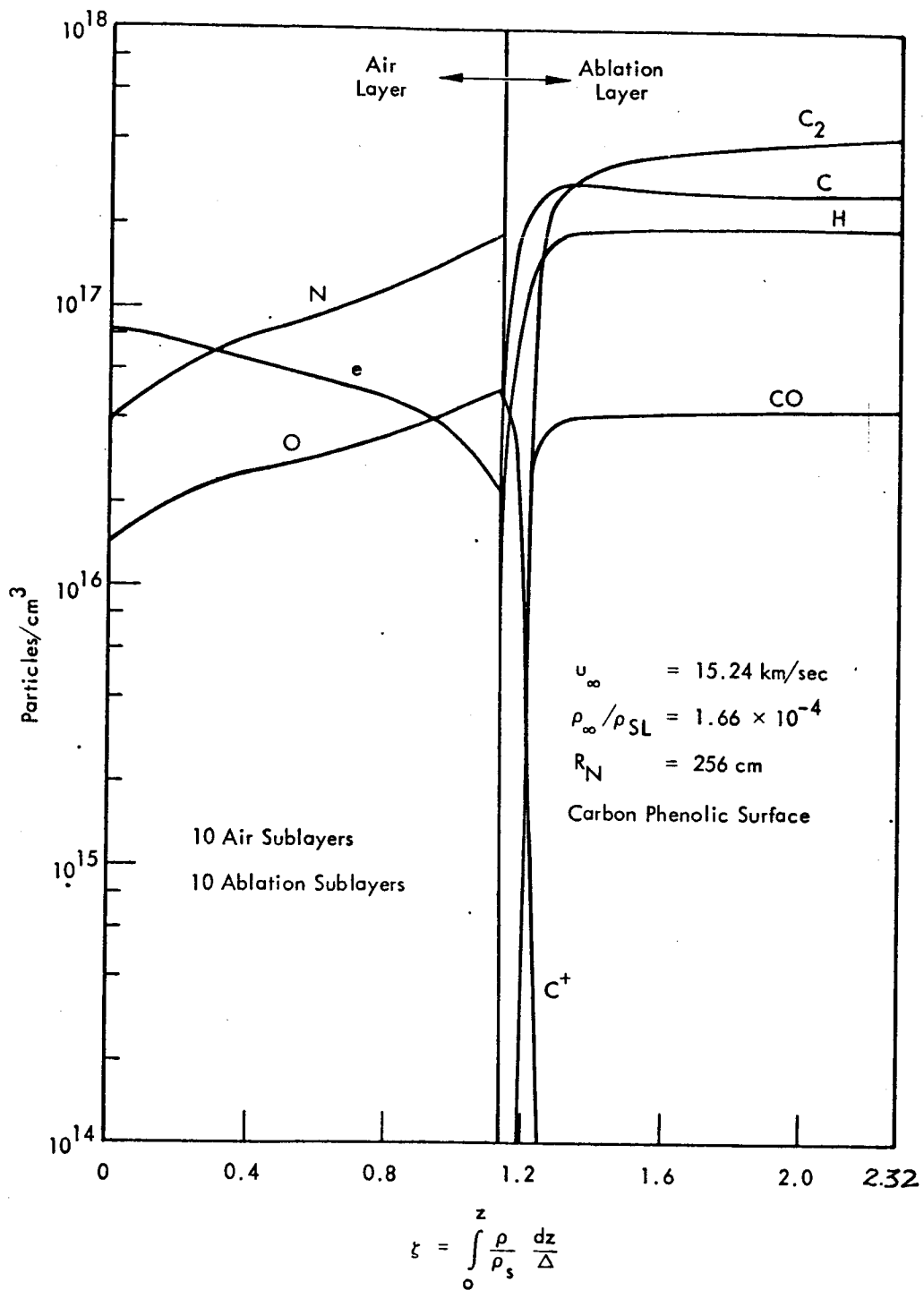


Fig. 11 Particle Density Distributions

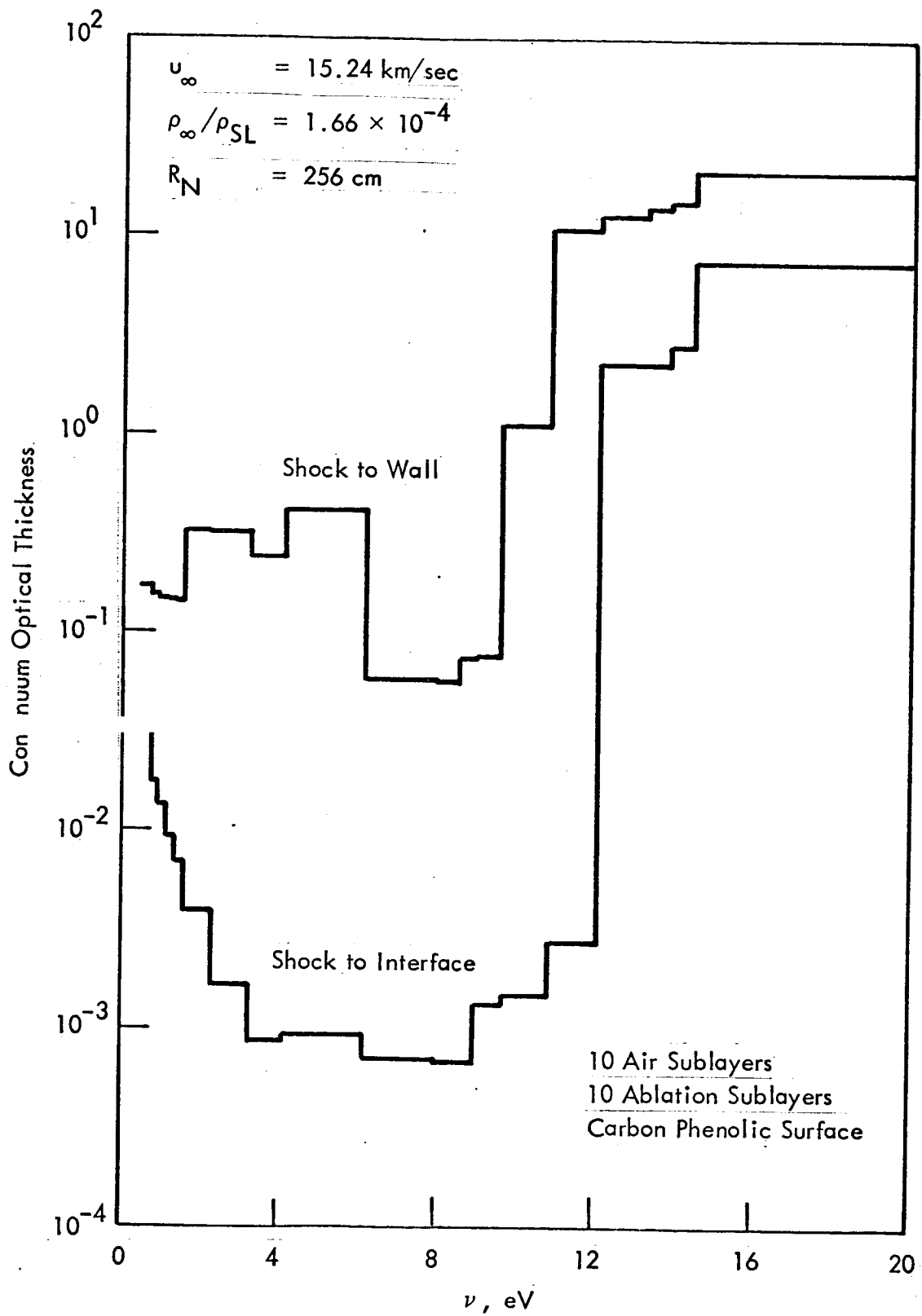


Fig. 12 Continuum Optical Thicknesses

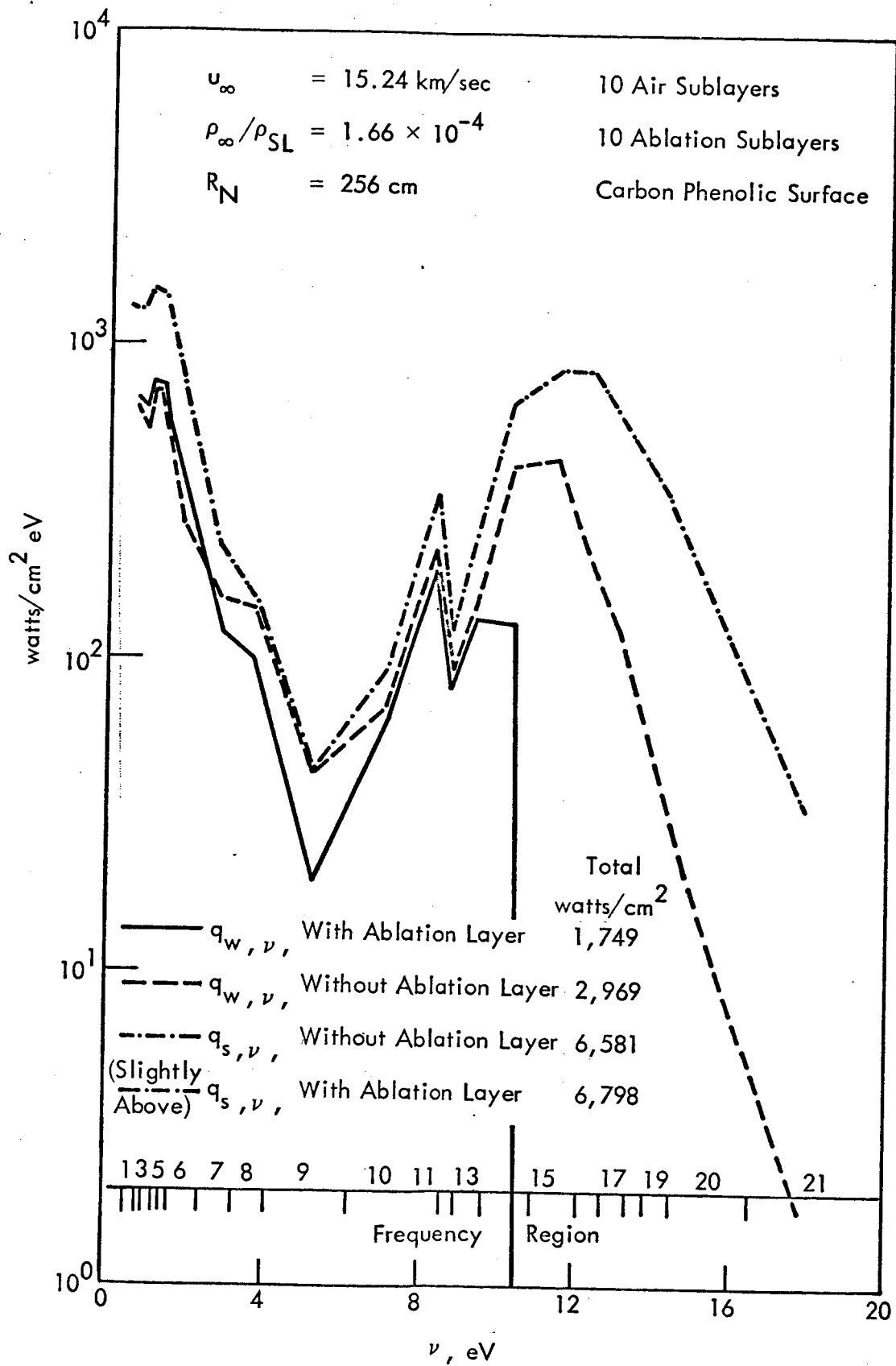


Fig. 13 Spectral Heat Flux to Wall and Shock

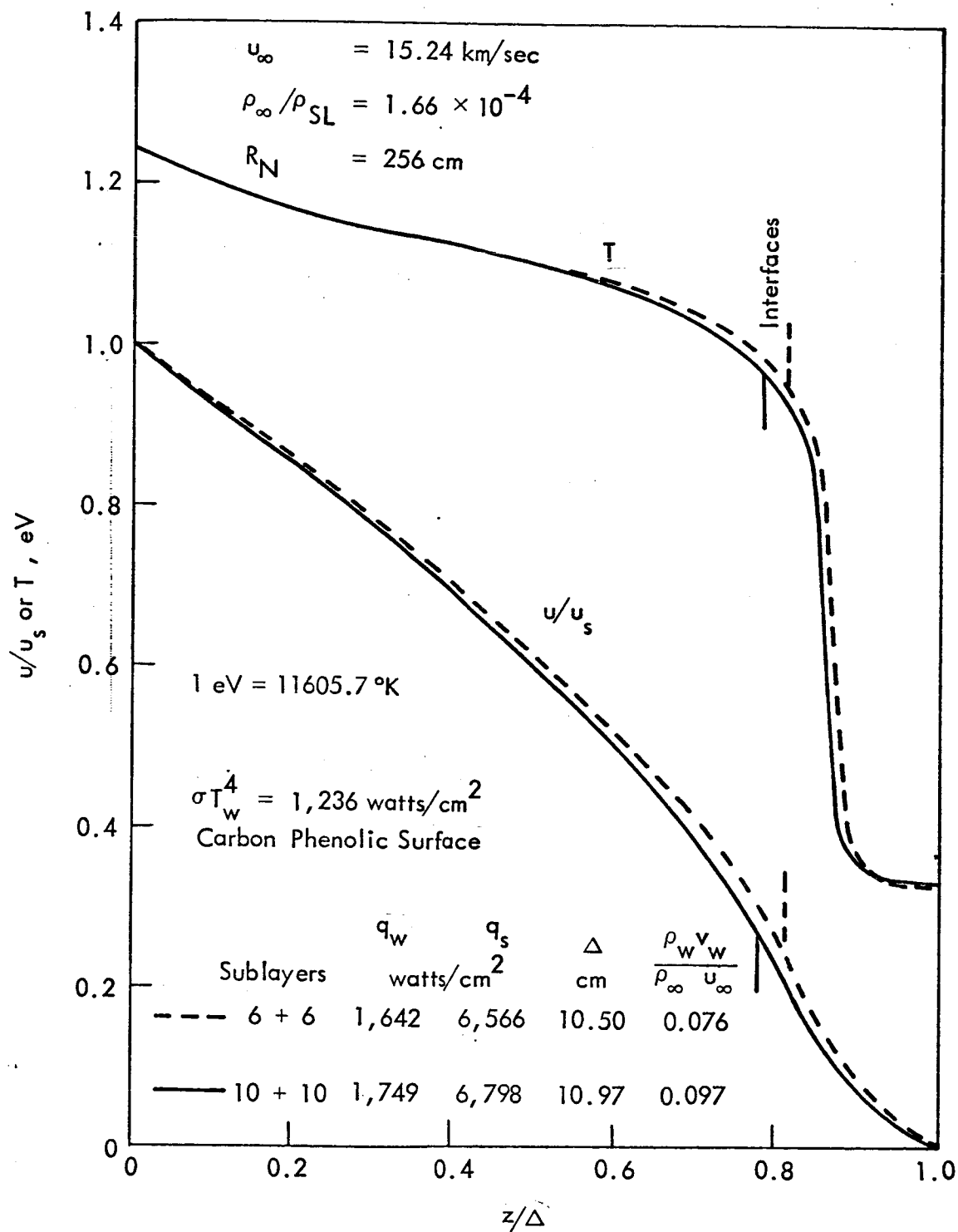


Fig. 14 Effects of Number of Sublayers

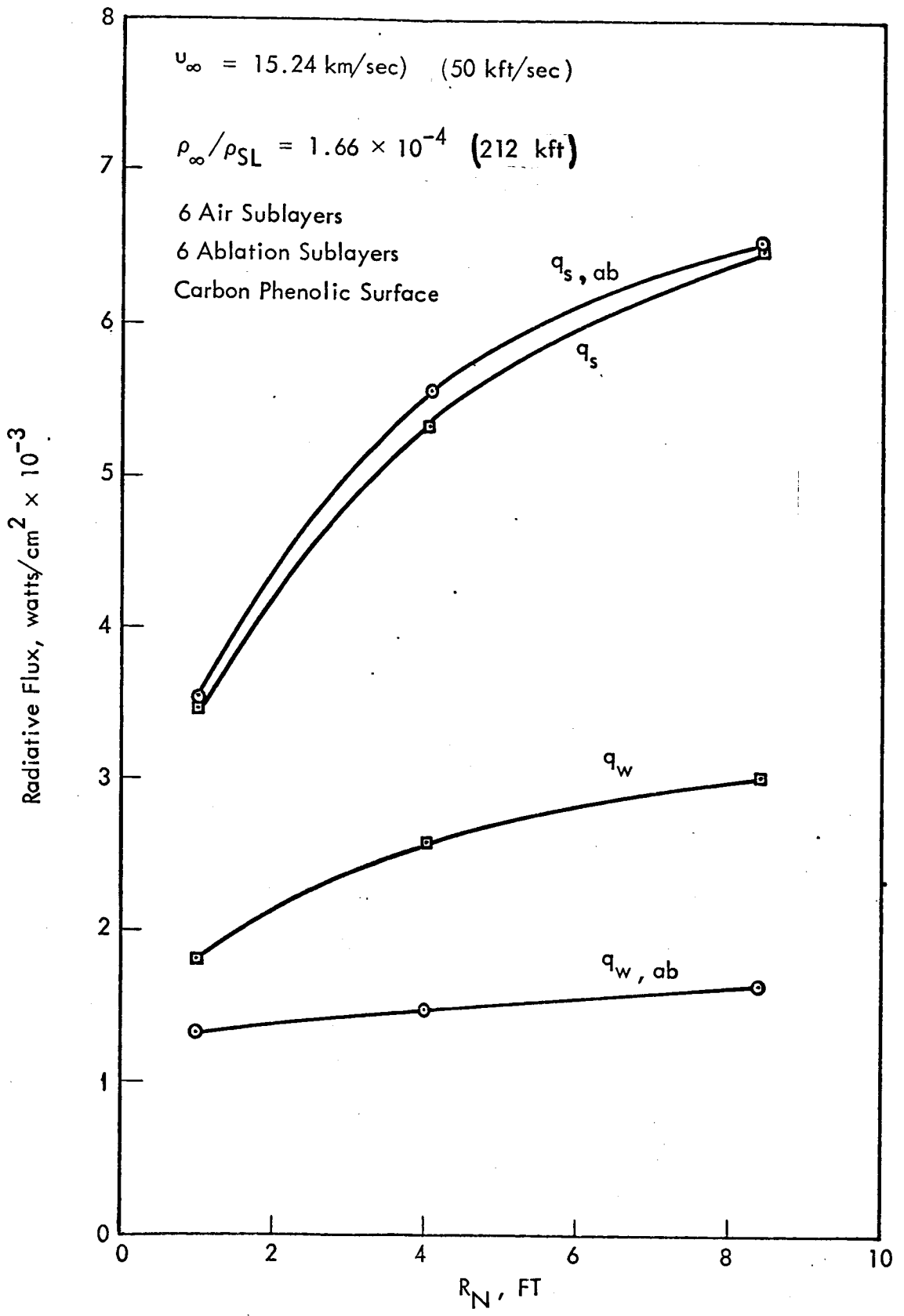


Fig. 15 Effects of Nose Radius, Constant Velocity and Altitude

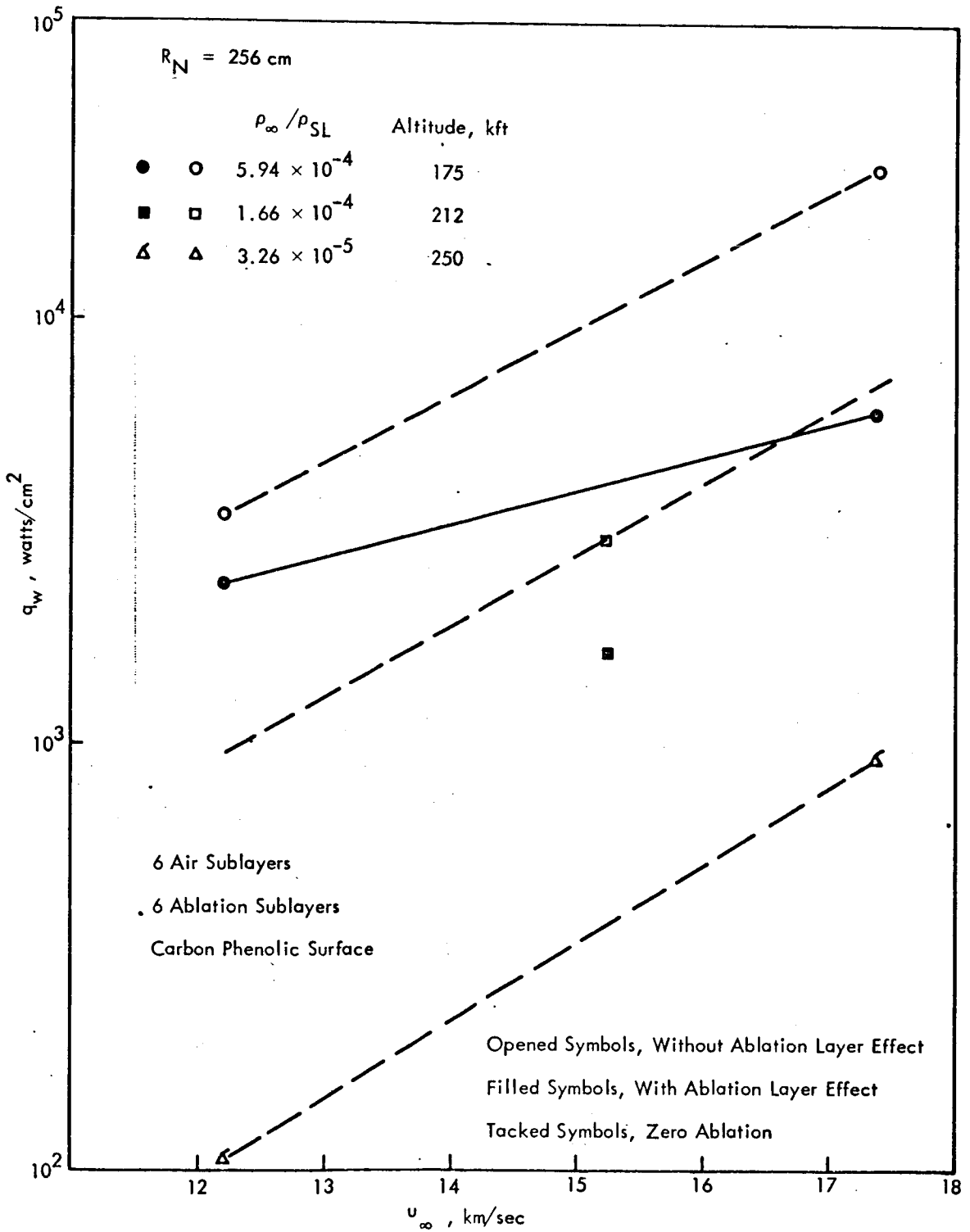


Fig. 16 Effects of Velocity, Constant Nose Radius

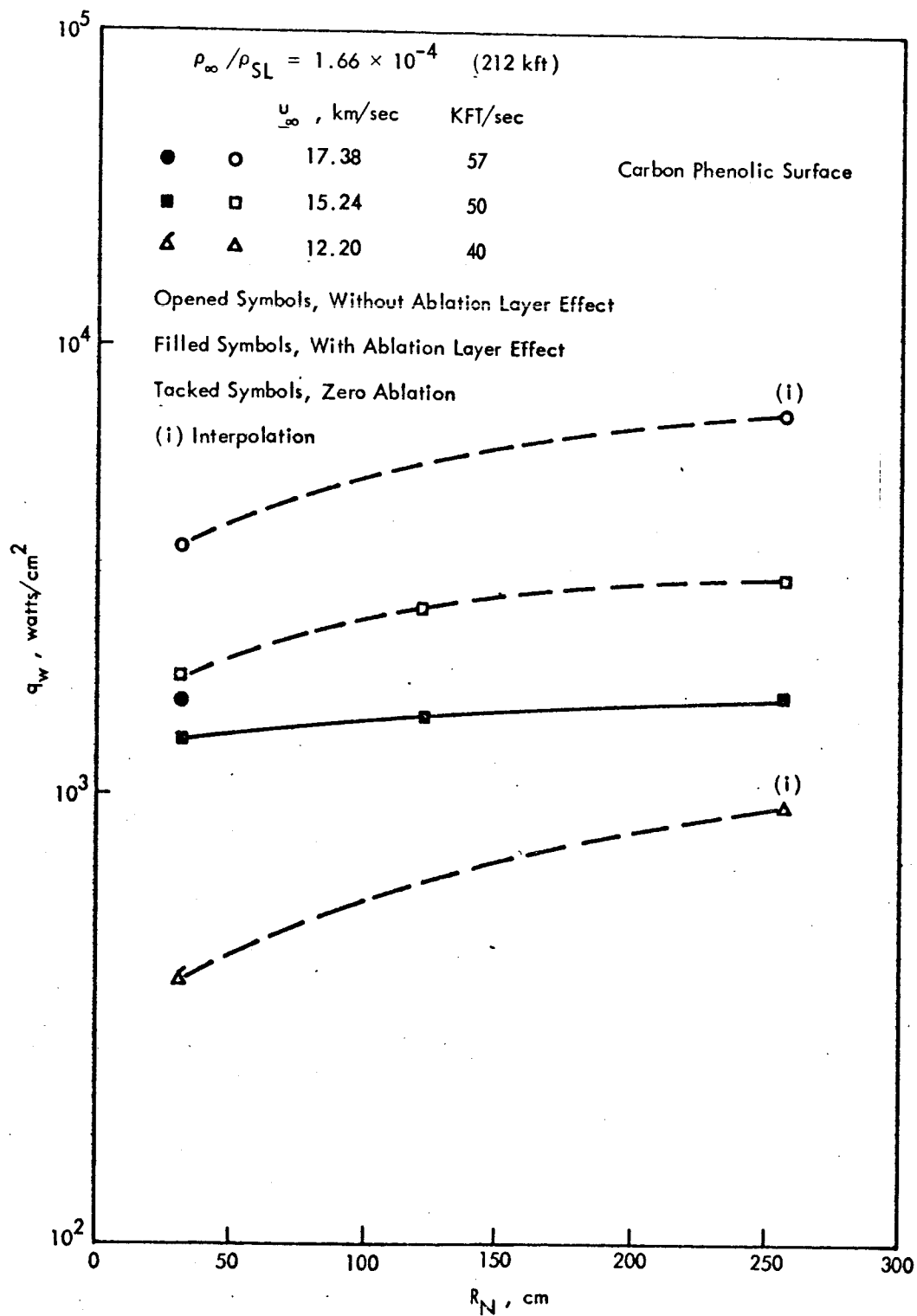


Fig. 17. Effects of Nose Radius, Constant Altitude

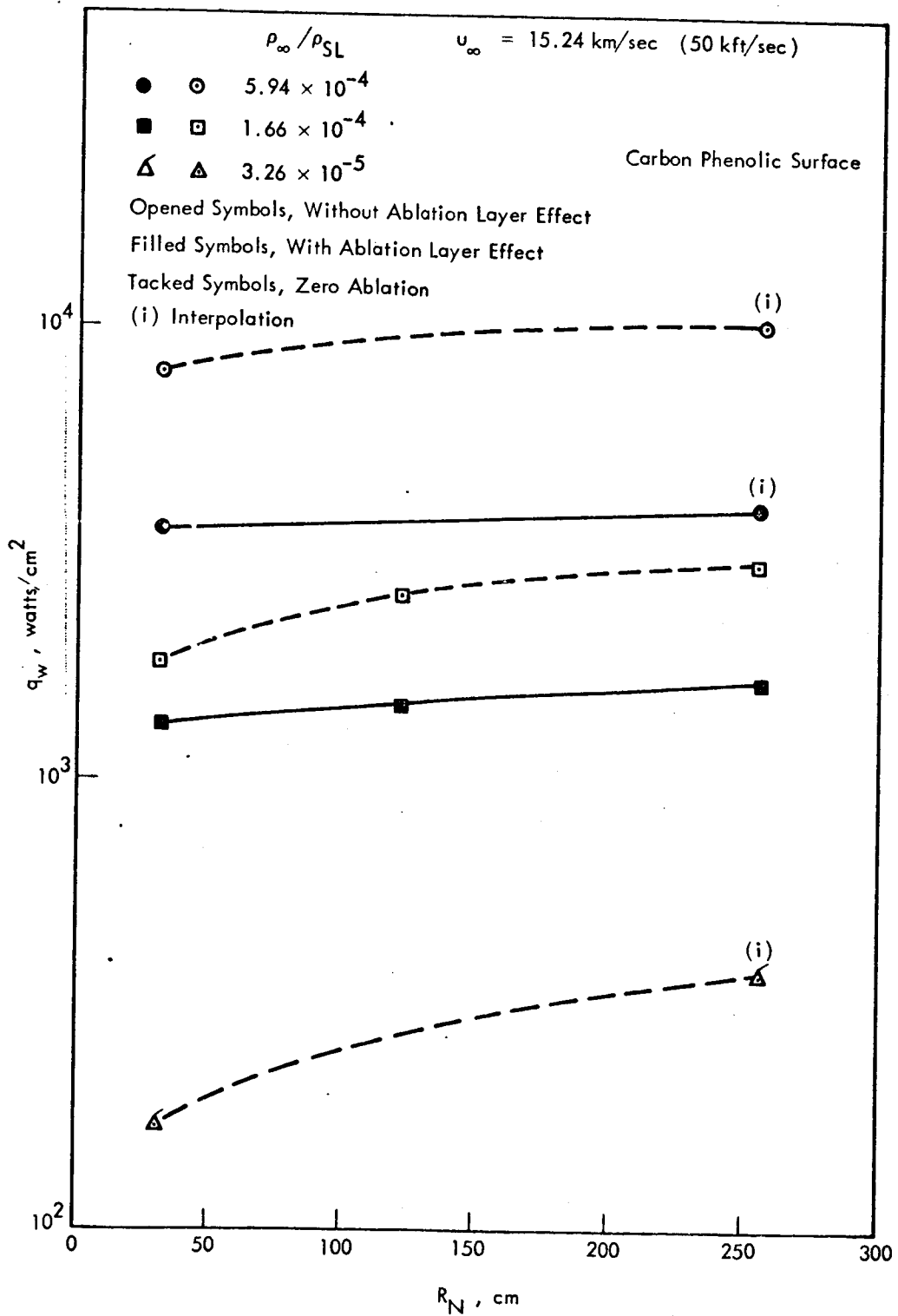


Fig. 18 Effects of Nose Radius, Constant Velocity

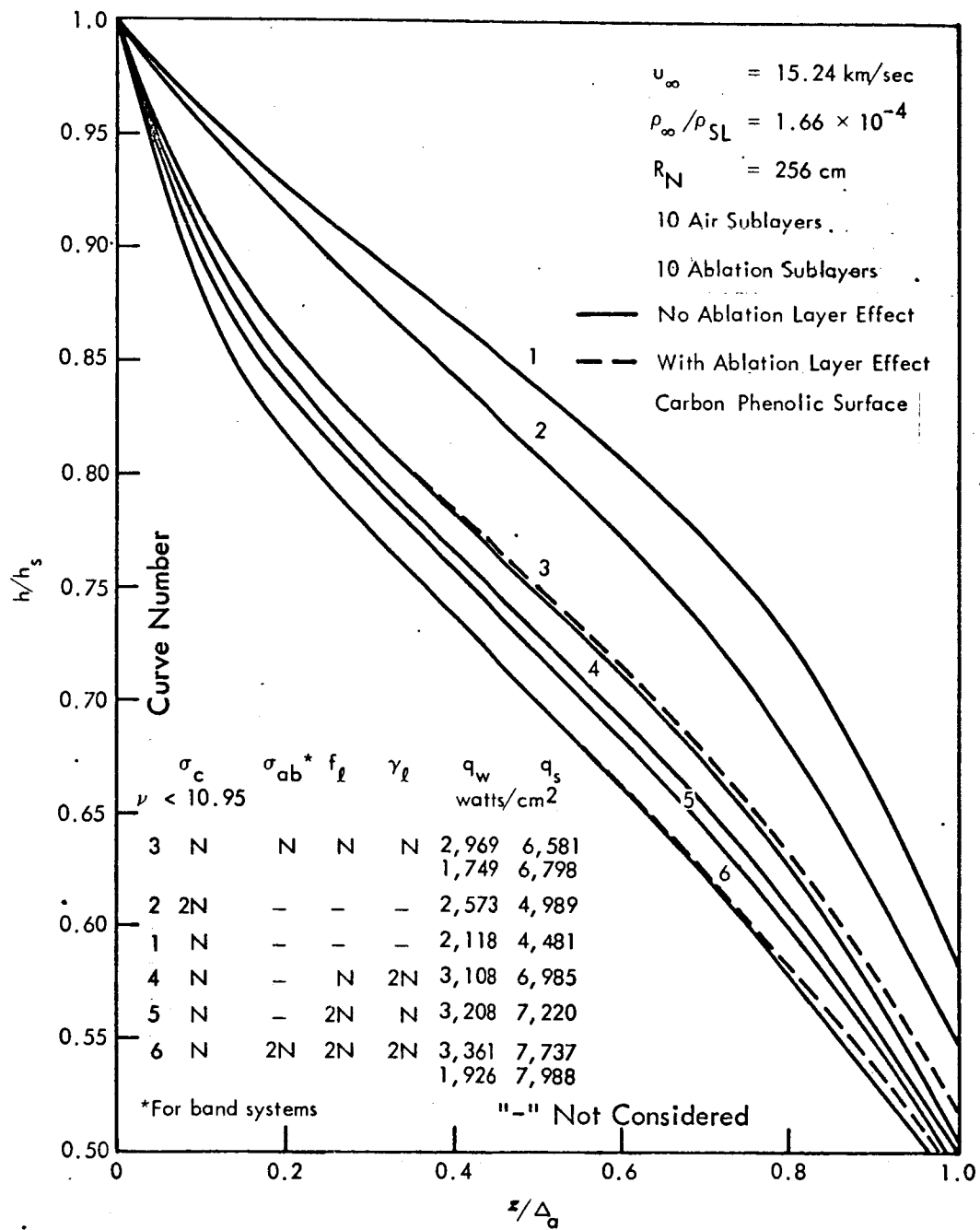


Fig. 19 Effects of Perturbation of Radiative Properties

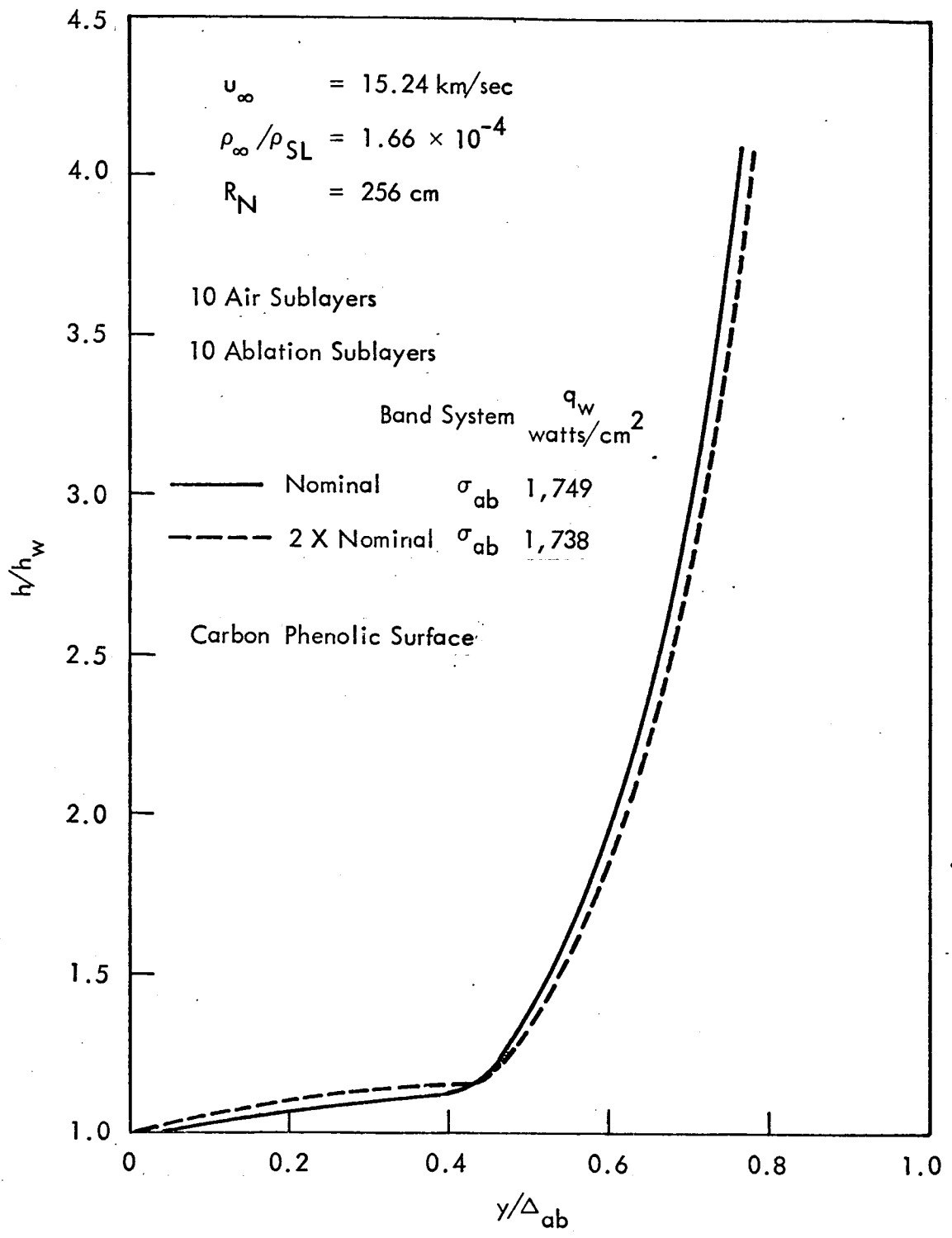


Fig. 20 Effects on Ablation Layer Enthalpy Distribution and Heat Flux to Wall by Perturbing Ablation Molecular Species f-numbers

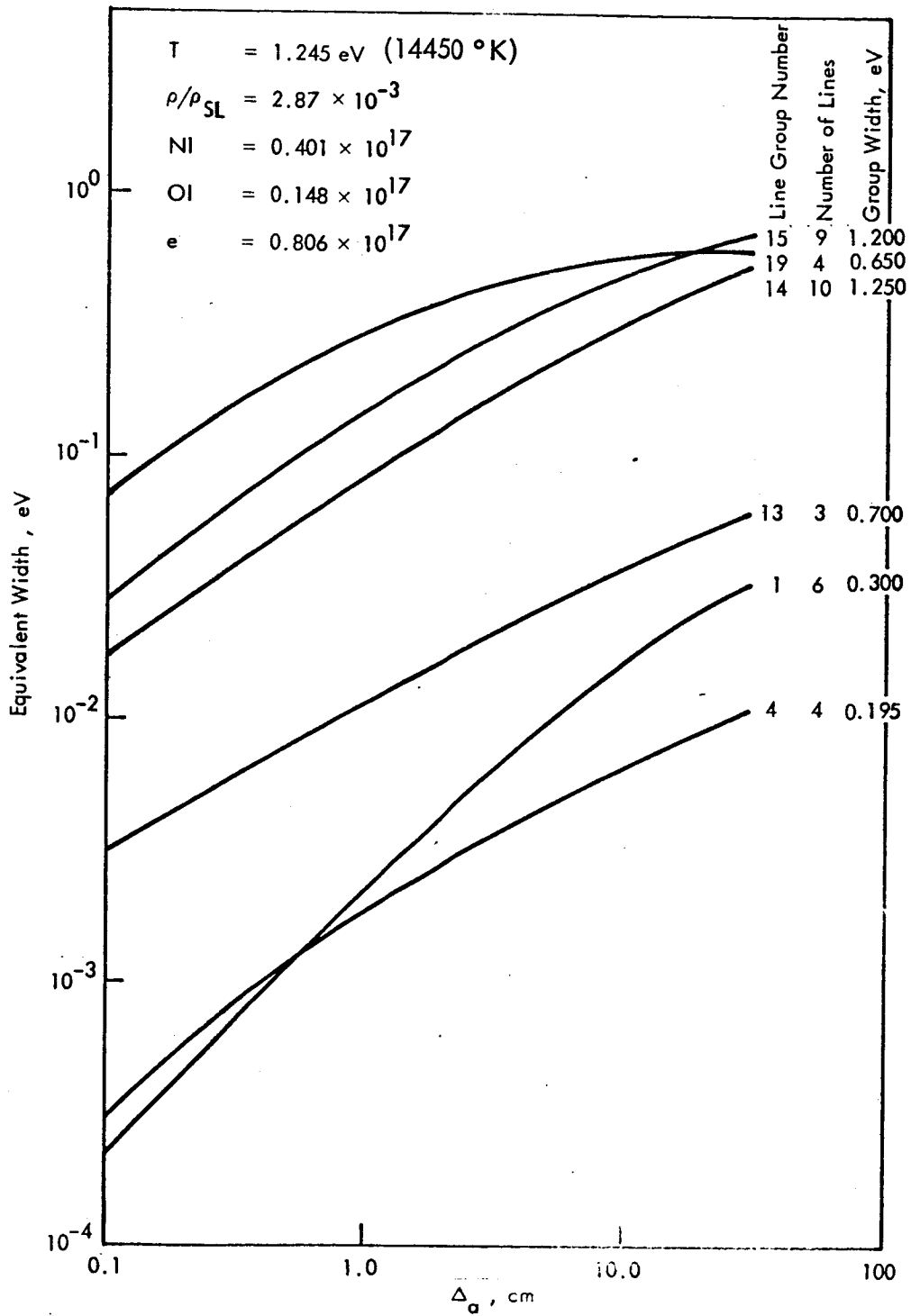


Fig. 21 Equivalent Widths for Isothermal Layers of Different Thickness

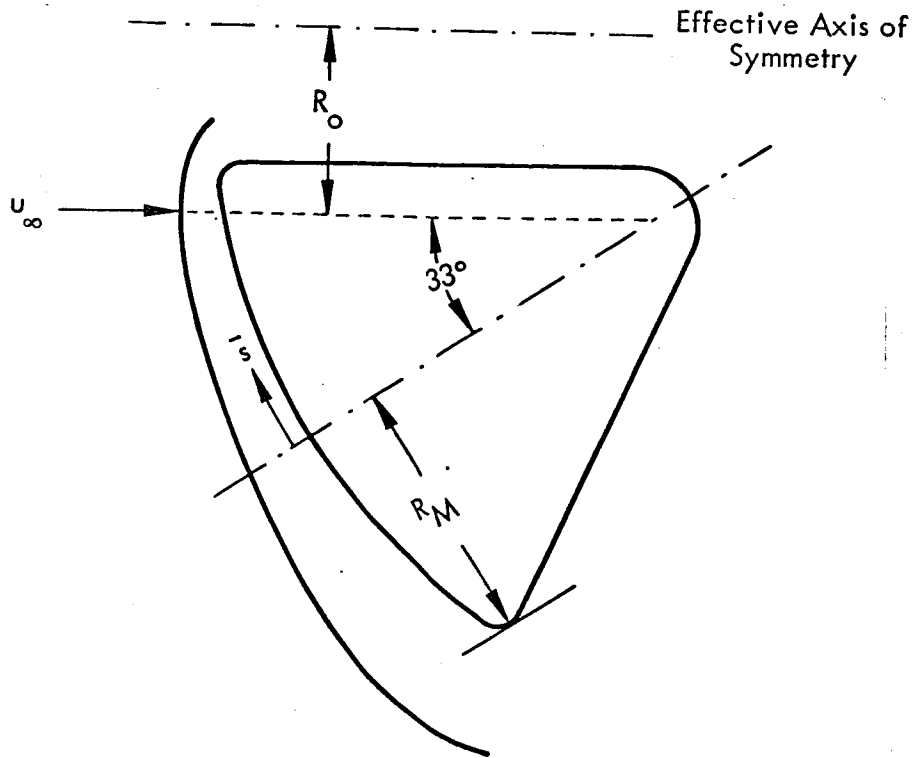


Fig. 22 Blunt Vehicle Configuration for STRADS Calculations

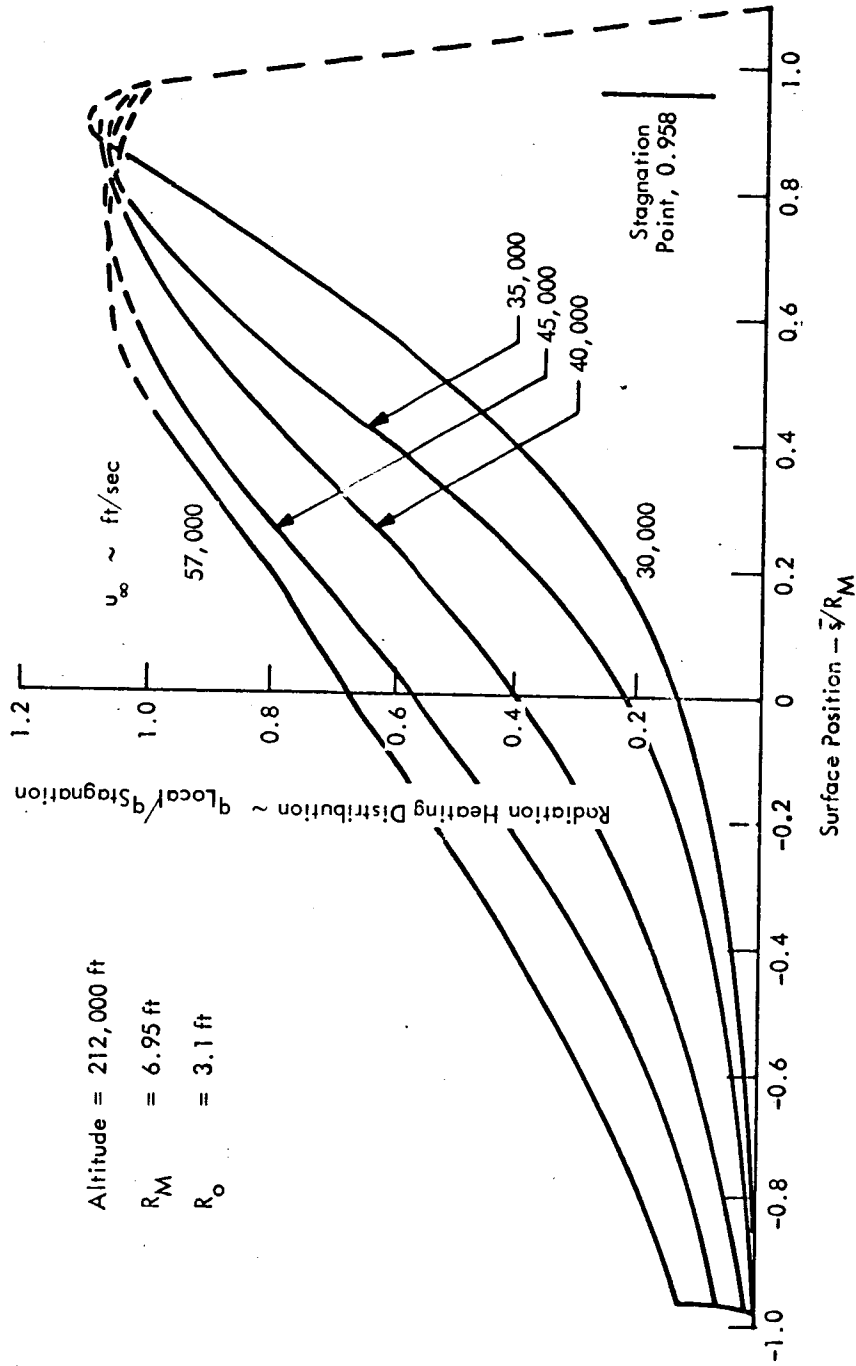


Fig. 23 Effect of Velocity on Radiation Heating Distribution, Blunt Vehicle

C.1 Listing of STAGRADS and Input Data

```

C LISTING OF STAGRADS AND INPUT DATA
C LISTING DATE NOVEMBER, 1967 LMSC, SUNNYVALE, CALIF J H CHIN

      VIT FOR MAIN
      C STAGRADS-AIR WITH LINES AND ABLATION FALL, 1967
        DIMENSION FVA(10),FUA(10),GH(10),GHC(11),GHA(10),GAL(10),GA2(10),
        1GC1(10),GC2(10),Y(11),H(10),SIT(13),VIW(13),
        2VIS(13),Z(10),PART(10),PARTE(10),DYNQ(10),DYNQI(10)
        3,FNU(10),DNU(10),SQW(10),SQWS(10),GEE(8),FF(80)
        4,VIABO(3),TTABO(14),SPTABO(14,3,3)
        DIMENSION TC(14,27)
        DIMENSION PPATOM(3,3)
        DIMENSION FUAB(10)
        COMMON/RNGB/FNUL(10),FNUU(10),QW(10),TAU(11,10),IKT(2,10),QWS(10),
        1QBST,NA,KK
        COMMON/RNGCR/DY(10),T(10),V(10),XN(10,4),TW,N,NPI,I
        COMMON/MCRLN/FHVP(24),FHVM(24),FHVPM(24),FHV(24),ISOE(24),NU(24),N
        1URINT(24),KL1(24),KL2(24),QWCO(24),QWCSO(24),TAUC(21,24)
        2,QGF(80),GAMDA(80),HVL(80),ND(80),EPS(8),LINEOP,NA,QWTS
        3,NLINE,NLST,NHV,NSAB
        COMMON/MABSPC/RTEM(20),IRTEM(20),INTFRE
        COMMON/RGADAS/FCONTN
        COMMON/HINTEG/CNAG,ERR,FRAC
        COMMON/MLINE/NRITES,NRITE4,NRITES,NRITE6
        COMMON/STAGAH/PRTAB(3),TTAB(3,20),ENTAB(3,20),RHOTAB(3,20),C2TAB(3
        1,20),C1TAB(3,20),COTAB(3,20),HTAB(3,20),CPTAB(3,20),EMTAB(3,20)
        COMMON/RSTACR/NT,NTP1,NAB,DYAB(10),TAB(10),NCGAB,IAB
        COMMON/SPABH/COSR(25)
        LOGICAL SWCHA,SWCHAB,SWCHC
        DATA(TC(I,J),J=1,9),I=1,14)/
        1.2,349, 0.500, 0.500, 0.500, 0.500, 0.500, 17.204, 17.412,
        2.34466, 4.996, 3.788, 2.469, 1.980, 1.415, 16.604, 18.212, 18.416,
        3.43082, 9.315, 9.439, 9.566, 9.847, 10.607, 17.501, 18.824, 19.021,
        4.31699, 11.671, 11.552, 11.505, 11.665, 12.426, 18.096, 19.230, 19.425,
        5.80315, 13.311, 13.055, 12.904, 12.990, 13.723, 18.513, 19.522, 19.710,
        6.68932, 14.541, 14.180, 13.962, 13.998, 14.695, 18.820, 19.738, 19.919,
        7.86165, 16.256, 15.756, 15.485, 15.431, 16.047, 19.235, 20.028, 20.198,
        81.0340, 17.394, 16.808, 16.465, 16.398, 16.939, 19.495, 20.209, 20.373,
    
```

EV, LOG+
38, 2-9
2-9
2-9
2-9
2-9
2-9
2-9

```

91.2069,18.200,17.558,17.138,17.091,17.566,19.669,20.330,20.487,
A1.3786,18.796,18.119,17.725,17.603,18.030,19.787,20.405,20.556,
B1.5510,19.245,18.536,18.131,17.991,18.373,19.862,20.445,20.593,
C1.7233,19.589,18.857,18.440,18.281,18.625,19.901,20.454,20.597,
D1.8956,19.829,19.084,18.660,18.489,18.601,19.905,20.431,20.570,
E2.0679,20.067,19.250,18.619,18.634,18.918,19.882,20.383,20.518/
DATA((TC(I,J),J=10,18),I=1,14)/
120.895, 0.500, 0.500, 0.500,20.605, 0.500, 0.500, 0.500, 0.500, 0.500,
220.895, 5.162, 6.549, 8.243,20.604, 4.919, 6.103, 3.780, 6.824,
320.896, 9.560, 9.868,10.803,20.602, 9.361, 9.759, 9.448,10.018,
420.896,11.664,11.794,12.501,20.600,11.621,11.817,11.549,11.955,
520.902,13.244,13.169,13.710,20.595,13.180,13.291,13.033,13.326,
620.907,14.461,14.215,14.618,20.591,14.329,14.397,14.137,14.356,
720.915,16.086,15.691,15.903,20.580,15.894,15.879,15.664,15.786,
820.925,17.181,16.688,16.774,20.568,16.902,16.847,16.666,16.734,
920.931,17.976,17.415,17.409,20.556,17.597,17.531,17.371,17.411,
A20.930,18.556,17.960,17.892,20.541,18.100,18.030,17.886,17.915,
B20.815,19.045,18.401,18.273,20.521,18.470,18.428,18.270,18.312,
C20.882,19.407,18.738,18.568,20.487,18.745,18.725,18.556,18.614,
D20.824,19.688,18.996,18.818,20.439,18.932,18.963,18.755,18.861,
E20.750,19.896,19.189,18.979,20.392,19.061,19.123,18.894,19.025/
DATA((TC(I,J),J=19,27),I=1,14)/
1 0.500, 0.500, 0.500, 0.500, 0.500, 0.500, 0.500, 0.500, 0.500,
2 3.302, 4.577, 3.856, 3.228, 2.466, 5.466, 4.753, 6.181, 7.209,
3 9.314, 9.316, 9.434, 9.459, 9.578, 9.498, 9.584, 9.831, 9.981,
4 11.781, 11.626, 11.575, 11.491, 11.517, 11.645, 11.671, 11.783, 11.821,
5 13.479, 13.248, 13.102, 12.949, 12.916, 13.439, 13.166, 13.181, 13.144,
6 14.752, 14.465, 14.248, 14.048, 13.973, 14.670, 14.386, 14.254, 14.146,
7 16.530, 16.164, 15.855, 15.597, 15.465, 16.357, 15.995, 15.761, 15.589,
8 17.709, 17.292, 16.928, 16.639, 16.467, 17.494, 17.081, 16.781, 16.568,
9 18.544, 18.091, 17.693, 17.386, 17.182, 18.318, 17.868, 17.525, 17.286,
A 19.162, 18.684, 18.261, 17.942, 17.708, 18.913, 18.447, 18.081, 17.826,
B 19.626, 19.129, 18.689, 18.364, 18.103, 19.424, 18.929, 18.533, 18.263,
C 19.984, 19.469, 19.016, 18.685, 18.397, 19.800, 19.290, 18.876, 18.597,
D 20.234, 19.709, 19.247, 18.915, 18.606, 20.090, 19.568, 19.141, 18.854,
E 20.420, 19.885, 19.416, 19.082, 18.752, 20.307, 19.774, 19.338, 19.046/
DATA(VTABO(J),J=1,3)/1.97634,2.97634,3.97634/
DATA(TTABO(I),I=1,14)/.25849,.34466,.43082,.51699,.60515,.68932,.7
17546,.86165,1.0340,1.2063,1.3789,1.5510,1.7233,2.0679/
DATA(((SPTABO(I,J,K),K=1,3),J=1,3),I=1,14)/

```

--LOGP/AT


```

1 4.738, 1.213, 7.370, 4.235, 0.875, 5.947, 3.736, 0.718, 6.618, SPTAB0
2 2.693, 0.725, 5.430, 2.193, 0.688, 5.162, 1.695, 0.680, 4.907, SPTAB0
3 1.478, 0.689, 4.379, 0.998, 0.680, 4.132, 0.561, 0.678, 3.900, SPTAB0
4 0.712, 0.687, 3.684, 0.340, 0.679, 3.432, 0.152, 0.677, 3.080, SPTAB0
5 0.294, 0.680, 3.120, 0.139, 0.678, 2.698, 0.112, 0.679, 2.210, SPTAB0
6 0.148, 0.679, 2.519, 0.115, 0.680, 2.027, 0.120, 0.688, 1.533, SPTAB0
7 0.120, 0.679, 2.066, 0.126, 0.684, 1.518, 0.194, 0.717, 0.980, SPTAB0
8 0.120, 0.689, 1.600, 0.137, 0.708, 1.081, 0.306, 0.770, 0.561, SPTAB0
9 0.166, 0.714, 0.930, 0.290, 0.798, 3.489, 0.649, 1.075, 0.161, SPTAB0
A 0.312, 0.819, 0.444, 0.611, 1.018, 3.174, 1.162, 1.585, 0.051, SPTAB0
B 0.523, 0.984, 0.230, 1.061, 1.377, 3.061, 1.825, 2.222, 0.010, SPTAB0
C 0.778, 1.187, 0.118, 1.588, 1.830, 3.016, 2.563, 2.914, 0.000, SPTAB0
D 1.066, 1.444, 0.056, 1.988, 2.293, 3.005, 3.000, 3.525, 0.000, SPTAB0
E 1.699, 2.114, 0.008, 2.684, 3.072, 4.034, 3.786, 4.050, -0.146/ SPTAB0

```

C INPUT LINE AND LINE-GROUP DATA

```

READ(5,9101),NHV,NLST
IF(NHV.LE.0)GO TO 8
READ(5,9100) (GEE(I),I=1,NLST)
READ(5,9100) (EPS(I),I=1,NLST)
READ(5,9100) (FHVM(I),I=1,NHV)
READ(5,9100) (FHVP(I),I=1,NHV)
READ(5,9100) (FHV(I),I=1,NHV)
READ(5,9101) (ISOE(I),I=1,NHV)
READ(5,9101) (NUMINT(I),I=1,NHV)
READ(5,9101) ( NU(I),I=1,NHV)

```

```

9100 FORMAT(6E12.1)
9101 FORMAT(36I2)

```

```

NLIN = 0
KL2(1)=NU(1)
KL1(1)=1
IF(NU(1).EQ.0)KL1(1)=0
DO 9504 I=1,NHV
  FHVP(I)=FHVP(I)-FHVM(I)
  IF(I.EQ.1)GO TO 9504
  KL1(I)=KL2(I-1)+1
  IF(NU(I).EQ.0)KL1(I)=KL2(I-1)
  KL2(I)=KL2(I-1)+NU(I)

```

```

9504 NLIN =NLIN +NU(I)
      NLINE=NLIN
      READ(5,9102) (ND(I),HVL(I),FF(I),GAMBA(I),I=1,NLINE)

```

```

9102 FORMAT(11,11X,3E12.1)
DO 9508 I=1,NLINE
ID=ND(I)
9508 BGF(I)=1.11276E4*GEE(ID)*FF(I)
C OUTPUT LINE AND LINE-GROUP DATA
IC1=0
9121 FORMAT(6H1GROUP,6X,2HHV,12X,3HHV+,11X,3HHV-,10X,1HN,8X,4HLINE,5X,
14HNLST,7X,5HHV(I),7X,4HF(I),7X,6HGAM( ),6X,6HDFG(I))
9122 FORMAT(14,F12.3,2F14.3,112,111,18,2X,f 12.3,1P3E12.2)
9124 FORMAT(56X,111,18,2X,F12.3,1P3E12.2)
WRITE(6,9121)
DO 9530 I=1,NHV
IC2=IC1+NU(I)
IC1=IC1+1
IF(NU(I).EQ.0)WRITE(6,9122)I,FHV(I),FFVP(I),FHVM(I),NU(I)
IF(NU(I).EQ.0) GO TO 9530
WRITE(6,9122) I,FHV(I),FHVP(I),FHVM(I),NU(I),IC1,ND(IC1),HVL(IC1),
1FF(IC1),GAMBA(IC1),BGF(IC1)
IF(IC1.EQ.IC2) GO TO 9530
IC3=IC1+1
DO 9525 J=IC3,IC2
9525 WRITE(6,9124) J,ND(J),HVL(J),FF(J),GAMBA(J),BGF(J)
9530 IC1=IC2
9186 FORMAT(1H0,8X,5HGROUP,7X,4HISOE,7X,6HUMINT,/)
9188 FORMAT(10I12)
WRITE(6,9186)
DO 9535 I=1,NHV
9535 WRITE(6,9188)I,ISOE(I),NUMINT(I)
WRITE(6,9192)(GEE(I),I=1,NLST)
WRITE(6,9194)(EPS(I),I=1,NLST)
9192 FORMAT(9H GEE(I) =,10E12.5)
9194 FORMAT(9H EPS(I) =,10E12.5)
1 FORMAT(6E12.8)
2 FORMAT(12,5E12.6)
3 FORMAT(1H 7E18.5)
4 FORMAT(1H 15,7E18.5)
5 FORMAT(1H 2E20.5)
7 FORMAT(1H )
9000 FORMAT(1H0/,30H
9001 FORMAT(30H FREE STREAM PRESSURE =,E15.5)
CASE =,E15.8)

```



```

WRITE(6,7)
DO 75 I=1,14
75 WRITE(6,9020)I,TC(I,1),(TC(I,J),J=19,27)
WRITE(6,7)
DO 78 I=1,14
DO 77 J=1,3
DO 77 K=1,3
77 PPATOM(J,K)=10.0*(-SPTAB0(I,J,K))
TAB0=TTAB0(I)*11605.7
78 WRITE(6,9020)I,TAB0,((PPATOM(J,K),K=1,3),J=1,3)
8 READ(5,2) NC
IF(NC)99,99,9
9 GO TO(10,80,7010,7020),NC
10 READ(5,2)L,CASE,PA,RHOA,UA,RN
READ(5,2)NS,ES,HA,TW
READ(5,2)MODEL
READ(5,2)LINEOP
READ(5,1)FCONTN,FDHAB
READ(5,9101)NRITE1,NRITE2,NRITE3,NRITE4,NRITE5,NRITE6,NRITE7
READ(5,1)CMAG,ERR,FRAC
READ(5,2)NSAB
IF(TW.LT.0.02)TW=0.02
LINEO=LINEOP
IF(NRITE1.GT.0)NRITE7=1
WRITE(6,9000)CASE
WRITE(6,9003)UA
WRITE(6,9001)PA
WRITE(6,9002)RHOA
WRITE(6,9005)HA
WRITE(6,9004)RN
WRITE(6,9006)ES
WRITE(6,9037)MODEL
WRITE(6,9059)FCONTN
IF(NSAB.GT.0)WRITE(6,7913)FDHAB
7913 FORMAT(30H FDHAB =,E15.5)
WRITE(6,7901)L,NS,NSAB
7901 FORMAT(1H0,5H L =,I6,6H NS =,I6,8H NSAB =,I6)
WRITE(6,9131)LINEO
IF(MODEL.LE.0)CALL EXIT
IF(NHV.LE.0.AND.LINEOP.GT.1)CALL EXIT

```

TEM
TEMTEM
TEM
TEM

TM

TEM
TEM

```

9190 WRITE(6,9190)CMAG,ERR,FRAC
9190 FORMAT(26H ABS(AV INTEGRAND)*1.E-4 =,E12.5,6H ERR =,E12.5,
124H FIRST NORMALIZED STEP =,E12.5)
IF(NS.GT.20.OR.NSAB.GT.10)CALL EXIT
IF(NS.GT.10)CALL EXIT
GO TO 8
C WIDTH CALCULATION ONLY WITH INPUT T,V,DELTA,N
80 READ(5,2)N,DELTA
READ(5,1)(T(I),I=1,N)
READ(5,1)(V(I),I=1,N)
READ(5,1)CMAG,ERR,FRAC
READ(5,9101)NRITE1,NRITE2,NRITE3,NRITE4,NRITE5,NRITE6
DYY=DELTA/FLOAT(N)
NPI=N+1
LINEOP=2
WRITE(6,9126)N,DELTA,DYY
9126 FORMAT(/5H N =,I8,10X,8H DELTA =,E16.5,4H CM,10X,5H DYY=,E16.5,4
1H CM)
WRITE(6,9128) (T(I),I=1,N)
WRITE(6,9129) (V(I),I=1,N)
9129 FORMAT(/12H RHOSL/RHO =,10E12.4)
9128 FORMAT(/12H TEMP(EV) =,10E12.4)
WRITE(6,9021)
DO 81 I=1,N
CALL DOUBL(ALOG10(V(I)),VTAB0,T(I),TTAB0,XN,SPTAB0,I,3,14,3)
PARTE(I)=10.0**(-XN(I,3))*5.07E+19/V(I)
PART(1)=10.0**(-XN(I,1))/V(I)*5.07E+19
PART(2)=10.0**(-XN(I,2))/V(I)*5.07E+19
PART(3)=PARTE(I)
WRITE(6,9020)I,(PART(J),J=1,3)
DYNQ(I)=(PART(1)+PART(2))*DYY/(5.07E+19*(4.+10.*EXP(-2.384/T(I))
1+6.*EXP(-3.576/T(I))))
81 CONTINUE
WRITE(6,7)
WRITE(6,9190)CMAG,ERR,FRAC
DO 85 KI=1,NHV
NELMC=0
KNU=NU(KI)+1
DO 82 J=1,N
IF(NU(KI).GT.0)DYNQI(J)=DYNQ(J)*(1.-EXP(-FHV(KI)/T(J)))

```

```

82 CONTINUE
DO 84 J=1,N
  JPI=J+1
DO 83 JJ=1,J
  CALL LINE(JPI,JJ,KI,LINEOP,WIDTH,NELMC,KL1(KI),KL2(KI),
  IFHVM(KI),FHVP(KI),FHVPM(KI),ISOE(KI),N,NP1,PARTE,DYNGI,GAMBA,ND,EP
  2S,BGF,NU(KI),HVL,T,NUNINT(KI))
83 CONTINUE
84 CONTINUE
85 CONTINUE
GO TO 8
7010 READ(5,2)IP
      READ(5,2)IT
7500 FORMAT(9E8.4)
      DO 7506 I=1,IP
        READ(5,7500)PRTAB(I)
        WRITE(6,7501)PRTAB(I)
7501 FORMAT(//1H,E15.6//)
      DO 7505 J=1,IT
        READ(5,7500)TTAB(I,J),ENTAB(I,J),RHOTAB(I,J),C2TAB(I,J),C1TAB(I,J)
        1,COTAB(I,J),HTAB(I,J),CPTAB(I,J),ENTAB(I,J)
        WRITE(6,7502)TTAB(I,J),ENTAB(I,J),RHOTAB(I,J),C2TAB(I,J),C1TAB(I,J)
        1,COTAB(I,J),HTAB(I,J),CPTAB(I,J),ENTAB(I,J)
7502 FORMAT(1H,9E12.6)
        TTAB(I,J)=TTAB(I,J)/11605.7
        ENTAB(I,J)=1.441E-4*ENTAB(I,J)
        RHOTAB(I,J)=ALOG10(1.23E-3/RHOTAB(I,J))
        C2TAB(I,J)=ALOG10(C2TAB(I,J))
        C1TAB(I,J)=ALOG10(C1TAB(I,J))
        COTAB(I,J)=ALOG10(COTAB(I,J))
        HTAB(I,J)=ALOG10(HTAB(I,J))
        CPTAB(I,J)=ALOG10(CPTAB(I,J))
        ENTAB(I,J)=ALOG10(ENTAB(I,J))
7505 CONTINUE
7506 CONTINUE
GO TO 8
7020 READ(5,2)ICOSR
      READ(5,7500)(COSR(I),I=1,ICOSR)
      WRITE(6,7)
      WRITE(6,3)(COSR(I),I=1,ICOSR)

```

```

GO TO 8
99 C22=12.1555
   IF(LINEOP.LE.0.OR.LINEOP.GT.3)CALL EXIT
   SWCHA=.FALSE.
   SWCHAB=.FALSE.
   SWCHC=.FALSE.
   C44=0.0172
   C55=0.0578
   L1=L+1
   CLI=L1
   ES1=1.0-ES
   ES2=ES**2
   ES21=1.0-ES2
   UA2=UA**2
   DYP1=C22*RHQA*UA2
   AMS=NS
   DYP=DYP1*ES1
   STP=DYP+PA
   ENT=C44*ES21*UA2
   AE=2.0*ES*ES1
   ESRN=ES*RN
   DYER=0.70/ANS
   DYER1=DYER*CLI
   DYER2=DYER1*0.35
   DYY=DYER*ESRN
   DYY2=DYY*0.35
   HO=ENT+HA
   PO=STP
   IF(NSAB.LE.0)GO TO 98
   IF(NSAB.GT.0)LINEOP=3
   IF(NSAB.GT.0)CALL SESB(PO,HW,VW,TW)
   CALL PROT(HW,ENTAB,D,RHOTAB,PO,PRTAB,TW,TTAB,D,C2TAB,D,C1TAB,D,
1COTAB,D,HTAB,D,CPTAB,3,20)
98 WRITE(6,9026)TW
   NAB=0
   NO1=-1
   INTFRE=0
   MODELL=MODEL
   IF(MODELL.GT.8)CALL EXIT
   CALL PROPT(PO,HO,VO,TO,ZO,NO1)

```

TEM

MP100

MP102
MP103
MP105

MP108
MP109
MP110

```

Z(1)=ZO
VO=VO/PO
CALL DOUBL(ALOG10(VO),VTABO,TO,TTABO,XN,SPTABO,1,3,14,3)
SIG=C55/(RHOA*UA*HO)
DELH=0.01
DELTA=0.0
Y(1)=0.
YER=0.0
NA=1
NAA=1
NCOUNT=0
NCNTR1=0
NCNTR2=0
NCNTR3=0
NCGAB=0
NGMT=0
CALL MODL1(FNUL,FNUU,IKT,KK)
CALL ABSORP(TO,VO,XN,IKT,SPMUO,1,1)
IF(LINEO.EQ.3)GO TO 830
810 GO TO (811,812,813,814,815,816,817,818),MODELL
811 CALL MODL1(FNUL,FNUU,IKT,KK)
GO TO 830
812 CALL MODL2(FNUL,FNUU,IKT,KK)
GO TO 830
813 CALL MODL3(FNUL,FNUU,IKT,KK)
GO TO 830
814 CALL MODL4(FNUL,FNUU,IKT,KK)
GO TO 830
815 CALL MODL5(FNUL,FNUU,IKT,KK)
GO TO 830
816 CALL MODL6(FNUL,FNUU,IKT,KK)
GO TO 830
817 CALL MODL7(FNUL,FNUU,IKT,KK)
GO TO 830
818 CALL MODL8(FNUL,FNUU,IKT,KK)
890 ND=0
201 J=1
GAMAO=2.0*SIG*TO**4*SPMUC*ESRN
GAMA5=5.0*GAMAO
GHW=(1.0+38.8*GAMA5)**(-0.25)

```

MP206


```

GH(1)=1.0
GHC(1)=1.0
SIT(1)=0.0
VIS(1)=1.0
202 DO 205 I=2,NS
YER=YER+DYER/GH(I-1)
SIT(I)=SIT(I-1)+DYY
IF(YER-0.99)204,203,203
203 GH(I)=GHW
GO TO 205
204 GH(I)=(1.0+GAMA5*((1.0-YER)**(-0.8)-1.0))**(-0.25)
205 VIS(I)=GH(I)
206 DO 209 I=1,NS
IF(I.EQ.NS)GO TO 209
207 GH(I)=(GH(I)+GH(I+1))/2.0
209 CONTINUE
SIT(NS+1)=2.0*SIT(NS)
VIS(NS+1)=VIS(NS)
IF(LINEC.EQ.3)GO TO 104
100 WRITE (6,9011)
WRITE (6,9012)
DO 101 J=1,KK
AC=1.0
FNU(J)=(FNUU(J)+FNUL(J))/2.0
DNU(J)=FNUU(J)-FNUL(J)
FNUC=FNU(J)*8067.0
FNULC=FNUL(J)*8067.0
FNUUC=FNUU(J)*8067.0
FNUM=1.2395/FNU(J)
FNULM=1.2395/FNUL(J)
FNUMM=1.2395/FNUU(J)
WRITE(6,9020)J,AB ,FNU(J),FNUL(J),FNUU(J),FNUC,FNULC,FNUM,
1FNULM,FNUMM
101 CONTINUE
104 WRITE(6,9131)LINEO
220 N=NS
CALL VEL(1,SIT,VIS,-1.0,DYY2,AE,CL1,N,ANS,DUM,DUM,DY,FVA,FUA,
1DYER2)
221 DO 227 I=1,N
Y(I+1)=Y(I)+DY(I)

```

```

227 CONTINUE
DELTA=Y(N+1)
NPI=N+1
NT=N+RAB
IF(NT.GT.20)CALL EXIT
NTP1=NT+1
301 DO 302 I=1,N
H(I)=GH(I)*HO
CALL PROPT(PO,H(I),V(I),T(I),Z(I),NO1)
V(I)=V(I)/PO
CALL DOUBL(ALOG10(V(I)),VTABO,T(I),TTABO,XN,SPTABO,I,3,14,3)
CONTINUE
302 DO 307 I=1,N
IF(NA.GT.1.AND.I.EQ.1)NA=2
IF(NA.GT.1.AND.I.GT.1)NA=3
IF(NAA.GT.1.AND.I.EQ.1)NAA=2
IF(NAA.GT.1.AND.I.GT.1)NAA=3
GO TO (910,910,911),LINEO
910 CALL NGGDS(CQ)
IF(LINEO.EQ.1)GO TO 912
CALL CRLINE(CQL)
CQ=CQ-CQL
GO TO 912
911 CALL CRLINE(CQ)
912 DOH=SIG*CQ/FVA(I)
GHC(I+1)=GHC(I)+DGH
GHA(I)=(GHC(I)+GHC(I+1))/2.0
IF(ABS(GHA(I)-GH(I))/GH(I)-DELH)205,305,304
304 NB=1
IF(GHA(I).GT.1.2)GHA(I)=1.2
IF(GHA(I)*HO.LT.0.3)GHA(I)=0.3/HO
305 IF(NCOUNT-1)3051,3053,3053
3051 GA2(I)=GH(I)
GC2(I)=GHA(I)
GAL(I)=GA2(I)+GC2(I)
GCL(I)=0.0
3052 GH(I)=(GHA(I)+GH(I))/2.0
GO TO 3057
3053 GAL(I)=GA2(I)
GCL(I)=GC2(I)

```

```

GA2(I)=GH(I)
GC2(I)=GHA(I)
GG=(GC2(I)-GC1(I))/(GA2(I)-GA1(I))
IF(GG)3055,3052,3052
3055 GH(I)=(GC1(I)-GG*GA1(I))/(1.0-GG)
3057 CONTINUE
IF(GH(I).LT.0.001)GH(I)=0.001
H(I)=GH(I)*HO
CALL PROPT(PO,H(I),V(I),T(I),Z(I),NO1)
V(I)=V(I)/PO
VIS(I+1)=V(I)/VO
CALL DOUBL(ALOG10(V(I)),VTABO,T(I),TTABO,XN,SPTABO,I,3,14,3)
307 CONTINUE
VIS(N+2)=VIS(N+1)+VIS(N+1)-VIS(N)
VIS(N+3)=VIS(N+2)
WRITE(6,9031)NCOUNT
321 IF(NB)330,330,322
334 NB=0
NA=2
NCCAB=0
IF(LINEO.GT.1)NAA=2
GO TO 220
322 NB=0
NA=2
NCCAB=0
IF(LINEO.GT.1)NAA=2
IF(NRITE1.LE.0)GO TO 412
DO 411 I=1,N
411 WRITE(6,9020)I,GA1(I),GC1(I),GA2(I),GC2(I),GH(I)
412 NCOUNT=NCOUNT+1
SWCHA=.FALSE.
SWCHAB=.FALSE.
IF(NCOUNT-50)220,220,350
330 CONTINUE
NCNTRI=NCNTRI+1
332 NA=4
IF(LINEO.GT.1)NAA=4
NCCAB=0
GO TO (930,930,931),LINEO
930 CALL NGBSP(QWTC)

```

```

IF(LINEO.EQ.1)QWT=QWTC
IF(LINEO.EQ.1)QSHOK=QWST
IF(LINEO.EQ.1)GO TO 331
CALL CRLINE(QWTL)
QWT=QWTC-QWTL
QSHOK=QWST-QWTS
GO TO 331

931 CALL CRLINE(QWT)
QWTL=QWT
QSHOK=QWTS

331 CONTINUE
IF(SWCHAB)SWCHC=.TRUE.
IF(SWCHC)GO TO 333
IF(NSAB.LE.0)GO TO 333
IF(NAB.GT.0)SWCHA=.TRUE.
7030 IF(SWCHA.AND.SWCHAB)SWCHC=.TRUE.
IF(SWCHC)GO TO 333
NCNTR3=NCNTR3+1
IF(NRITE7.LE.0)GO TO 7031
IF(SWCHAB)GO TO 334
333 WRITE (6,9013)
WRITE (6,9030)DELTA,PO,HO,TO,QWT,QSHOK
WRITE (6,9014)
DO 335 I=1,N
YC=(Y(I)+DY(I)/2.0)/DELTA
UC=-FUA(I)
VC=FVA(I)*V(I)/VO
HC=GH(I)
335 WRITE(6,9020)I,YC,UC,VC,HC,T(I),V(I),Z(I)
IF(NSAB.GT.0)TS=T(N)
WRITE(6,9021)
DO 735 I=1,N
DO 734 J=1,3
734 PART(J)=10.0*(-XN(I,J))*5.07E+19/V(I)
IF(LINEO.EQ.1)GO TO 735
PARTE(I)=PART(3)
DYNQ(I)=(PART(1)+PART(2))*DY(I)/(5.07E+19*(4.+10.*EXP(-2.384/T(I))
1+6.*EXP(-3.576/T(I))))
735 WRITE(6,9020)I,(PART(J),J=1,3)
IF(LINEO.EQ.3)GO TO 950

```

```

DO 750 J=1, KK
SQW(J)=QW(J)/DNU(J)
SQWS(J)=QWS(J)/DNU(J)
750 CONTINUE
WRITE(6,9015)(FNUL(J),J=1, KK)
WRITE(6,9016)(FNUU(J),J=1, KK)
WRITE(6,9017)(QW(J),J=1, KK)
IF(LINEOP.LT.3)WRITE(6,9022)QWTC
WRITE(6,9028)(QWS(J),J=1, KK)
WRITE(6,9027)QWST
WRITE(6,9056)(SQW(J),J=1, KK)
WRITE(6,9058)(SQWS(J),J=1, KK)
WRITE(6,9018)
NI=N+1
DO 340 K=1, NI
340 WRITE(6,9019) K, (TAU(K, J), J=1, KK)
9131 FORMAT(/, 9H LINEOP =, I12, /)
IF(LINEO.EQ.1)GO TO 7031
950 WRITE(6,9133)
9133 FORMAT(/, 6H GROUP, 8X, 2HHV, 12X, 3HHV+, 11X, 3HHV-, 8X, 5HNLINE, 11X,
15H TAUC, 15X, 6H QWALL, 14X, 7H QSHOCK, 8X, 6H TAUCT, /)
DO 955 J=1, NHV
WRITE(6,9135)J, FHV(J), FHVP(J), FHM(J), NU(J), TAUC(NP1, J), QWCO(J), QW
ICSO(J), TAUC(NTP1, J)
9135 FORMAT(I4, F12.3, 2F14.3, I12, 3E20.5, E14.5)
955 CONTINUE
WRITE(6,9137)LINEO, QWTL, QWTS
9137 FORMAT(/, 66H (IF LINEOP=2, VALUES ARE NEGATIVE CORRECTION TO CONTIN
IUCH)LINEOP=, I2, 8H, TOTAL=, 2E20.5)
9139 IF(NRITE2.LE.0)GO TO 7031
IF(NSAB.LE.0. OR.SWCHC)GO TO 9128
GO TO 7031
9138 CONTINUE
NRITE3=NRITE2
IF(NRITE4.GE.0)NRITE4=1
IF(NRITE5.GE.0)NRITE5=1
IF(NRITE6.GE.0)NRITE6=1
DO 962 KI=1, NHV
NELXC=0
DO 960 J=1, N

```

```

960 IF(NU(KI).GT.0)DYNQI(J)=DYNQ(J)*(1.-EXP(-FHV(KI)/T(J)))
CONTINUE
CALL LINE(JP1,JJ,KI,LINEOP,WIDTH
,NELMC,KL1(KI),KL2(KI),
1FHVA(KI),FHVP(KI),FHVPM(KI),ISOE(KI),N,NP1,PARTE,DYNQI,GAMBA,ND,EP
2S,BGF,NU(KI),HVL,T,NUMINT(KI))
962 CONTINUE
7031 IF(NSAB.LE.0)GO TO 8
IF(SWCHC)GO TO 7032
IF(SWCHAB)GO TO 322
IF(NRITE7.LE.0)GO TO 7033
7032 WRITE(6,7911)
7911 FORMAT(/,31H. STAGRADS=ABLATION CALCULATION,/)
7033 CALL STAGAB(C22,C44,C55,L,L1,ES1,RHOA,UA,PO,RN,NSAB,HV,TW,DELTA
1B,QWT,EMD,TS,SWCHA,SWCHAB,SWCHC,NRITE1,NRITE7,FUAB,N,NGWT,FDHAB,
2V1W)
IF(EMD.LT.0.11E-2)NSAB=0
IF(EMD.LT.0.11E-2)GO TO 9139
IF(SWCHC)GO TO 7040
NCNTR2=NCNTR2+1
SWCHAB=.TRUE.
GO TO 7030
350 WRITE (6,9031) NCOUNT
DO 352 I=1,N
352 WRITE (6,9020) I,GH(I),GHA(I)
360 GO TO 8
7040 DELTAT=DELTA+DELTAB
VROD=VW*DELTAT/VO
WRITE(6,7903)DELTA,DELTAB,DELTAT
7903 FORMAT(/8H DELTA =,E20.5,10X,9H DELTAB =,E20.5,10X,9H DELTAT =,
1E20.5,/)
YAB=DELTA
ZETA=0.0
WRITE(6,7905)
7905 FORMAT(6H I ,12H Y/DELTAT ,6X,4HU/US,9X,1HT,10X,
24RZETA,12X,3HIAB,/,65X,2H 0)
DO 7045 I=1,NT
IF(I.GT.N)GO TO 7041
DZETA=DY(I)/(VIS(I+1)*DELTAT)
ZETA=ZETA+DZETA
YC=(Y(I)+DY(I)/2.0)/DELTAT

```

```

UC=-FUA(I)
WRITE(6,7907)I,YC,UC,T(I),ZETA
GO TO 7045
7041 IAB=NTPI-I
DZETA=DYAB(IAB)/(VIW(IAB+1)*VWOD)
ZETA=ZETA+DZETA
YC=(YAB+DYAB(IAB))/2.0)/DELTAT
YAB=YAB+DYAB(IAB)
UC=FUAB(IAB)
WRITE(6,7907)I,YC,UC,TAB(IAB),ZETA,IAB
7045 CONTINUE
7907 FORMAT(I6,4E12.5,I12)
WRITE(6,7909)NCNTR1,NCNTR2,NCNTR3
7909 FORMAT(/10X,9H NCNTR1 =,I6,10X,9H NCNTR2 =,I6,10X,9H NCNTR3 =,I6)
GO TO 8
END

```

```

VIT FOR STAGAB
SUBROUTINE STAGAB(C22,C44,C55,L,L1,ES1,RHOA,UA,PO,RN,NS,HW,VW,TW,
1DELTA,QWT,EMD,TS,SWCHA,SWCHAB,SWCHC,NRITE1,NRITE7,FUA,NAIR,NQWT,
2FDHAB,VIW)
DIMENSION FVA(10),FUA(10),GH(10),GHC(11),GHA(10),GA1(10),GA2(10),
1GC1(10),GC2(10),Y(11),H(10),SIT(13),
2VIW(13),V(10)
COMMON/STAGAH/PRTAB(3),TTAB(3,20),ENTAB(3,20),RHOTAB(3,20),C2TAB(3
1,20),C1TAB(3,20),COTAB(3,20),HTAB(3,20),CPTAB(3,20),EMTAB(3,20)
COMMON/MSTACR/NT,NTPI,N,DY(10),T(10),NCQAB,I
COMMON/SPADST/FC2(10),FCO(10),FH(10),FCL(10),FCP(10)
LOGICAL SWCHA,SWCHAB,SWCHC
3 FORMAT(1H 7E18.5)
9013 FORMAT(119H DELTA UR PO QWT EMD TW RMOM,
1W VCV
25X,6H URMAS)
9014 FORMAT(/124H IAB YC UC VC HC
1 T NCI NC2 NCO NH
2 NC+)
9020 FORMAT(I6,11E11.5)
9030 FORMAT(1H 10E12.5,11.5)
9031 FORMAT(15H NCOUNT =,I10)

```

```

IF(SRCHC) GO TO 334
IF(NQWT.GT.0)GO TO 105
C8=0.463E-6/(RHOA*UA)
RB=RN
ANS=NS
CL1=LI
DZETA=0.12
NO1=-1
INL=3
INL=20
CALL PROT( HW ,ENTAB,V(1),RHOTAB,PO,PRTAB,T(1),TTAB,FC2(1),C2TAB,
1FC1(1),C1TAB,FCO(1),COTAB,FH(1),HTAB,FCP(1),CPTAB,INL,IML)
VW=V(1)
TW=T(1)
AEE= RN*SQRT(RHOA*VW/(2.0*ES1))/CL1
SIG=C55/(RHOA*UA)
DELTA=0.0
GHC(1)=1.0
SIT(1)=0.0
DSI=5.0/ANS
Y(1)=0.0
F=1.20
FI=1.0/F
NCOUNT=0
GHE=(TS/TW)**1.35
HVAP=0.61*(1.386-1.13*TW)*FDHAB
RW=1.03E+5*TW**4
QS=QWT
DELH=0.03
105 NHHH=10
NB=0
NCGAB=1
NCONH=0
131 EMD=C6*(QWT-1.03E+5*TW**4)/(1.386-1.13*TW)
EMD=EMD/FDHAB
IF(NCOUNT.EQ.0)WRITE(6,9040)EMD
9040 FORMAT(/38H NC ABLATION LAYER ATTENUATION, EMD =,E18.5,/)
IF(EMD.LT.0.10E-2)RETURN.
QWT1=QWT
EMDHN=EMD*HW

```



```

AEYZ=AEZ*EMD
IF(NQWT.EQ.0)GO TO 206
NQWT=0
GO TO 220
206 DO 209 I=1,NS
SIT(I+1)=SIT(I)+DSI
209 CONTINUE
N=NS
SIT(N+2)=SIT(N+1)+DSI/2.0
SIT(N+3)=2.0*SIT(N+2)
MH=-1
220 N=NS
MH=MH+1
NS=0
NHHH=10
IF(MH-1)800,800,221
800 DC 810 I=1,N
801 GH(I)=1.0+(GHE-1.0)*((FLOAT(I)-0.5)/FLOAT(N))
807 V(I)=GH(I)**1.50*VW
VIM(I+1)=V(I)/VW
810 CONTINUE
VIM(N+2)=VIM(N+1)+VIM(N+1)-VIM(N)
VIM(N+3)=VIM(N+2)
IF(MH.GT.0)GO TO 221
BL=HVAP/(HVAP+HW*(GHE-1.0))
IF(NRITE1.GT.0)WRITE(6,3)BL
MH=MH+1
221 SUM=0.0
CALL VEL(2,SIT,VIM,0.0,DZETA,1.0,CL1,N,ANS,FUE,AEYZ,DY,FVA,FUA,
IDUM)
DO 227 I=1,N
SUM=SUM+FUA(I)*DY(I)/V(I)
DY(I)=DY(I)/(1.0+Y(I)/RB)**L
Y(I+1)=Y(I)+DY(I)
227 CONTINUE
DELTA=Y(N+1)
NT=N+IR+N
IF(NT.GT.20)CALL EXIT
NTP1=NT+1
GHC(1)=1.0

```

```

IF(MH.GT.1)GO TO 303
301 DO 302 I=1,N
   H(I)=GH(I)*HW
302 CALL PROT( H(I),ENTAB,V(I),RHOTAB,PO,PRTAB,T(I),TTAB,FC2(I),C2TAB,
   1FC1(I),C1TAB,FCO(I),COTAB,FH(I),HTAB,FCP(I),CPTAB,INL,IML)
303 DO 307 I=1,N
   IF(I.EQ.1)NCGAB=1
   IF(I.GT.1)NCGAB=2
   CALL CRLINE(CQ)
   DGH = SIG*CQ/(FVA(I)*EMDHW)
   GHC(I+1)=GHC(I)+DGH
   GHA(I)=(GHC(I)+GHC(I+1))/2.0
   ABDH=ABS((GHA(I)-GH(I))/GH(I))
   IF(ABDH.GT.0.20)NHHH=25
   IF(ABDH-DELH)305,305,304
304 NB=1
305 IF(NCOUNT-1)3058,3051,3053
3051 GA2(I)=GH(I)
   GC2(I)=GHA(I)
   GA1(I)=GA2(I)+GC2(I)
   GC1(I)=0.0
3052 GACH=(GA2(I)+GC2(I))/2.0
   IF(GC2(I)-GA2(I))701,3057,702
701 FGA=FI*GA2(I)
   GH(I)=AMAX1(GACH,FGA)
   GO TO 3057
702 FGA=F*GA2(I)
   GH(I)=AMIN1(GACH,FGA)
   GO TO 3057
3053 GA1(I)=GA2(I)
   GC1(I)=GC2(I)
   GA2(I)=GH(I)
   GC2(I)=GHA(I)
   GG=(GC2(I)-GC1(I))/(GA2(I)-GA1(I))
   IF((GC1(I)-GA1(I))*(GC2(I)-GA2(I)))3055,3057,3052
3055 GH(I)=(GC1(I)-GG*GA1(I))/(1.0-GG)
3057 H(I)=GH(I)*HW
   CALL PROT( H(I),ENTAB,V(I),RHOTAB,PO,PRTAB,T(I),TTAB,FC2(I),C2TAB,
   1FC1(I),C1TAB,FCO(I),COTAB,FH(I),HTAB,FCP(I),CPTAB,INL,IML)
3058 VW(I+1)=V(I)/VW

```

```

307 CONTINUE
   VIW(N+2)=VIW(N+1)+VIW(N+1)-VIW(N)
   VIW(N+3)=VIW(N+2)
   IF(NRITE1.LE.0)GO TO 413
   WRITE(6,9031)NCOUNT
   IF(NCOUNT.EQ.0)GO TO 413
   DO 411 I=1,N
411 WRITE(6,9020)I,GA1(I),GC1(I),GA2(I),GC2(I),GH(I)
413 CONTINUE
   NCONH=NCONH+1
   NCOUNT=NCOUNT+1
   IF(NCOUNT.GT.205)GO TO 350
321 IF(NB)332,332,322
322 CONTINUE
   SWCHA=.FALSE.
   IF(NCONH-NHHH)409,409,408
408 NCONH=0
   IF(NCOUNT-200)332,332,350
409 IF(NCOUNT-200)410,410,350
410 NCGAB=3
   CALL CRLINE(QWT)
   IF(NRITE1.GT.0)WRITE(6,3)QWT
   IF(NCOUNT.GT.1)GO TO 220
   QWTL=BL*(QS-RW)+RW
   IF(NRITE1.GT.0)WRITE(6,3)QWTL
   QWT=AMAX1(QWT,QWTL)
   NQWT=1
   GO TO 105
332 NCGAB=3
   CALL CRLINE(QWT)
   IF(ABS(QWT-QWT1)/QWT<0.02)400,400,500
400 IF(NB)453,453,401
453 IF(DE LH<0.029)333,333,401
401 DELH=0.01
   IF(NRITE1.GT.0)WRITE(6,3)DELH
500 IF(NQWT-1)451,451,464
451 QWTA1=QWT1
   QWTC1=QWT
   QWTA2=QWTA1+QWTC1
   QWTC2=0.0

```

```

462 QWT1=(QWTA2+QWTC2)/2.0
GO TO 470
452 QWTA2=QWT1
QWTC2=QWT
GO TO 465
464 QWTA1=QWTA2
QWTC1=QWTC2
QWTA2=QWT1
QWTC2=QWT
465 XX1=(QWTC2-QWTC1)/(QWTA2-QWTA1)
IF((QWTC1-QWTA1)*(QWTC2-QWTA2))466,462,462
466 QWT1=(QWTC1-XX1*QWTA1)/(1.0-XX1)
470 IF(NRITE1.LE.0)GO TO 471
WRITE(6,9050)NQWT,NCONH,NCOUNT
9050 FORMAT(11H NQWT =,I10,11H NCONH =,I10,11H NCOUNT =,I10)
WRITE(6,9051)QWTA1,QWTC1,QWTA2,QWTC2,QWT1
9051 FORMAT(8H QWTA1 =,E18.5,8H QWTC1 =,E18.5,8H QWTA2 =,E18.5,8H QWTC2
1 =,E18.5,8H QWT1 =,E18.5)
471 CONTINUE
NCONH=0
NQWT=NQWT+1
EMD=C8*(QWT1-1.03E+5*TW**4)/(1.386-1.13*TW)
EMD=EMD/FDHAB
AEYZ=AEEM*EMD
GO TO 220
333 VCW=EMD*RHOA*VW
RMOM=EMD*VCW
UR=-SQRT(2.0*ES1*RHOA*VW)*FUE
URMAS=EMD*RHOA*RB*FUE/(CL1*SUM)
IF(NRITE7.LE.0)RETURN
334 CONTINUE
WRITE(6,9013)
WRITE(6,9030)DELTA,PO,HW,TW,VW,VCW,UR,QWT,EMD,RMOM,URMAS
WRITE(6,9014)
DO 335 I=1,N
YC=(Y(I)+DY(I))/2.0)/DELTA
UC=FUA(I)/FUE
VC=FVA(I)*V(I)/VW
HC=GH(I)
H(I)=HC*HW

```

```

IF(SWCHC)FUA(I)=UC*URMAS
335 WRITE(6,9020)I,YC,UC,VC,HC,T(I),V(I),FCL(I),FC2(I),FCO(I),FH(I),FC
1P(I)
RETURN
350 WRITE (6,9031) NCOUNT
DO 352 I=1,N
352 WRITE(6,9020)I,GH(I),GHA(I)
EMD=-0.1E+4
RETURN
END

```

VIT FOR NGG6SP

```

SUBROUTINE NGGBSP(CQ)
DIMENSION T4(10),TFBB(10,10),TFBW(10),G(10,10)
COMMON/HNGB/FNUL(10),FNUU(10),QW(10),TAU(11,10),IKT(2,10),QWS(10),
1QWST,NA,KT
COMMON/HNGCR/DY(10),T(10),V(10),XN(10,4),TW,N,NP1,I
COMMON/MGADAS/FCONTN
E3F(A)=0.50*EXPF(-2.0*A)
GO TO (2,312,32,66),NA
2 DO 4 KK=1,KT
4 TAU(1,KK)=0.0
TW4=TW**4
DO 30 KK=1,KT
CALL PLANCK(FNUL(KK),FNUU(KK),TW,FBW)
TFBW(KK)=FBW*TW4
50 CONTINUE
NA=NA+1
312 DO 15 J=1,N
T4(J)=T(J)**4
DO 14 KK=1,KT
CALL PLANCK(FNUL(KK),FNUU(KK),T(J),FBB)
CALL ABSORP(T(J),V(J),XN,IKT,SPMU,J,KK)
TAU(J+1,KK)=TAU(J,KK)+SPMU*DY(J)
14 TFBB(J,KK)=T4(J)*FBB
15 CONTINUE
NA=NA+1
32 CG=0.0
33 DO 50 KK=1,KT

```

NG 2
NG 3
NG16
NG17

NG31

NG 5
NG 6

NG14

NG34
NG36

```

43 G(I, KK)=E3F(TAU(N+1, KK)-TAU(I+1, KK))-E3F(TAU(N+1, KK)-TAU(I, KK))
   CG=CQ+TFBW(KK)*G(I, KK)
   DO 48 J=1, N
   FF=E3F(ABS(TAU(I, KK)-TAU(J+1, KK)))-E3F(ABS(TAU(I, KK)-TAU(J, KK)))+E
13F(ABS(TAU(I+1, KK)-TAU(J, KK)))-E3F(ABS(TAU(I+1, KK)-TAU(J+1, KK)))
   FF=FF*TFBB(J, KK)
48 CG=CQ+FF
50 CONTINUE
   RETURN
66 QWT=0.0
   QWST=0.
   DO 75 KK=1, KT
   QW(KK)=0.0
   QWS(KK)=0.0
701 DO 74 I=1, N
72 QW(KK)=QW(KK)+TFBB(I, KK)*G(I, KK)
   QWS(KK)=QWS(KK)+TFBB(I, KK)*(E3F(TAU(I, KK))-E3F(TAU(I+1, KK)))
74 CONTINUE
   QWS(KK)=QWS(KK)+TFBW(KK)*E3F(TAU(N+1, KK))
   QWT=QWT+QW(KK)
   QWST=QWST+QWS(KK)
   QW(KK)=QW(KK)*2.06E+5
   QWS(KK)=QWS(KK)*2.06E+5
75 CONTINUE
   QWT=QWT*2.06E+5
   QWST=QWST*2.06E+5
   CG=QWT
   RETURN
   END

```

NG47
NG48
NG49
NG50

NG52
NG53
NG54
NG69

NG70

NG79

NG81

NG82
NG83

```

VIT FOR CRLINE
SUBROUTINE CRLINE(CG)
  DIMENSION EI(20,24), BIW(24), ETAU12(21,21), G(20,24), GS(20,24),
1GWS(24), DYNGI(10), DYNGI(10), PARTE(10), WIDTH(11,11),
2STORE(55,24), TNPIJ(10,24)
  DIMENSION FFF(20)
  DIMENSION C1(10), C2(10), C3(10), C4(10), C5(10), C9(10), C10(10), C14(10)
1), C15(10), C18(10), C21(10), C23(10), SPM1(10), SPM2(10), SPM3(10), SPM5(
210), SPM6(10), SPM8(10), SPM9(10), SPM(10)

```

```

COMMON/HNGCR/DY(10),T(10),V(10),XN(10,4),TW,N,NP1,I
COMMON/MCRLN/FHVP(24),FHM(24),FHVPM(24),FHV(24),ISOE(24),NU(24),N
IUMINT(24),KL1(24),KL2(24),QWCO(24),QWCSO(24),TAUC(21,24)
2,DGF(30),GAMBA(80),HVL(80),ND(80),EPS(8),LINEOP,NAA,QWTS
3,NLINE,NLST,NHV,MSAB
COMMON/MSTACR/NT,NTP1,NAB,DYAB(10),TAB(10),NCGAB,IAB
E3F(A)=0.50*EXP(-2.0*A)
5IF(FRE,TT)=FRE**3/(EXP(FRE/TT)-1.0)*0.153990
IF(NCGAB.LE.0)GO TO 1001
GO TO (1002,1006,60),NCGAB
1001 CONTINUE
GO TO (2,20,51,60),NAA
2 GO TO (3,4,5),LINEOP
3 CALL EXIT
4 CCC=0.0
GO TO 6
5 CCC=1.0
6 CONTINUE
DO 10 KK=1,NHV
TAUC(1,KK)=0.
BIW(KK)=BIF(FHV(KK),TW)
WRITE(6,100)KK,KL1(KK),KL2(KK),FHV(KK)
100 FORMAT(17H (KK,KL1,KL2,FHV),3110,E20.6)
10 CONTINUE
NAA=NAA+1
1002 CONTINUE
20 DO 25 J=1,NT
IF(NCGAB.GT.0)GO TO 1010
IF(J.GT.N)GO TO 1010
PARTE(J)=10.0**(-XN(J,3))*5.07E+19/V(J)
DYNQ(J)=(10.0**(-XN(J,1))+10.0**(-XN(J,2)))*DY(J)/(V(J)*(4.+10.*EXP
1(-2.384/T(J))+6.*EXP(-3.576/T(J))))
1010 FFF(J)=0.
25 CONTINUE
DO 50 KK=1,NHV
WIDTH(1,1) =CCC*FHVPM(KK)
ETAU12(1,1)=0.50*WIDTH(1,1)
IF(NCGAB.GT.0)GO TO 1003.
NELMC=0
DO 26 J=1,N

```

```

IF(NU(KK).LE.0)GO TO 27
DYNQI(J)=DYNQ(J)*(1.-EXP(-FHV(KK)/T(J)))
26 CONTINUE
27 CONTINUE
DO 40 J=1,N
  JP1=J+1
  BI(J,KK)=BIF(FHV(KK),T(J))
  CALL ABSORC(T(J),V(J),XN,SPMUC,J,KK,FHV(KK),NHV,LINEOP)
  TAUC(JP1,KK)=TAUC(J,KK)+SPMUC*DY(J)
  DO 30 JJ=1,J
    ETAU=E3F(TAUC(JP1,KK)-TAUC(JJ,KK))
    CALL LINE(JP1,JJ,KK,LINEOP,WIDTH(JP1,JJ) ,NELMC,KL1(KK),KL2(KK),
    1FHV(KK),FHVP(KK),FHVPM(KK),ISOE(KK),N,NP1,PARTE,DYNQI,GAMBA,ND,EP
    2S,BGF,NU(KK),HVL,T,NUMINT(KK))
    WIDTH(JJ,JP1 )=WIDTH(JP1,JJ )
    ETAU=ETAU*WIDTH(JP1,JJ )
    ETAU12(JP1,JJ)=ETAU
    ETAU12(JJ,JP1)=ETAU
    IF(NSAB.LE.0)GO TO 30
    K=J*(J-1)/2+JJ
    IF(K.GT.55)CALL EXIT
    STORE(K,KK)=ETAU
    IF(J.EQ.N.AND.LINEOP.EQ.3)TNP1JJ(JJ,KK)=WIDTH(JP1,JJ)
30 CONTINUE
40 CONTINUE
1005 CONTINUE
IF(NSAB.LE.0)GO TO 1042
DO 1041 J=1,NT
  JP1=J+1
  IF(J.LT.NP1)GO TO 1004
  JAB=NTP1-J
  BI(J,KK)=BIF(FHV(KK),TAB(JAB))
  CALL SPABCO(SPMUC,KK,JAB,TAB(JAB),C1(JAB),C2(JAB),C3(JAB),C4(JAB),
  1C5(JAB),C9(JAB),C10(JAB),C14(JAB),C15(JAB),C18(JAB),C21(JAB),C23(J
  2AB),SPM1(JAB),SPM2(JAB),SPM3(JAB),SPM5(JAB),SPM6(JAB),SPM8(JAB),SP
  3M9(JAB),SPM(JAB))
  TAUC(JP1,KK)=TAUC(J,KK)+SPMUC*DYAB(JAB)
1004 DO 1930 JJ=1,J
  IF(J.GE.NP1)GO TO 1005
  K=J*(J-1)/2+JJ

```



```

TEM=STORE(K,KK)
ETAU12(JP1,JJ)=TEM
ETAU12(JJ,JP1)=TEM
GO TO 1930
1005 IF(JJ-NP1)1102,1105,1105
1102 ETAU=E3F(TAUC(JP1,KK)-TAUC(JJ,KK))*TNPIJJ(JJ,KK)
GO TO 1106
1105 ETAU=E3F(TAUC(JP1,KK)-TAUC(JJ,KK))*WIDTH(I,1)
1106 ETAU12(JP1,JJ)=ETAU
ETAU12(JJ,JP1)=ETAU
1930 CONTINUE
1041 CONTINUE
1042 DO 45 J=1,NT
JP1=J+1
ETAU12(JP1,JP1)=ETAU12(I,1)
WIDTH(JP1,JP1)=WIDTH(I,1)
G(J,KK)=ETAU12(NTP1,JP1)-ETAU12(NTP1,J)
GS(J,KK)=ETAU12(J,1)-ETAU12(JP1,1)
DO 43 IJ=1,NT
FF=BI(IJ,KK)*( ETAU12(J,IJ+1)-ETAU12(J,IJ)+ETAU12(JP1,IJ)-ETAU12(
IJ+1,IJ+1))
43 FFF(J)=FFF(J)+FF
44 FFF(J)=FFF(J)+BIW(KK)*G(J,KK)
45 CONTINUE
GWS(KK)=ETAU12(NTP1,1)
50 CONTINUE
IF(NCGAB.GT.0)NCGAB=NCGAB+1
IF(NCGAB.GT.0)GO TO 1006
NAA=NAA+1
IF(NCGAB.LE.0) GO TO 51
1006 I=NTP1-IAB
51 CS=FFF(I)
RETURN
60 QWT=0.
QWTS=0.
DO 75 KK=1,NHV
QWCO(KK)=0.
QWCSO(KK)=0.
DO 74 I=1,NT
QWCO(KK)=QWCO(KK)+BI(I,KK)*G(I,KK)

```

LS

LS

```

      QWCSS(KK)=QWCSS(KK)+BI(I,KK)*GS(I,KK)
74  CONTINUE
      QWCSS(KK)=QWCSS(KK)+BIW(KK)*GWS(KK)
      QWT=QWT+QWCSS(KK)
      QWTS=QWTS+QWCSS(KK)
      QWCO(KK)=QWCO(KK)*2.06E+5
75  CONTINUE
      QWT=QWT*2.06E+5
      QWTS=QWTS*2.06E+5
      CQ=QWT
      RETURN
      END

```

LS

LS

LS

VIT FOR ABSORC

```

      SUBROUTINE ABSORC(T,V,XN,SPMUC,IL,K,FHV,NHV,LINEOP)
      INTFRE=GT.0 BYPASS FREQ INTERPOLATION
      DIMENSION FRET(24),IT(14),IL(2,14,24),TC(2,14,24),XN(10,4)
      COMMON/MABSPC/RTEM(20),IRTEM(20),INTFRE
      DATA(IT(I),I=1,14)/.25849,.34466,.43082,.51699,.60315,.68932,.8616
      DATA(FRET(J),J=1,24)/.25,.50,.75,1.0,2.0,3.0,4.0,5.0,6.0,7.0,8.0,9
      214.501,30.00/
      DATA((TL(I,I),I,J),J=1,9),I=1,14)/
      1 .500, .500, .500, .500, .500, .500, .500, .500, .500, .500, .500,
      2 6.721, 5.816, 5.286, 4.911, 4.009, 3.481, 2.576, 2.290, 2.053,
      3 10.453, 9.598, 9.346, 9.320, 9.585, 9.228, 9.849, 9.820,
      4 12.960, 12.161, 11.865, 11.763, 11.542, 11.626, 11.272, 11.680, 11.639,
      5 14.761, 13.937, 13.598, 13.455, 13.124, 13.093, 12.739, 13.021, 12.968,
      6 16.117, 15.274, 14.905, 14.730, 14.316, 14.199, 13.846, 14.045, 13.981,
      7 18.023, 17.155, 16.744, 16.525, 15.993, 15.761, 15.408, 15.507, 15.425,
      8 19.303, 18.420, 17.977, 17.723, 17.117, 16.817, 16.462, 16.498, 16.405,
      9 20.220, 19.324, 18.861, 18.590, 17.925, 17.577, 17.223, 17.215, 17.111,
      A 20.905, 20.000, 19.524, 19.236, 18.530, 18.149, 17.792, 17.751, 17.636,
      B 21.427, 20.516, 20.029, 19.728, 18.992, 18.585, 18.228, 18.158, 18.037,
      C 21.835, 20.920, 20.425, 20.111, 19.348, 18.923, 18.562, 18.471, 18.342,
      D 22.130, 21.210, 20.709, 20.387, 19.606, 19.167, 18.806, 18.698, 18.563,
      E 22.356, 21.433, 20.927, 20.598, 19.801, 19.350, 18.987, 18.863, 18.723/

```

EVLOG+38

A20.651,19.763,19.265,16.994,18.299,16.025,17.685,17.991,17.927,
 B21.223,20.323,19.818,19.528,18.792,18.476,18.137,16.364,18.301,
 C21.648,20.748,20.233,19.929,19.170,18.525,18.484,18.657,18.592,
 D21.982,21.079,20.558,20.246,19.467,19.097,18.757,18.918,18.848,
 E22.241,21.332,20.808,20.486,19.652,19.305,18.963,19.079,19.009/
 DATA((TL(2,I),J),J=10,18),I=1,14)/

EVLOG+38

1 .500, .500, .500, .500, .500, .500, .500, .500, .500, .500,
 2 8.824, 8.766, 8.733, 8.731, 8.724, 8.718, 8.712, 8.243, 8.243,
 3 11.167, 11.114, 11.086, 11.083, 11.076, 11.068, 11.064, 10.803, 10.803,
 4 12.740, 12.688, 12.666, 12.660, 12.655, 12.651, 12.647, 12.501, 12.501,
 5 13.869, 13.822, 13.803, 13.799, 13.796, 13.793, 13.790, 13.710, 13.710,
 6 14.726, 14.684, 14.668, 14.667, 14.666, 14.664, 14.663, 14.618, 14.618,
 7 15.951, 15.919, 15.911, 15.913, 15.914, 15.915, 15.917, 15.903, 15.903,
 8 16.794, 16.771, 16.769, 16.773, 16.777, 16.782, 16.785, 16.774, 16.774,
 9 17.417, 17.400, 17.401, 17.408, 17.413, 17.418, 17.423, 17.409, 17.409,
 A 17.893, 17.881, 17.887, 17.894, 17.900, 17.907, 17.913, 17.892, 17.892,
 B 16.267, 18.258, 18.267, 18.274, 18.281, 18.290, 18.297, 18.273, 18.273,
 C 18.561, 18.554, 18.562, 18.571, 18.579, 18.587, 18.593, 18.568, 18.568,
 D 18.814, 18.804, 18.811, 18.818, 18.826, 18.834, 18.840, 18.818, 18.818,
 E 18.976, 18.966, 18.974, 18.981, 18.989, 18.997, 19.004, 18.979, 18.979/
 DATA((TL(2,I),J),J=19,24),I=1,14)/

EVLOG+38

120.605,20.605,20.605,20.605,20.605,20.605,20.605,20.605,
 220.604,20.604,20.604,20.604,20.604,20.604,20.604,20.604,
 320.602,20.602,20.602,20.602,20.602,20.602,20.602,20.602,
 420.600,20.600,20.600,20.600,20.600,20.600,20.600,20.600,
 520.595,20.595,20.595,20.595,20.595,20.595,20.595,20.595,
 620.591,20.591,20.591,20.591,20.591,20.591,20.591,20.591,
 720.580,20.580,20.580,20.580,20.580,20.580,20.580,20.580,
 820.568,20.568,20.568,20.568,20.568,20.568,20.568,20.568,
 920.556,20.556,20.556,20.556,20.556,20.556,20.556,20.556,
 A20.541,20.541,20.541,20.541,20.541,20.541,20.541,20.541,
 B20.521,20.521,20.521,20.521,20.521,20.521,20.521,20.521,
 C20.487,20.487,20.487,20.487,20.487,20.487,20.487,20.487,
 D20.439,20.439,20.439,20.439,20.439,20.439,20.439,20.439,
 E20.392,20.392,20.392,20.392,20.392,20.392,20.392,20.392/
 IF(INTFRE.GT.0) GO TO 35

10 J=1

4 IF(FRET(J)-FHV)1,2,3

1 J=J+1

1 IF(J.EQ.24)GO TO 8

```

GO TO 4
2 R=1.0
GO TO 5
3 IF(J.EQ.1)J=2
8 R=(FHV-FRET(J-1))/(FRET(J)-FRET(J-1))
5 DO 30 N=1,2
DO 20 I=1,14
20 TC(N,I,K)=R*( TL(N,I,J)- TL(N,I,J-1))+ TL(N,I,J-1)
30 CONTINUE
IF(K.EQ.NHV) INTFRE=1
35 IF(LINEOP-2)36,37,40
36 CALL EXIT
37 I=IRTEM(IL)
GO TO 50
40 I=1
44 IF(TT(I)-T)41,42,43
41 I=I+1
41 IF(I.EQ.14)GO TO 48
GO TO 44
42 RTEM(IL)=1.0
GO TO 50
43 IF(I.EQ.1)I=2
48 RTEM(IL)=(T-TT(I-1))/(TT(I)-TT(I-1))
50 SMUC=0.0
DO 60 N=1,2
SIGA=RTEM(IL)*(TC(N,I,K)-TC(N,I-1,K))+TC(N,I-1,K)
AB=-10.295+SIGA-XN(IL,N)
AB=10.0**AB
60 SMUC=SMUC+AB
SPMUC=SMUC/V
RETURN
END

```

VIT FOR LINE

```

SUBROUTINE LINE(I2,I1,N,LINEOP,WIDTRN,NELMC,K1,K2,X1,X2,X12,ISOE,N
1,KP1,PART,DYNGI,GAMBA,ND,EPS,BGF,HU,
HVL,T,NUMINT)
DIMENSION BGF(80),DYNGI(10),EPS(8),GAM(10),GAMBA(80),GAM2
1(10,12),HVL(80),ND(80),PARTE(10),SGAM(10,12),SGAMP(10,12),SGAMT(11
2),SS(10),SST(11),WID12(11,11),T(10),TAUD(10),TAUDT(11),WIDISO(11,1

```

```

31) COMMON/MLINE/NRITE3,NRITE4,NRITE5,NRITE6
SST(I)=0.
TAUDT(I)=0.
SGAMT(I)=0.
IF(NU)1,1,5
1 GO TO (2,3,4),LINEOP
2 CALL EXIT
3 WIDTRN=0.
RETURN
4 WIDTRN=X12
RETURN
5 IF(NELMC)2,6,100
6 NELMC=NELMC+1
DO 10 I=1,N
DO 10 J=1,I
10 WID12(I+1,J)=0.
DO 50 K=K1,K2
KM=K-K1+1
JD=ND(K)
DO 40 I=1,N
IPI=I+1
GAM(I)=GAMBA(K)*PARTE(I)
IF(NUMINT.EQ.0) GO TO 21
GAM2(I,KM)=GAM(I)**2
21 IF(KM.GT.1.AND.ISOE.GT.0)GO TO 22
DYGI(I)=DYNQI(I)*EXP(-EPS(JD)/T(I))
22 SS(I)=DYGI(I)*BGF(K)
TAUD(I)=SS(I)/(3.1415927*GAM(I))
SGAM(I,KM)=SS(I)*GAM(I)
IF(NUMINT.GT.0) SGAMP(I,KM)=SGAM(I,KM)*0.31830989
SST(IPI)=SST(I)+SS(I)
TAUDT(IPI)=TAUDT(I)+TAUD(I)
SGAMT(IPI)=SGAMT(I)+SGAM(I,KM)
IF(NRITE6.LE.0)GO TO 801
WRITE(6,902)M,K,KM,JD,I,GAM(I),SS(I),SST(IPI),SGAM(I,KM),SGAMT(IPI)
1),TAUD(I),TAUDT(IPI)
902 FORMAT(/25H M K KM JD I,6X,7H GAM(I),7X,6H SS(I),4X,9
1H SST(I+1),2X,11H SGAM(I,KM),2X,11H SGAMT(I+1),5X,6H TAUD(I),2X,11
2H TAUDT(I+1),/5I5,8E13.4)

```

```

801 CONTINUE
DO 30 J=1,I
SS12=SST(IP1)-SST(J)
TAU12=TAUDT(IP1)-TAUDT(J)
SGAM12=SGAMT(IP1)-SGAMT(J)
GAME12=SGAM12/SS12
TPG12=6.2831854*GAME12
ZETA12=SGAM12/(TPG12*GAME12)
WID12K=TPG12 *FLR(ZETA12)
WID12(IP1,J)=WID12(IP1,J)+WID12K
IF(NWRITE5.LE.0)GO TO 802
WRITE(6,904)M,K,KM,JD,IP1,J,SS12,SGAM12,GAME12,ZETA12,WID12K,WID12
1(IP1,J),TAU12
904 FORMAT(/30H M K KM JD IP1 J,8X,5H SS12,6X,7H SGAM12,
16X,7H GAME12,6X,7H ZETA12,6X,7H WID12K,2X,13H WID12(IP1,J),5X,6H T
2AU12,/6I5,7E13.4)
802 CONTINUE
30 CONTINUE
40 CONTINUE
50 CONTINUE
810 NINT=0
GO TO 814
812 NINT=1
814 CONTINUE
IF(NWRITE3.LE.0.AND.NINT.LE.0)GO TO 100
DO 60 I=1,N
IPL=I+1
DO 60 J=1,I
WIDISO(IP1,J)=WID12(IP1,J)
IF(NWRITE3.GT.0.AND.NUMINT.EQ.0)GO TO 816
IF(NINT.GT.0)GO TO 60
WRITE(6,906)M,IP1,J,WID12(IP1,J)
FORMAT(19H ISOLATED LINES, M=,I5,9H WIDTH(,I3,1H,,I3,2H)=,E15.8)
CALL FWIDTH(M,X12,WID12(IP1,J))
WRITE(6,908)M,IP1,J,WID12(IP1,J)
FORMAT(20H FROM CORRELATION,M=,I5,8H WIDTH(,I3,1H,,I3,2H)=,E15.8)
60 CONTINUE
61 CONTINUE
IF(NINT.LE.0)GO TO 100

```

```

IF(NUMINT.EQ.0) GO TO 100
CALL INTEG(X1,X2,N,NP1,WID12,K1,K2,HVL,GAM2,SGAMP,NRITE4)
IF(NRITE3.LE.0)GO TO 100
WRITE(6,910)
910 FORMAT(/,5H M,4X,3HIP1,4X,1HI,9X,9HISO.WIDTH,9X,9HACT.WIDTH,
110X,7HDNU*TRN,7X,13HISO-ACT WIDTH)
DO 70 I=1,N

```

```

IPI=I+1
DO 70 J=1,I
WMWS=HIDISO(IPI,J)-WID12(IPI,J)
DNUTRN=X12-WID12(IPI,J)
WRITE(6,912)M,IPI,J,WIDISO(IPI,J),WID12(IPI,J),DNUTRN,WMWS
70 CONTINUE
912 FORMAT(3I6,6E18.8)
100 GO TO (101,102,103),LINEOP
101 STOP
102 WIDTRN=WID12(I2,I1)
RETURN
103 WIDTRN=X12-WID12(I2,I1)
RETURN
END

```

```

VIT FOR FLR
FUNCTION FLR(ZETA)
IF(ZETA=0.22019566)1,1,2
1 FLR=ZETA
RETURN
2 IF(ZETA=1.8405672)3,3,4
3 FLR=0.685*ZETA**0.75
RETURN
4 FLR=0.79788455*SQRT(ZETA)
RETURN
END

```

```

VIT FOR INTEG
SUBROUTINE INTEG(XLA,XUA,NL,NLPI,ANS,K1,K2,HVL,GAM2,SGAMP,NRITE4)
DIMENSION TA(11,11),T1(11,11),T2(11,11),T3(11,11),TB(11,11),ANS(11
1,11),GAM2(10,12),SGAMP(10,12),HVL(80)
DIMENSION DXX(50)
COMMON/NINTEG/CMAG,ERR,FRAC

```



```

LOGICAL SWCHX
H=(XUA-XLA)*FRAC
RERR = 1. / ERR
DX = H
FX=DX
XA = XLA
SWCHX = .FALSE.
NREJE=0
NCOUNT=1
DO 300 I=1,NL
DO 300 J=1,I
300 ANS(I+1,J)=0.
CALL INTRND(XA,TA,NL,NLPI,K1,K2,HVL,GAM2,SGAMP)
401 X1 = XA + DX
X2 = X1 + DX
X3 = X2 + DX
XB = X3 + DX
DX13=0.33333333*DX
DX23=0.66666667*DX
C TEST FOR END OF X INTERVAL
C IF( XB - XUA )405,404,403
403 IF OVERSTEPPING END, ADJUST
DX = 0.25 * ( XUA - XA )
DX23=0.66666667*DX
DX13=0.33333333*DX
X1 = XA + DX
X2 = X1 + DX
X3 = X2 + DX
XB = XUA
404 SWCHX = .TRUE.
C USE TEMPORARY STORAGE TO SAVE RECOMPUTING FUNCT
405 CALL INTRND(X1,I1,NL,NLPI,K1,K2,HVL,GAM2,SGAMP)
CALL INTRND(X2,I2,NL,NLPI,K1,K2,HVL,GAM2,SGAMP)
CALL INTRND(X3,I3,NL,NLPI,K1,K2,HVL,GAM2,SGAMP)
CALL INTRND(XB,IB,NL,NLPI,K1,K2,HVL,GAM2,SGAMP)
IF(NCOUNT.GT.50)GO TO 901
DXX(NCOUNT)=DX
901 CONTINUE
DO 700 I=1,NL
IPI=I+1

```

```

DO 600 J=1,I
AU=2.*T2(IP1,J)
ABC=TA(IP1,J)+ TB(IP1,J)+AB
COARSE AND FINE APPROXIMATIONS
S1=DX23*(ABC+AB)
S2=DX13*(ABC+4.*(T1(IP1,J)+T3(IP1,J)))
DEL S = S2 - S1
FORM TEST RATIO
IF(IP1.GT.2)GO TO 423
450 RATIO = (RERR * ABS(DEL S) ) / AMAX1(ABS(S2), CMAG )
HT = DX
C RATIO TEST
500 IF( RATIO - 1.0 )502,501,501
502 IF( RATIO - 0.5 )504,503,503
504 IF( RATIO - .01 )506,406,406
C REJECT CYCLE, BRANCH TO X LINE OR Y STRIP.
501 HT = 0.66666667 * HT
GO TO 402
C ACCEPT CYCLE, BRANCH TO X LINE OR Y STRIP
503 HT = 0.66666667 *.HT
GO TO 406
506 HT = 1.5 * HT
C RESUME X LINE
406 HX=AMIN1(HT,HX)
DX = HT
C ADD EXTRAPOLATED VALUE TO PARTIAL SUM.
423 ANS(IP1,J)=ANS(IP1,J)+S2+0.066666667*DELS
600 CONTINUE
700 CONTINUE
C CHECK SWCHX IF DONE, IF NOT MAKE ANOTHER PASS
IF(SWCHX)GO TO 800
GO TO 407
C RETURN FROM RATIO, CYCLE REJECTED.
402 DX = HT
NREJE=NREJE+1
SWCHX = .FALSE.
GO TO 401
C STEP FOR NEW PASS, FIFTH ORDINATE IS NOW FIRST.
407 XA = XB
NCOUNT=NCOUNT+1

```

```

DO 408 I=1,NL
  IP1=I+1
  DO 408 J=1,I
    408 TA(IP1,J)=TB(IP1,J)
  GO TO 401
800 CONTINUE
  XULA=XUA-XLA
  DO 820 I=1,NL
    DO 820 J=1,I
      IF(ANS(I+1,J).GT.XULA)ANS(I+1,J)=XULA*0.9999999990
820 CONTINUE
  IF(NRITE4.LE.0)RETURN
  HXR=HX/XULA
  WRITE(6,100)NCOUNT,HX,ERR,XULA,HXR
  WRITE(6,101)NREJE
  IF(NCOUNT.GT.50)NCOUNT=50
  WRITE(6,102)
  WRITE(6,103)(DXX(I), I=1,NCOUNT)
100 FORMAT(9H NCOUNT =,I6,16H SMALLEST STEP =,E12.5,7H ERR =,E12.5,
101 FORMAT(8H NREJE =,I12)
102 FORMAT(20H DXX(I) VALUES BELOW)
103 FORMAT(12E11.3)
  RETURN
  END

```

```

VIT FOR INTRND
SUBROUTINE INTRND(XX,PRODK,N,NP1,K1,K2,HVL,GAM2,SGAMP)
DIMENSION PRODK(11,11),GAM2(10,12),SGAMP(10,12),HVL(80),TIJ(10),EX
1PTIJ(10),HVLNU(12)
  K11=K1-1
  DO 20 K=K1,K2
    KM=K-K11
    20 HVLNU(KM)=(XX-HVL(K))**2
  DO 50 I=1,N
    TIJ(I)=0.
  DO 30 K=K1,K2
    KN=K-K11
    TIKJ=SGAMP(I,KM)/(HVLNU(KM)+GAM2(I,KM))

```

```

30 TIJ(I)=TIJ(I)+TIKJ
   EXPTIJ(I)=EXPF(-TIJ(I))
   IPI=I+1
   PRODK(IPI,IPI)=1.0
   DO 40 J=1,I
   IJ=IPI-J
40 PRODK(IPI,IJ)=PRODK(IPI,IJ+1)*EXPTIJ(IJ)
   DO 45 J=1,I
45 PRODK(IPI,J)=1.0-PRODK(IPI,J)
50 CONTINUE
   RETURN
   END

VIT FOR DOUBL
SUBROUTINE DOUBL(X,XT,Y,YT,Z,ZT,IL,NX,NY,NZ)
DIMENSION XT(3),YT(14),ZT(14,3,3),Z(10,4)
10 I=1
4 IF(YT(I)-Y)1,2,3
1 I=I+1
IF(I.EQ.NY)GO TO 8
2 RY=1.0
GO TO 20
3 IF(I.EQ.1)I=2
8 RY=(Y-YT(I-1))/(YT(I)-YT(I-1))
20 J=1
14 IF(XT(J)-X)11,12,13
11 J=J+1
IF(J.EQ.NX)GO TO 18
GO TO 14
12 RX=1.0
GO TO 30
13 IF(J.EQ.1)J=2
18 RX=(X-XT(J-1))/(XT(J)-XT(J-1))
30 DO 40 N=1,NZ
ZA=RY*(ZT(I,J-1,N)-ZT(I-1,J-1,N))+ZT(I-1,J-1,N)
ZB=RY*(ZT(I,J,N)-ZT(I-1,J,N))+ZT(I-1,J,N)
40 Z(IL,N)=RX*(ZB-ZA)+ZA
RETURN
END

```

END

VIT FOR PROPT

SUBROUTINE PROPT(P,H,V,T,Z,I,J)

DIMENSIONPT(4),HT(4),BO(4,3),B1(4,3),B2(4,3),B3(4,3),B4(4,3),
1 A0(4,3),A1(4,3),A2(4,3),A3(4,3),A4(4,3),A5(4,3),C0(3),C1(3),C4(3)
2),C5(3),C2(3),C3(3),D0(3),D1(3),D2(3),D3(3),D4(3),D5(3),B5(4,3)
3,E0(4,3),E1(4,3),E2(4,3),E3(4,3),E4(4,3),F0(3),F1(3),F2(3),F3(3),
4F4(3)

DATA((A0(I,J),I=1,4),J=1,3)/1.1835678E-1,1.0487607E-1,9.6979514E-2
1,1.1613734E-1,-1.5819349,-1.9278666,-1.8226109,-1.2891001,1.920540
26,192.95706,28.774962,-7.3068604E-2/((A1(I,J),I=1,4),J=1,3)/6.581
52617E-1,9.5327098E-1,1.1433393,1.0843619,3.3455871,3.8547943,3.6499
43767,2.5154559,-5.1167326,-132.56946,-13.395786,93749066 / ,((A2(
5I,J),I=1,4),J=1,3)/9.3439634E-1,2.2467991E-3,-3.5657184E-1,1.10343
620E-1,-1.8624081,-2.0904657,-1.7229472,-1.0005790,2.2507384,35.826
7685,2.1445183,-.19204991 / ,((A3(I,J),I=1,4),J=1,3)/-3.053483,-1.5
8121987,-1.0256365,-1.6526663,+5.2266841,+5.7519457,+4.3881665,+2.11
912489,-.37221565,-4.7585249,-.11088207,1.5081737E-2/((A4(I,J),I=1
1,4),J=1,3)/2.4147548,1.5027109,1.0029850,1.3729724,-7.2395315E-2,-
27.8194046E-2,-5.5808957E-2,-2.2369219E-2,2.7502427E-2,3.1126795,0.
3,0. / ,((A5(I,J),I=1,4),J=1,3)/-.58669396,-.30545366,-.24502322,-.3
43199664,3.9710259E-3,4.2031910E-3,2.8371443E-3,9.6330532E-4,-7.470
5516E-4,-8.0365421E-3,0.0. /

DATA ((B0(I,J),I=1,4),J=1,3)/4.1466486,3.4124600,3.1948184,3.77508
171,-127.24814,-142.84936,-135.49011,-73.263048,-635.40412, 25708.6
208,3671.9114,117.14926/((B1(I,J),I=1,4),J=1,3)/31.607714,45.71565
35,50.919528,48.311173,255.36017,273.19929,248.8272,134.73468,-173.
410620,-17743.649,-1746.7649,17.900484/((B2(I,J),I=1,4),J=1,3)/70.
5980384,22.226337,16.382194,36.479840,-138.07613,-141.79945,-116.59
6636,-36.334566,183.82531,4824.4025,285.18962,-2.9186889/((B3(I,J)
7,I=1,4),J=1,3)/-170.31562,-83.560087,-73.823582,-98.644062,40.6781
868,40.480512,31.199285,6.1591101,-36.014227,-642.77878,-14.827085,
9.75179851/((B4(I,J),I=1,4),J=1,3)/127.68093,63.467061,57.745495,7
12.579584,-5.8860258,-5.672231,-4.1153845,-.42335399,2.8527773,42.
215.685,0.0. / ,((B5(I,J),I=1,4),J=1,3)/-29.994045,-13.608968,-12.95
36107,-16.722375,33852682,31539598,21737420,9.2513935E-3,-8.1544
4340E-2,-1.0911416,0.0. /
DATA((E0(I,J),I=1,4),J=1,3)/.9020421,.89964231,.90237509,.88730931

```

1,1.2756413,1.3501822,1.3665294,1.4055444,2.8602478,2.86146,-.13604
2584,-.640844/,((E1(I,J),I=1,4),J=1,3)/1.3765963,1.3061862,1.168661
38,1.129664,.50509824,.44379041,.3933847,.33971451,.16921459,.15494
49,1.0478795,1.1224999/,((E2(I,J),I=1,4),J=1,3)/-1.5847662,-1.46265
525,-1.1587565,-1.058127,-.54156490E-2,.97737477E-3,.48567755E-2,.8
62709458E-2,.25006779E-2,.32019459E-2,-.6454679E-1,-.66709173E-1/,
7(E3(I,J),I=1,4),J=1,3)/1.5546703,1.4298675,1.1151654,.95701218,.0,
8.0,.0,.0,.0,.0/,((E4(I,J),I=1,4),J=1,3)/-.51615931,-.4698722
9,-.36066937,-.29414222,.0,.0,.0,.0,.0,.0,0/
DATA(PT(I),I=1,4)/-2.0,-1.0,0.0,1.0/, (HT(I),I=1,4)/11.0,9.9,7.43,6
1.78/
900 FORMAT(1H 2E30.8)
994 FORMAT(25H= PRESSURE IS ABOVE TABLE)
995 FORMAT(25H= ENTHALPY IS ABOVE TABLE)
PL=ALOG10(P)
IF(H=0.01)100,100,102
100 H=0.01
GO TO 1
102 IF(H=0.0785)1,1,2
1 T=SQRT(0.264+2.642*H)-0.5138
V=40.27*T
Z=1.0
RETURN
H2=H**2
H3=H2*H
H4=H3*H
H5=H4*H
IF(IJ)3,19,19
3 DO 4 I=1,4
IF(PL-PT(I))5,15,4
4 CONTINUE
I=4
GO TO 17
5 IF(I=1)999,999,17
999 I=2
GO TO 17
15 DO 16 J=1,3
F0(J)=E0(I,J)
F1(J)=E1(I,J)
F2(J)=E2(I,J)

```

```

F3(J)=E3(I,J)
F4(J)=E4(I,J)
C0(J)=B0(I,J)
C1(J)=B1(I,J)
C2(J)=B2(I,J)
C3(J)=B3(I,J)
C4(J)=B4(I,J)
C5(J)=B5(I,J)
D0(J)=A0(I,J)
D1(J)=A1(I,J)
D2(J)=A2(I,J)
D3(J)=A3(I,J)
D4(J)=A4(I,J)
16 D5(J)=A5(I,J)
GO TO 19
17 RR=(PL-PT(I-1))/(PT(I)-PT(I-1))
DO 18 J=1,3
FC(J)=E0(I-1,J)+RR*(E0(I,J)-E0(I-1,J))
F1(J)=E1(I-1,J)+RR*(E1(I,J)-E1(I-1,J))
F2(J)=E2(I-1,J)+RR*(E2(I,J)-E2(I-1,J))
F3(J)=E3(I-1,J)+RR*(E3(I,J)-E3(I-1,J))
F4(J)=E4(I-1,J)+RR*(E4(I,J)-E4(I-1,J))
C0(J)=B0(I-1,J)+RR*(B0(I,J)-B0(I-1,J))
C1(J)=B1(I-1,J)+RR*(B1(I,J)-B1(I-1,J))
C2(J)=B2(I-1,J)+RR*(B2(I,J)-B2(I-1,J))
C3(J)=B3(I-1,J)+RR*(B3(I,J)-B3(I-1,J))
C4(J)=B4(I-1,J)+RR*(B4(I,J)-B4(I-1,J))
C5(J)=B5(I-1,J)+RR*(B5(I,J)-B5(I-1,J))
D0(J)=A0(I-1,J)+RR*(A0(I,J)-A0(I-1,J))
D1(J)=A1(I-1,J)+RR*(A1(I,J)-A1(I-1,J))
D2(J)=A2(I-1,J)+RR*(A2(I,J)-A2(I-1,J))
D3(J)=A3(I-1,J)+RR*(A3(I,J)-A3(I-1,J))
D4(J)=A4(I-1,J)+RR*(A4(I,J)-A4(I-1,J))
D5(J)=A5(I-1,J)+RR*(A5(I,J)-A5(I-1,J))
18 IF(H-1.5)20,20,21
19 J=1
GO TO 25
21 IF(H-5.5)22,22,23
22 J=2
GO TO 25

```

```

23 IF(H-HT(I))24,24,998
998 WRITE (6,995)
X=HT(I)
V=C0(2)+X*(C1(3)+X*(C2(3)+X*(C3(3)+X*(C4(3)+X*C5(3))))
T=D0(3)+X*(D1(3)+X*(D2(3)+X*(D3(3)+X*(D4(3)+X*D5(3))))
Z=F0(3)+X*(F1(3)+X*(F2(3)+X*(F3(3)+X*(F4(3))))
HX=H/X
Z=Z*HX*.051
T=T*HX*.036
V=V*HX*.087
RETURN
24 J=3
25 V=C0(J)+C1(J)*H+C2(J)*H2+C3(J)*H3+C4(J)*H4+C5(J)*H5
T=D0(J)+D1(J)*H+D2(J)*H2+D3(J)*H3+D4(J)*H4+D5(J)*H5
Z=F0(J)+F1(J)*H+F2(J)*H2+F3(J)*H3+F4(J)*H4
IJ=2
RETURN
END

FIT FOR ABSORP
SUBROUTINE ABSORP(T,V,XN,IKT,SPMU,IL,K)
CHARMSTRONG CONTINUUM,LMSC4-17-66-5
C XN=-LOG10(PART/AIR ATOM),SIGA=LOG10(CROSS-SECTION)+38,IL=LAYER NUMBER,
C K=BAND NUMBER,NI AND OI ONLY,PLANCK MEANS EXCEPT J=7-10,14
DIMENSION IKT(2,10),XN(10,4),TC(14,27)
COMMON/MABSPC/RTEM(20),IRTEM(20),INTFRE
COMMON/MGADAS/FCONTN
DATA(TC(I,J),J=1,9),I=1,14)/
1.25649, 0.500, 0.500, 0.500, 0.500, 0.500, 0.500, 0.500, 15.103, 17.204, 17.412,
2.34466, 4.996, 3.788, 2.469, 1.980, 1.415, 16.604, 18.212, 18.416,
3.43082, 9.515, 9.439, 9.566, 9.847, 10.607, 17.501, 18.824, 19.021,
4.51699, 11.671, 11.552, 11.503, 11.665, 12.426, 18.096, 19.230, 19.425,
5.60315, 13.311, 13.055, 12.904, 12.990, 13.723, 18.513, 19.522, 19.710,
6.68932, 14.541, 14.160, 13.962, 13.998, 14.695, 18.820, 19.738, 19.919,
7.66165, 16.256, 15.756, 15.485, 15.431, 16.047, 19.235, 20.028, 20.198,
81.0340, 17.394, 16.808, 16.465, 16.398, 16.939, 19.495, 20.209, 20.373,
91.2063, 18.200, 17.558, 17.188, 17.091, 17.568, 19.669, 20.330, 20.487,
A1.3786, 18.796, 18.115, 17.725, 17.603, 18.030, 19.787, 20.405, 20.556,
51.5510, 19.245, 18.536, 18.131, 17.991, 18.373, 19.862, 20.445, 20.593,
EV, LOG+
38, 2-9
2-9
2-9
2-9
2-9
2-9
2-9
2-9
2-9
2-9
2-9

```



```

C1.7233,19.589,18.857,18.440,18.281,18.625,19.901,20.454,20.597,
D1.8956,19.829,19.084,18.660,18.489,18.801,19.905,20.431,20.570,
E2.0679,20.007,19.250,18.619,18.634,18.918,19.882,20.383,20.518/
DATA((TC(I,J),J=10,16),I=1,14)/
120.895, 0.500, 0.500, 0.500,20.605, 0.500, 0.500, 0.500, 0.500, 0.500,
220.695, 5.162, 6.549, 8.243,20.604, 4.919, 6.103, 3.780, 6.824,
320.696, 9.560, 9.868,10.803,20.602, 9.361, 9.759, 9.448,10.018,
420.898,11.664,11.794,12.501,20.600,11.621,11.817,11.549,11.955,
520.902,13.244,13.169,13.710,20.595,13.180,13.291,12.033,13.326,
620.907,14.461,14.215,14.618,20.591,14.329,14.397,14.137,14.356,
720.915,16.086,15.691,15.903,20.580,15.894,15.879,15.664,15.786,
820.925,17.181,16.688,16.774,20.568,16.902,16.847,16.666,16.734,
920.931,17.976,17.415,17.409,20.556,17.597,17.531,17.371,17.411,
A20.930,18.556,17.960,17.892,20.541,18.100,18.030,17.886,17.915,
B20.915,19.045,18.401,18.273,20.521,18.470,18.428,18.270,18.312,
C20.882,19.407,18.738,18.566,20.487,18.745,18.725,18.556,18.614,
D20.824,19.688,18.996,18.818,20.439,18.932,18.963,18.755,18.861,
E20.750,19.896,19.189,18.979,20.392,19.061,19.123,18.894,19.025/
DATA((TC(I,J),J=19,27),I=1,14)/
1 0.500, 0.500, 0.500, 0.500, 0.500, 0.500, 0.500, 0.500, 0.500, 0.500,
2 5.302, 4.577, 3.836, 3.228, 2.466, 5.466, 4.753, 6.161, 7.209,
3 9.314, 9.316, 9.434, 9.459, 9.578, 9.498, 9.584, 9.831, 9.981,
4 11.781,11.626,11.575,11.491,11.517,11.645,11.671,11.763,11.821,
5 13.479,13.248,13.102,12.949,12.916,13.439,13.166,13.181,13.144,
6 14.752,14.465,14.248,14.048,13.973,14.670,14.386,14.254,14.146,
7 15.530,16.164,15.855,15.597,15.465,16.357,15.995,15.761,15.589,
8 17.709,17.292,16.928,16.639,16.467,17.494,17.081,16.781,16.568,
9 18.544,18.091,17.693,17.386,17.182,18.318,17.868,17.525,17.286,
A 19.162,18.684,18.261,17.942,17.708,18.913,16.447,16.081,17.826,
B 19.626,19.129,18.689,18.364,18.103,19.424,18.929,18.533,18.263,
C 19.984,19.469,19.016,18.685,18.397,19.800,19.290,18.876,18.597,
D 20.234,19.709,19.247,18.915,18.606,20.090,19.568,19.141,18.854,
E 20.420,19.885,19.416,19.082,18.752,20.307,19.774,19.338,19.046/
IF(K.GT.1)GO TO 20
10 I=1
4 IF(TC(I,1)-T)1,2,3
1 I=I+1
IF(I.EQ.14)GO TO 8
GO TO 4
2 R=1.0

```

2-9

2-9

2-9

LOG+38

10-18

10-18

10-18

10-18

10-18

10-18

10-18

10-18

10-18

10-18

10-18

10-18

10-18

10-18

10-18

10-18

LOG+38

19-27

19-27

19-27

19-27

19-27

19-27

19-27

19-27

19-27

19-27

19-27

19-27

19-27

19-27

```

GO TO 20
3 IF(I.EQ.1)I=2
8 R=(T-TC(I-1,1))/(TC(I,1)-TC(I-1,1))
20 SMU=0.0
RTEM(IL)=R
IRTEM(IL)=I
DO 30 N=1,2
JA=IKT(N,K)
SIGA=R*(TC(I,JA)-TC(I-1,JA))+TC(I-1,JA)
AB=-18.295+SIGA-XN(IL,N)
AB=10.0**AB
IF((JA.LT.7).OR.((JA.GT.10).AND.(JA.NE.14)))AB=AB*FCNTN
30 SMU=SMU+AB
SPMU=SMU/V
RETURN
END

VIT FOR SPABCO
SUBROUTINE SPABCO(SPMUC,K,J,TT,C1,C2,C3,C4,C5,C9,C10,C14,C15,C18,
IC21,C23,SPM1,SPM2,SPM3,SPM5,SPM6,SPM8,SPM9,SPM)
COMMON/SPABN/COSR(25)
COMMON/SPABST/FC2(10),FCO(10),FH(10),FC1(10),FCP(10)
GO TO (10,11,11,11,11,20,21,30,40,50,51,60,61,70,80,81,81,90,91,91
1,91),K
10 C1=FC2(J)*COSR(1)
C2=FC2(J)*COSR(2)
C3=FC2(J)*COSR(3)
C4=FC2(J)*COSR(4)
C5=FC2(J)*COSR(5)
C9=FCO(J)*COSR(9)
C10=FCO(J)*COSR(10)
C14=FH(J)*COSR(14)*EXP(-10.2/TT)
C15=FH(J)*COSR(15)
C18=FC1(J)*COSR(18)
C21=FCP(J)*COSR(21)*EXP(-5.4/TT)
C23=FCP(J)*COSR(23)*1.0E-18
SPMUC=C1*1.81E-16*EXP(-1.20/TT)
SPMUC=SPMUC*10.0
SPMUC=SPMUC+C23*FCP(J)*2.43E-18/SQRT(TT)

```

```

SPM1=SPMUC
RETURN
11 SPMUC=SPM1
RETURN
20 SPMUC=C1 *1.14E-16+C2*3.94E-18*EXP(-0.29/TT)+C3*3.26E-18*EXP(-0.65
1/TT)
SPM2=SPMUC
RETURN
21 SPMUC=SPM2
RETURN
30 SPMUC=C1*3.19E-18*EXP(-0.27/TT)+C2*2.44E-17+C3*1.31E-17*EXP(-0.79/
1TT)+C4*2.41E-16*EXP(-1.52/TT)+C14*3.38E-17
SPM3=SPMUC
RETURN
40 SPMUC=C3*4.5E-19*EXP(-1.17/TT)+C4*3.98E-16*EXP(-.72/TT)+C5*1.5E-17
1+C9*3.52E-17*EXP(-1.6/TT)+C14*1.19E-17
SPMUC=SPMUC+SPM3
RETURN
50 SPMUC=C9*6.23E-17+C14*5.55E-18+C18*2.0E-19*EXP(-7.46/TT)
SPM5=SPMUC
RETURN
51 SPMUC=SPM5
RETURN
60 SPMUC=C9*6.75E-17+C14*3.09E-18+C18*1.3E-18*EXP(-2.67/TT)
SPM6=SPMUC
RETURN
61 SPMUC=SPM6
RETURN
70 SPMUC=C9*6.35E-18*EXP(-0.46/TT)+C14*2.1E-18+C18*2.05E-17*EXP(-1.26
1/TT)
RETURN
80 SPM=C18*1.8E-17*(1.0+1.17*EXP(-1.26/TT))
SPMUC=SPM+C14*1.32E-18
SPM8=SPMUC
RETURN
81 SPMUC=SPM8
RETURN
90 SPMUC=SPM+C10*1.0E-17+C15*4.85E-18+C21*3.4E-20/TT
SPM9=SPMUC
RETURN

```

```

91 SPHUC=SPM9
RETURN
END

```

```

VIT FOR PROT

```

```

SUBROUTINE PROT(XX,XT,YY,YT,ZP,ZT,AA,AT,BB,BT,CC,CT,DD,DT,EE,ET,F
1,FT,NL,ML)
CEC3208 DOUBLE INTERPOLATION SUBROUTINE
DIMENSION ZT(NL),YT(NL,ML),XT(NL,ML),AT(NL,ML),BT(NL,ML),CT(NL,ML)
1,DT(NL,ML),ET(NL,ML),FT(NL,ML)
ZT=ALOG10(ZP)
801 IF(ZZ-ZT(1)) 802,801,801
802 IF(XX-XT(1,1))802,803,803
802 YY = 0.0
L=2
LM=1
IF(ZZ-ZT(1)).LT.0.0.AND.XX-XT(1,1).GT.0.0)GO TO 902
GO TO 906
803 DO 800 I=1,NL
L=I
LL=I-1
IF (ZZ-ZT(I)) 902,804,800
800 CONTINUE
L=2
LM=1
GO TO 906
902 A=ZZ-ZT(LL)
B=ZI(L)-ZT(LL)
RATIP = A/B
GO TO 1111
804 DO904 J=1,ML
LLM=J
LLM=J-1
IF (XX-XT(L,J)) 905,906,904
904 CONTINUE
L=2
LM=20
GO TO 906
905 A=XX-XT(L,LLM)

```

```

$ A202
$ B202
$ C202

```

```

$ 202
$ 203
$ 204
$ 205
$ 206

```

```

$ 207
$ 208
$ 2

```

```

$ 210
$ 211
$ 212
$ 213
$ 214

```

```

$ 215

```

\$ 216
\$ 217
\$ 218
\$ 219

\$ 220
\$ 221

\$ 222
\$ 223
\$ 224
\$ 225

B=XT(L,LM)-XT(L,LLM)
RATIO=A/B
C=YT(L,LM)-YT(L,LLM)
YY = C*RATIO+YT(L,LLM)
C=AT(L,LM)-AT(L,LLM)
AA=C*RATIO+AT(L,LLM)
C=BT(L,LM)-BT(L,LLM)
BB=C*RATIO+BT(L,LLM)
C=CT(L,LM)-CT(L,LLM)
CC=C*RATIO+CT(L,LLM)
C=DT(L,LM)-DT(L,LLM)
DD=C*RATIO+DT(L,LLM)
C=ET(L,LM)-ET(L,LLM)
EE=C*RATIO+ET(L,LLM)
C=FT(L,LM)-FT(L,LLM)
FF=C*RATIO+FT(L,LLM)

YY=10.0**YY
FF=10.0**FF
EE=10.0**EE
DD=10.0**DD
CC=10.0**CC
BB=10.0**BB

RETURN

906 YY = YT(L,LM)

AA=AT(L,LM)
BB=BT(L,LM)
CC=CT(L,LM)
DD=DT(L,LM)
EE=ET(L,LM)
FF=FT(L,LM)
YY=10.0**YY
FF=10.0**FF
EE=10.0**EE
DD=10.0**DD
CC=10.0**CC
BB=10.0**BB

RETURN

1111 DO 913 J=1,ML
LM=J
LLM=J-1

\$ 226
\$ 227

```

913 IF (XX-XT(L,J)) 911,912,913
CONTINUE
L=2
LM=20
GO TO 906
912 C1=YT(L,LM)
C2=AT(L,LM)
C3=BT(L,LM)
C4=CT(L,LM)
C5=DT(L,LM)
C6=ET(L,LM)
C7=FT(L,LM)
2005 DO 2000 J=1,ML
LM=J
LLM=J-1
IF (XX-XT(LL,J)) 2001,2002,2000
CONTINUE
L=2
LM=20
GO TO 906
2002 YY=YT(LL,LM)+RATIP*(C1-YT(LL,LM))
AA=AT(LL,LM)+RATIP*(C2-AT(LL,LM))
BB=BT(LL,LM)+RATIP*(C3-BT(LL,LM))
CC=CT(LL,LM)+RATIP*(C4-CT(LL,LM))
DD=DT(LL,LM)+RATIP*(C5-DT(LL,LM))
EE=ET(LL,LM)+RATIP*(C6-ET(LL,LM))
FF=FT(LL,LM)+RATIP*(C7-FT(LL,LM))
YY=10.0**YY
FF=10.0**FF
EE=10.0**EE
DD=10.0**DD
CC=10.0**CC
BB=10.0**BB
RETURN
2001 RATIO=(XX-XT(LL,LLM))/(XT(LL,LM)-XT(LL,LLM))
C11=YT(LL,LLM)+RATIO*(YT(LL,LM)-YT(LL,LLM))
C22=AT(LL,LLM)+RATIO*(AT(LL,LM)-AT(LL,LLM))
C33=BT(LL,LLM)+RATIO*(BT(LL,LM)-BT(LL,LLM))
C44=CT(LL,LLM)+RATIO*(CT(LL,LM)-CT(LL,LLM))
C55=DT(LL,LLM)+RATIO*(DT(LL,LM)-DT(LL,LLM))

```

```

C66=ET(LL,LLM)+RATIO*(ET(LL,LM)-ET(LL,LLM))
C77=FT(LL,LLM)+RATIO*(FT(LL,LM)-FT(LL,LLM))
YY=C11+RATIP*(C1-C11)
AA=C22+RATIP*(C2-C22)
BB=C33+RATIP*(C3-C33)
CC=C44+RATIP*(C4-C44)
DD=C55+RATIP*(C5-C55)
EE=C66+RATIP*(C6-C66)
FF=C77+RATIP*(C7-C77)
YY=10.0**YY
FF=10.0**FF
EE=10.0**EE
DD=10.0**DD
CC=10.0**CC
BB=10.0**BB
RETURN
911 RATIO=(XX-XT(L,LLM))/(XT(L,LM)-XT(L,LLM))
C1=YT(L,LLM)+RATIO*(YT(L,LM)-YT(L,LLM))
C2=AT(L,LLM)+RATIO*(AT(L,LM)-AT(L,LLM))
C3=BT(L,LLM)+RATIO*(BT(L,LM)-BT(L,LLM))
C4=CT(L,LLM)+RATIO*(CT(L,LM)-CT(L,LLM))
C5=DT(L,LLM)+RATIO*(DT(L,LM)-DT(L,LLM))
C6=ET(L,LLM)+RATIO*(ET(L,LM)-ET(L,LLM))
C7=FT(L,LLM)+RATIO*(FT(L,LM)-FT(L,LLM))
GO TO 2005
END

```

```

VIT FOR SESB
SUBROUTINE SESB(P,HB,VB,TW)
DIMENSION PT(3),HT(3),VT(3),TT(3)
DATA(PT(I),I=1,3)/-1.0,0.0,1.0/, (HT(I),I=1,3)/0.882,0.882,0.882/,
1(VT(I),I=1,3)/14.45,13.37,13.82/, (TT(I),I=1,3)/0.31,0.342,0.388/
PL=ALOG10(P)
I=1
4 IF(PT(I)-PL)1,2,3
1 I=I+1
GO TO 4
2 HB=HT(I)
VB=VT(I)/P

```

```

TW=TT(I)
RETURN
3 R=(PL-PT(I-1))/(PT(I)-PT(I-1))
RR=1.0-R
HB=R*HT(I)+RR*HT(I-1)
VB=(R*VT(I)+RR*VT(I-1))/P
TW=R*TT(I)+RR*TT(I-1)
RETURN
END

```

VT FOR PLANCK

```

SUBROUTINE PLANCK(FNUL,FNUU,T,FBB)

```

```

N=0
I=1
X=FNUL/T
1 IF(X<0.30)2,2,3
2 X2=X*X
FBB=0.153990*X*X2*(0.333333333-0.125*X+X2*(0.01666667-X2*1.984127E-
14))
GO TO 19
3 IF(X<2.0)4,4,5
4 X2=X*X
FBB=0.153990*X*X2*(0.333333333-0.125*X+X2*(0.01666667+X2*(-1.984127
1E-4+X2*(3.6743092E-6+X2*(-7.5156325E-8+X2*1.6059025E-9))))
GO TO 19
5 N=N+1
FBB=0.0
IF(X<5.0)6,6,7
6 MT=5
GO TO 14
7 IF(X<10.0)8,9,9
8 MT=4
GO TO 14
9 IF(X<15.0)10,11,11
10 MT=3
GO TO 14
11 IF(X<20.0)12,13,13
12 MT=2
GO TO 14

```

PL 1
PL 2
PL 3
PL 4
PL 5
PL 6
PL 7
PL 8
PL 9
PL 10
PL 11
PL 12
PL 13
PL 14
PL 15
PL 16
PL 17
PL 18
PL 19
PL 20
PL 21
PL 22
PL 23
PL 24
PL 25
PL 26
PL 27
PL 28

PL29
PL30
PL31

PL34
PL35
PL36
PL37
PL38
PL39
PL40
PL41
PL42
PL43

PL45
PL46
PL47
PL48

```
13 MT=1
14 FBS=0.0
15 DO 17 M=1,MT
16 CM=M
17 X2=CM*X
18 FDB=FDB+EXPF(-X2)*((X2+3.0)*X2+6.0)*X2+6.0)/CM**4
19 CONTINUE
20 FDB=FDB*0.153990
21 IF(I-1)20,20,21
22 FBB1=FBB
23 I=I+1
24 X=FNUU/T
25 GO TO 1
26 IF(M-1)22,23,24
27 FBB=FBB-FBB1
28 GO TO 25
29 FDB=1.0-FDB-FBB1
30 GO TO 25
31 FDB=FBB1-FBB
32 RETURN
33 END
34 VIT FOR EXPF
35 FUNCTION EXPF(X)
36 IF(ABS(X)-85.0)1,1,2
37 2 X=85.0*X/ABS(X)
38 1 EXPF=EXP(X)
39 RETURN
40 END
```

```
VIT FOR VEL
SUBROUTINE VEL(LA06,SIT,VI,FUI ,DZETA,AE,CLI,N,ANS,FUE,AEYZ,DY,
1FVA,FUA,DYER2)
DIMENSION ZETA(40),VIJ(40),FU(40),FV(40),SIT(13),VI(13),FVA(10),FU
1A(10),DY(10)
ZETA(1)=0.0
FV(1)=1.0
FU(1)=FUI
5 FDFW=1.0
DO 6200 J=1,39
```

```

CALL TBLP4(ZETA(J),SIT,VIJ(J),VI,DUM,FV,DUM,FU,1)
GO TO (10,20),LAOB
10 DX=DYER2/VIJ(J)
GO TO 25
20 DX=DZETA
25 DFV=FU(J)*DX
DFU=(FU(J)**2-AE*VIJ(J))*DX/(CL1*FV(J))
TEH=FV(J)+DFV
IF(TEM)6201,6202,6202
6201 FDFW=-FV(J)/DFV
6202 FU(J+1)=FU(J)+DFU*FDFW
FV(J+1)=FV(J)+DFV*FDFW
ZETA(J+1)=ZETA(J)+DZETA*FDFW
IF(TEM)6203,6203,6200
6200 CONTINUE
DZETA=1.20*DZETA
DYER2=1.20*DYER2
GO TO 5
6203 IF(J-20)6204,6205,6205
6204 C=FLOAT(J)/25.0
DZETA=C*DZETA
DYER2=C*DYER2
GO TO 5
6205 ZETAT=ZETA(J+1)
IF(J.GE.40)CALL EXIT
DSI=ZETAT/ANS
GO TO(35,30),LAOB
30 FUE=FU(J+1)
AEE=AEYZ*DSI
35 DO 6300 I=1,N
SIT(I+1)=SIT(I)+DSI
IF(I.EQ.1)SIT(2)=DSI/2.0
CALL TBLP4(SIT(I+1),ZETA,FVA(I),FV,FUA(I),FU,VI(I+1),VIJ,2)
GO TO (45,40),LABC
40 DY(I)=AEE*VI(I+1)
GO TO 6300
45 DY(I)=DSI
6300 CONTINUE
SIT(N+2)=SIT(N+1)+DSI/2.0
SIT(N+3)=2.0*SIT(N+2)

```

RETURN
END

```
VIT FOR TBLP4
SUBROUTINE TBLP4(A,AT,B,BT,C,CT,D,DT,JF)
DIMENSION AT(20),BT(20),CT(20),DT(20)
I=1
4 IF(AT(I)-A)1,2,3
1 I=I+1
GO TO 4
2 B=BT(I)
IF(JF.EQ.1)RETURN
C=CT(I)
D=DT(I)
RETURN
3 R=(A-AT(I-1))/(AT(I)-AT(I-1))
RR=1.0-R
B=R*BT(I)+RR*BT(I-1)
IF(JF.EQ.1)RETURN
C=R*CT(I)+RR*CT(I-1)
D=R*DT(I)+RR*DT(I-1)
RETURN
END
```

```
VIT FOR MODL1
SUBROUTINE MODL1(FNULL,FNUUU,IKTT,KKK)
DIMENSION FNUL(10),FNUU(10),IKT(2,10)
DIMENSION FNUL(10),FNUUU(10),IKTT(2,10)
DATA(FNUL(I),I=1,2)/.5,10.95/, (FNUU(I),I=1,2)/10.95,30.00/, ((IKT(J
1,I),I=1,2),J=1,2)/15,7,16,13/,KK/2/
KKK=KK
DO 20 I=1,KKK
FNUL(I)=FNUL(I)
FNUUU(I)=FNUUU(I)
DO 10 J=1,2
10 IKTT(J,I)=IKT(J,I)
20 CONTINUE
RETURN
```

END

VIT FOR MODL2

```

SUBROUTINE MODL2(FNULL,FNUUU,IKTTT,KKK)
  DIMENSION FNUL(10),FNUU(10),IKT(2,10)
  DIMENSION FNULL(10),FNUUU(10),IKTTT(2,10)
  DATA(FNUL(I),I=1,3)/.5,10.95,12.15/, (FNUU(I),I=1,3)/10.95,12.15,30
  1.00/, ((IKT(J,I),I=1,3),J=1,2)/15,7,8,16,13,13/,KK/3/
  KKK=KK
  DO 20 I=1,KKK
    FNUL(I)=FNUL(I)
    FNUUU(I)=FNUUU(I)
  DO 10 J=1,2
    10 IKTTT(J,I)=IKT(J,I)
  20 CONTINUE
  RETURN
  END

```

VIT FOR MODL3

```

SUBROUTINE MODL3(FNULL,FNUUU,IKTTT,KKK)
  DIMENSION FNUL(10),FNUU(10),IKT(2,10)
  DIMENSION FNULL(10),FNUUU(10),IKTTT(2,10)
  DATA(FNUL(I),I=1,4)/.5,10.95,12.15,13.61/, (FNUU(I),I=1,4)/10.95,12
  1.15,13.61,30.00/, ((IKT(J,I),I=1,4),J=1,2)/15,7,8,9,16,13,13,14/,KK
  2/4/
  KKK=KK
  DO 20 I=1,KKK
    FNUL(I)=FNUL(I)
    FNUUU(I)=FNUUU(I)
  DO 10 J=1,2
    10 IKTTT(J,I)=IKT(J,I)
  20 CONTINUE
  RETURN
  END

```

VIT FOR MODL4

```

SUBROUTINE MODL4(FNULL,FNUUU,IKTTT,KKK)

```

```

DIMENSION FNUL(10),FNUU(10),IKT(2,10)
DIMENSION FNUL(10),FNUU(10),IKTT(2,10)
DATA(FNUL(I),I=1,5)/.5,10.95,12.15,13.61,14.50/,
(FNUU(I),I=1,5)/10,
1.95,12.15,13.61,14.50,30.00/,
((IKT(J,I),I=1,5),J=1,2)/15,7,8,9,10,
216,13,13,14,14/,KK/5/
KKK=KK
DO 20 I=1,KKK
FNUL(I)=FNUL(I)
FNUU(I)=FNUU(I)
DO 10 J=1,2
10 IKTT(J,I)=IKT(J,I)
20 CONTINUE
RETURN
END

```

```

VIT FOR MODL5
SUBROUTINE MODL5(FNUL,FNUU,IKTT,KKK)
DIMENSION FNUL(10),FNUU(10),IKT(2,10)
DIMENSION FNUL(10),FNUU(10),IKTT(2,10)
DATA(FNUL(I),I=1,4)/.5,2.,10.95,12.15/,
(FNUU(I),I=1,4)/2.,10.95,12
1.15,30.00/,
((IKT(J,I),I=1,4),J=1,2)/2,17,7,8,11,18,13,13/,KK/4/
KKK=KK
DO 20 I=1,KKK
FNUL(I)=FNUL(I)
FNUU(I)=FNUU(I)
DO 10 J=1,2
10 IKTT(J,I)=IKT(J,I)
20 CONTINUE
RETURN
END

```

```

VIT FOR MODL6
SUBROUTINE MODL6(FNUL,FNUU,IKTT,KKK)
DIMENSION FNUL(10),FNUU(10),IKT(2,10)
DIMENSION FNUL(10),FNUU(10),IKTT(2,10)
DATA(FNUL(I),I=1,9)/.5,2.,4.,6.,9.,5,10.95,12.15,13.61,14.50/,
(FNUU
1(I),I=1,9)/2.,4.,6.,9.,5,10.95,12.15,13.61,14.50,30.00/,
((IKT(J,I),
2I=1,9),J=1,2)/2,3,4,5,6,7,8,9,10,11,12,13,13,13,14,14/,KK/9/

```

```

KKK=KK
DO 20 I=1,KKK
FNUL(I)=FNUL(I)
FNUU(I)=FNUU(I)
DO 10 J=1,2
10 IKTT(J,I)=IKT(J,I)
20 CONTINUE
RETURN
END

```

```

VIT FOR MODL7
SUBROUTINE MODL7(FNUL,FNUU,IKTT,KKK)
DIMENSION FNUL(10),FNUU(10),IKT(2,10)
DIMENSION FNUL(10),FNUU(10),IKTT(2,10)
DATA(FNUL(I),I=1,9)/.5,1.,2.,3.,4.,10.95,12.,15,13.,61,14.,50/, (FNUU(
11),I=1,9)/1.,2.,3.,4.,10.95,12.,15,13.,61,14.,50,30.0/, ((IKT(J,I),I=1
2,9),J=1,2)/19,20,21,22,23,7,8,9,10,24,25,26,27,13,13,14,14/,KK/
39/

```

```

KKK=KK
DO 20 I=1,KKK
FNUL(I)=FNUL(I)
FNUU(I)=FNUU(I)
DO 10 J=1,2
10 IKTT(J,I)=IKT(J,I)
20 CONTINUE
RETURN
END

```

```

VIT FOR MODL8
SUBROUTINE MODL8(FNUL,FNUU,IKTT,KKK)
DIMENSION FNUL(10),FNUU(10),IKT(2,10)
DIMENSION FNUL(10),FNUU(10),IKTT(2,10)
DATA(FNUL(I),I=1,5)/.5,2.,4.,10.95,12.,15/, (FNUU(I),I=1,5)/2.,4.,10
1.95,12.,15,30.00/, ((IKT(J,I),I=1,5),J=1,2)/2,3,23,7,8,11,12,13,13,1
23/,KK/5/
KKK=KK
DO 20 I=1,KKK
FNUL(I)=FNUL(I)

```


6	690	2.76	E-11.87	E-20
6	710	3.07	E-11.87	E-20
6	723	6.60	E-21.87	E-20
5	753	1.50	E-24.46	E-21
3	846	1.81	E-22.92	E-21
3	877	4.06	E-24.46	E-21
3	911	5.84	E-23.36	E-21
6	922	1.66	E-23.87	E-20
6	939	3.40	E-23.87	E-20
6	954	4.50	E-23.87	E-20
6	975	4.95	E-23.87	E-20
6	988	1.06	E-23.87	E-20
5	998	1.19	E-13.12	E-21
5	1.009	5.75	E-22.94	E-21
5	1.033	6.33	E-25.36	E-21
5	1.119	7.44	E-24.46	E-21
5	1.170	2.01	E-12.40	E-21
5	1.225	2.93	E-13.04	E-21
5	1.268	6.25	E-23.20	E-21
4	1.319	1.83	E-19.84	E-22
5	1.368	3.89	E-22.29	E-21
4	1.430	5.16	E-19.50	E-22
4	1.509	2.52	E-18.39	E-22
4	1.553	3.01	E-32.93	E-20
4	1.663	9.27	E-29.58	E-22
5	1.675	7.55	E-32.93	E-20
5	1.836	7.13	E-32.93	E-20
5	1.919	1.27	E-22.93	E-20
5	2.075	1.34	E-32.93	E-20
4	2.571	4.63	E-35.51	E-21
4	2.925	1.06	E-25.51	E-21
4	3.107	5.85	E-32.09	E-20
4	3.466	1.72	E-23.90	E-20
4	3.541	3.80	E-35.73	E-20
4	3.849	1.40	E-25.73	E-20
4	3.926	3.20	E-35.73	E-20
3	7.111	6.34	E-29.12	E-22
2	8.302	7.40	E-29.12	E-22
3	8.781	4.35	E-26.61	E-22
3	9.301	1.66	E-24.46	E-21

9	9.394	1.19	E-22.92	E-21
9	9.460	3.60	E-23.36	E-21
2	9.973	8.90	E-26.61	E-22
3	10.102	3.74	E-22.93	E-20
1	10.332	1.84	E-16.21	E-22
1	10.418	2.25	E-25.32	E-20
2	10.483	1.87	E-24.46	E-21
9	10.585	1.31	E-27.96	E-20
2	10.619	5.33	E-23.12	E-21
9	10.662	8.19	E-32.08	E-19
3	10.757	3.18	E-34.37	E-19
1	10.927	4.54	E-11.61	E-23
3	11.200	2.00	E-24.46	E-21
2	11.293	4.18	E-22.93	E-20
3	11.310	2.54	E-23.23	E-21
3	11.550	1.33	E-13.61	E-23
2	11.609	2.50	E-25.32	E-20
2	11.776	1.46	E-27.96	E-20
2	11.874	9.10	E-32.68	E-19
2	11.948	5.75	E-34.37	E-19
3	12.000	2.19	E-22.93	E-20
3	12.316	1.56	E-26.96	E-20
2	12.414	5.74	E-23.90	E-21
2	12.511	2.79	E-23.37	E-21
1	12.877	2.30	E-24.46	E-21
1	13.004	1.32	E-12.94	E-21
2	13.190	4.89	E-22.99	E-20
2	13.508	2.91	E-26.96	E-19
1	13.677	9.57	E-22.93	E-20
1	13.993	5.84	E-25.32	E-20
1	14.160	3.42	E-27.96	E-20
1	14.257	2.12	E-22.68	E-19
1	14.332	1.38	E-24.37	E-19

DATA CARDS FOR TABLE 01
 FOR INPUT FORMATS, SEE MAIN PROGRAM READ STATEMENTS
 NEAR STATEMENT NUMBERS 9, 10
 COLUMN NUMBER

5 0 5 0 5 0 5 0 5 0 5 0

2200+05+8197+05+2431-06+1873+05+7724+13+1673+03+4943+13+7824+16+1836+17
 2500+05+1097+06+1868-06+6913+03+1029+13+2152+01+1289+13+2347+16+1783+17
 0000+00
 3500+04+4600+04+1200-03+2000+19+3000+16+1000+13+5000+18+1000+13+1000+13
 4000+04+6110+04+8800-04+1000+19+4000+18+8500+17+4500+18+7000+13+7000+13
 5000+04+1303+05+3081-04+2012+18+7346+18+6900+17+3834+18+6786+14+5396+14
 6000+04+1622+05+2105-04+2823+17+8635+18+4657+17+2821+18+6611+15+6537+15
 7000+04+1735+05+1750-04+4437+16+7633+18+5013+17+2350+18+3255+16+3251+16
 8000+04+1876+05+1483-04+1046+16+6626+18+7546+16+1993+18+1065+17+1065+17
 9000+04+2019+05+1281-04+3197+15+5618+18+1161+16+1722+16+2626+17+2629+17
 1000+05+2219+05+1105-04+1120+15+4558+18+2023+15+1485+18+5237+17+5248+17
 1100+05+2538+05+9350-05+4064+14+3447+16+3837+14+1212+18+6561+17+9033+17
 1200+05+2990+05+7782-05+1379+14+2365+18+8116+13+9557+17+1217+18+1314+18
 1300+05+3567+05+6430-05+4183+13+1456+18+1741+13+7031+17+1504+18+1678+18
 1400+05+4200+05+5370-05+1149+13+8170+17+3684+12+4718+17+1655+18+1929+18
 1500+05+4795+05+4602-05+3049+12+4355+17+7634+11+2850+17+1683+18+2053+18
 1600+05+5282+05+4065-05+8454+11+2307+17+1564+11+1581+17+1641+18+2079+18
 1700+05+5647+05+3687-05+2580+11+1252+17+3263+10+3411+16+1571+18+2042+18
 1800+05+5919+05+3406-05+8648+10+7067+16+7214+09+4477+16+1495+18+1976+18
 1900+05+6137+05+3135-05+3414+10+4163+16+1741+09+2443+16+1419+18+1898+18
 2000+05+6336+05+2998-05+1468+10+2553+16+4649+06+1381+16+1341+16+1820+18
 2200+05+6807+05+2673-05+3509+09+1059+16+2285+07+4932+15+1165+18+1687+18
 2500+05+8217+05+2194-05+5415+08+3014+15+7309+05+1338+15+7745+17+1582+18
 1000+01
 3500+04+3900+04+1430-02+1000+20+2200+19+8800+13+5000+19+3000+13+3000+13
 4000+04+4170+04+1090-02+7000+19+3000+19+8200+13+4500+19+2000+14+2000+14
 5000+04+8050+04+5550-03+4000+19+4600+19+7000+13+3700+19+2000+15+2000+15
 6000+04+1406+05+2476-03+1622+19+6547+19+5537+13+3070+19+2188+16+1497+16
 7000+04+1658+05+1832-03+3944+18+7197+19+3976+13+2439+19+1025+17+9732+16
 8000+04+1784+05+1541-03+1035+18+6590+19+2570+13+2064+19+3381+17+3335+17
 9000+04+1916+05+1329-03+3488+17+5868+19+9098+17+1783+19+8517+17+8465+17
 1000+05+2044+05+1167-03+1426+17+5144+19+2230+17+1567+19+1763+18+1759+18
 1100+05+2195+05+1031-03+6679+16+4419+19+5365+16+1371+19+3080+18+3219+18
 1200+05+2294+05+9086-04+3353+16+3689+19+1512+16+1192+19+4849+18+5145+18
 1300+05+2661+05+7946-04+1733+16+2963+19+4706+15+1015+19+6897+18+7449+18
 1400+05+3008+05+6893-04+8892+15+2273+19+1558+15+8394+18+8974+18+9899+18
 1500+05+3431+05+5952-04+4427+15+1660+19+5323+14+6681+18+1079+19+1221+19
 1600+05+3913+05+5147-04+2126+13+1157+19+1838+14+5077+18+1212+19+1412+19
 1700+05+4418+05+4488-04+9955+14+7778+18+6344+13+3665+18+1288+19+1548+19
 1800+05+4906+05+3969-04+4646+14+5122+18+2182+13+2516+18+1315+19+1628+19

1900+05+5343+05+3569-04+2218+14+3356+16+7515+12+1661+18+1307+19+1660+19
 2000+05+5716+05+3262-04+1106+14+2216+18+2618+12+1070+18+1279+19+1657+19
 2200+05+6294+05+2827-04+3275+13+1023+18+1809+11+4411+17+1193+19+1592+19
 2500+05+7004+05+2395-04+3163+12+3701+17+8544+09+1298+17+1032+19+1458+19

C DARA CARDS FOR TABLE 04
 C FOR INPUT FORMATS, SEE MAIN PROGRAM READ STATEMENTS
 C NEAR STATEMENT NUMBERS 7020
 C COLUMN NUMBER

C 5 0 5 0 5 0 5 0 5 0 5 0 5 0

04
 23
 0059+00+0200+00+0060+00+0020+00+0200+00+0000+00+*00 + + + 170+00
 1000+01+0000+00+0000+0 + + 1000+01+1000+C1+0000+00+0000+00+1000+01
 0000+00+0000+00+1000+01+0000+00+0000+00

-1

C DARA CARDS FOR TABLE 02
 C FOR INPUT FORMATS, SEE MAIN PROGRAM READ STATEMENTS
 C NEAR STATEMENT NUMBERS 80
 C COLUMN NUMBER

C 5 0 5 0 5 0 5 0 5 0 5 0

02
 1+10000000+02
 12450000+01
 34900000+03
 50000000-04+10000000+00+50000000-01
 1 1 1 1 1 1

▽ EOF

C IF FULL E2F(X) INSTEAD OF EXPONENTIAL KERNAL APPROXIMATION IS USED (
 C ALLOWED ONLY LINEOP=1, OR CALCULATION WITHOUT LINE AND ABLATION),

C REPLACE E3F(X) IN SUBROUTINE NNGGSP AND CRLINE BY THE FOLLOWING
 C CARD AND ADD FUNCTION E2F(X) TO DECK.

E3F(A)=0.5*(EXPF(-A)-A*E2F(A))
 VIT FOR E2F

FUNCTION E2F(X)

IF(X)1,2,3

1 WRITE (6,90)

90 FORMAT(26H- NEGATIVE ARGUMENT IN E2F)

ZZZ=-1.0

ZZZ=SQRT(ZZZZ)

CALL EXIT

2 E2F=1.0

RETURN

3 IF(X-1.0)4,4,5

4 E2F=1.+X*(ALOG(X)-.42278435-X*(0.5-X*(0.08333333-X*(0.01368889-X*(
 10.20833333E-2-X*(0.27777778E-3-X*(0.33068783E-4))))))

RETURN

5 X1=1.0/X

Y=0.003130501+X1*(1.830847-X1*(3.5524186-X1*(4.8709437-X1*(3.69091
 195-X1*1.1347977))))

E2F=(1.0-Y)/(X*EXPF(X))

RETURN

END

E2F 1
 E2F 2
 E2F3

E2F 4
 E2F 5
 E2F 6
 E2F 7
 E2F8
 E2F 9
 E2F10
 E2F11
 E2F12
 E2F13
 E2F14
 E2F15

PRECEDING PAGE BLANK NOT FILMED.

OUTPUT DATA LISTING
INCLUDING DETAILS OF
LINE DATA USED

GROUP	NV	NV+	nv-	N	LINE	MLST	HV(I)	F(I)	GAM(I)	RFG(I)					
1	.500	.800	.500	6	1	6	.657	1.02-01	1.87-20	1.02+05					
					2	6	.674	2.08-01	1.87-20	2.08+05					
					3	6	.690	2.76-01	1.87-20	2.76+05					
					4	6	.710	3.07-01	1.87-20	3.07+05					
					5	6	.723	6.60-02	1.87-20	6.61+04					
					6	5	.753	1.50-02	4.46-21	9.01+03					
2	.900	.965	.800	6	7	5	.846	1.81-02	2.92-21	1.09+04					
					8	5	.877	4.46-21	4.46+04	2.44+04					
					9	5	.911	5.84-02	3.36-21	3.51+04					
					10	6	.922	1.66-02	3.87-20	1.66+04					
					11	6	.939	3.40-02	3.87-20	3.41+04					
					12	6	.954	4.50-02	3.87-20	4.51+04					
					13	6	.975	4.95-02	3.87-20	4.96+04					
					14	6	.998	1.06-02	3.87-20	1.06+04					
					15	5	.998	1.19-01	3.12-21	7.15+04					
3	1.050	1.200	.965	7	16	5	1.009	5.75-02	2.94-21	3.46+04					
					17	5	1.033	6.33-02	3.36-21	3.80+04					
					18	5	1.119	7.44-02	4.46-21	4.47+04					
					19	5	1.170	2.01-01	2.40-21	1.21+05					
					20	5	1.225	2.93-01	3.04-21	1.76+05					
					21	5	1.268	6.25-02	3.20-21	3.76+04					
					22	4	1.319	1.83-01	9.84-22	3.67+04					
					23	5	1.368	3.89-02	2.29-21	2.34+04					
					24	4	1.430	5.16-01	9.50-22	1.03+05					
					25	4	1.509	2.52-01	8.39-22	5.05+04					
					4	1.250	1.395	1.200	4	26	4	1.553	3.01-03	2.93-20	6.03+02
27	4	1.663	9.27-02	9.58-22						1.86+04					
28	5	1.675	7.55-03	2.93-20						4.54+03					
29	5	1.836	1.27-02	2.93-20						4.28+03					
30	5	1.919	1.34-03	2.93-20						7.63+03					
31	5	2.075	1.34-03	2.93-20						8.05+02					
32	4	2.571	4.63-03	5.51-21						9.27+02					
33	4	2.925	1.06-02	5.51-21						2.12+03					
34	4	3.107	5.85-03	2.09-20						1.17+03					
5	1.470	1.600	1.395	3						35	4	3.466	1.72-02	3.90-20	3.45+03
					36	4	3.541	3.90-03	5.73-20	7.61+02					
					37	4	3.849	1.40-02	5.73-20	2.80+03					
					38	4	3.926	3.20-03	5.73-20	6.41+02					
					39	3	7.111	6.34-02	9.12-22	4.23+03					
					40	2	8.302	7.40-02	9.12-22	8.23+03					
					41	3	8.781	4.35-02	6.61-22	2.90+03					
					42	3	9.301	1.66-02	4.46-21	1.11+03					
					43	3	9.394	1.19-02	2.92-21	7.95+02					
					6	1.650	1.600	1.600	5	44	3	9.460	3.60-02	3.36-21	2.40+03
45	3	9.973	6.90-02	6.61-22						9.90+03					
46	3	10.102	3.74-02	2.93-20						2.50+03					
47	1	10.332	1.84-01	6.21-22						8.19+03					
48	3	10.418	2.25-02	5.32-20						1.50+03					
49	2	10.483	1.87-02	4.46-21						2.08+03					
50	3	10.585	1.31-02	7.96-20						8.75+02					
51	3	10.619	5.33-02	3.12-21						5.93+03					
52	3	10.682	9.19-03	2.68-19						5.47+02					
7	1.850	2.350	2.350	3						53	3	10.757	5.18-03	4.37-19	3.46+02
					54	1	10.927	4.54-01	1.61-23	2.02+04					
					55	3	11.200	2.00-02	4.46-21	1.34+03					
					56	2	11.293	4.18-02	2.93-20	4.65+03					
					8	3.700	4.100	3.250	4	9	0	6.200	4.100		
										10	1	8.000	6.200		
										11	1	8.600	8.000		
										12	1	9.000	8.600		
										13	3	9.000	9.000		
										9	10.600	10.950	9.700	10	14
15	9	12.150	10.950												

16	12.410	12.700	12.150	3	57	11.310	2.54-02	3.23-21	1.70+03
					58	11.550	1.33-01	3.61-23	8.88+03
					59	11.609	2.50-02	5.32-20	2.78+03
					60	11.776	1.46-02	7.96-20	1.62+03
					61	11.874	9.10-03	2.68-19	1.01+03
					62	11.948	5.75-03	4.37-19	6.40+02
					63	12.000	2.19-02	2.99-20	1.46+03
					64	12.316	1.56-02	6.96-20	1.04+03
					65	12.414	5.74-02	3.90-21	6.39+03
					66	12.511	2.79-02	3.37-21	3.10+03
					67	12.877	2.30-02	4.46-21	1.02+03
					68	13.004	1.32-01	2.94-21	5.88+03
					69	13.190	4.89-02	2.99-20	5.44+03
					70	13.508	2.91-02	6.96-19	3.24+03
					71	13.677	9.57-02	2.93-20	4.26+03
					72	13.993	5.84-02	5.32-20	2.60+03
					73	14.160	3.42-02	7.96-20	1.52+03
					74	14.257	2.12-02	2.68-19	9.44+02
					75	14.332	1.38-02	4.37-19	6.14+02
17	13.040	13.350	12.700	3	66	12.877	2.30-02	4.46-21	1.02+03
18	13.580	13.850	13.350	2	69	13.190	4.89-02	2.99-20	5.44+03
19	14.260	14.500	13.850	4	71	13.677	9.57-02	2.93-20	4.26+03
20	15.300	16.500	14.500	0	73	14.160	3.42-02	7.96-20	1.52+03
21	17.850	24.000	16.500	0	75	14.332	1.38-02	4.37-19	6.14+02

GROUP ISOE NUMINT

GE(1) =	.40000+01	.10000+02	.60000+01	.18000+02	.54000+02	.90000+02
EPS(1) =	.90000	.23840+01	.35760+01	.10452+02	.11877+02	.13002+02
1	.50000+04	.31623-37	.31623-37	.31623-37	.31623-37	.31623-37
2	.40000+04	.95000+04	.61376-34	.29444-35	.95409-36	.40179-21
3	.50000+04	.20684-28	.27479-28	.34813-28	.70307-28	.31696-20
4	.60000+04	.46001-26	.35645-26	.31969-26	.46238-26	.12474-19
5	.70000+04	.20464-24	.11350-24	.80168-25	.97724-25	.16982-18
6	.80000+04	.84754-23	.15136-23	.91622-24	.99541-24	.32584-19
7	.90000+05	.18050-21	.57016-22	.30549-22	.26977-22	.66069-19
8	.10000+05	.24774-20	.64269-21	.29174-21	.11143-21	.54702-18
9	.14000+05	.15849-19	.36141-20	.15417-20	.25003-20	.17179-18
10	.16000+05	.02517-19	.13032-19	.53068-20	.12331-20	.10666-17
11	.18000+05	.17579-18	.34350-19	.13521-19	.40087-20	.16181-17
					.97949-20	.23605-19
						.25823-20
						.15996-20
						.16293-19
						.66681-19
						.26607-18
						.51286-18
						.82985-18
						.15776-17
						.82224-17
						.23605-17
						.84139-17
						.30690-17
						.85310-17
						.35975-17
						.85114-17
						.65313-17

12	.6000+05	.3815-18	.7194-19	.2754-19	.1909-19	.4217-19	.7961-18	.2844-17	.3953-17	.7620-17
13	.2300+05	.6745-18	.1213-19	.6576-19	.3082-19	.6324-19	.8035-18	.2697-17	.3715-17	.6668-17
14	.2399+05	.1016-17	.1763-18	.6591-19	.4303-19	.6279-19	.7620-18	.2415-17	.3296-17	.5623-17
1	.5000+04	.3162-37	.3162-37	.3162-37	.4022-17	.3162-37	.3162-37	.3162-37	.3162-37	.3162-37
2	.4000+04	.1452-38	.3540-31	.1743-29	.4017-17	.6298-33	.1277-31	.6025-34	.6668-31	.6668-31
3	.5000+04	.3630-28	.7379-28	.6533-27	.3994-17	.2296-28	.5781-28			
4	.6000+04	.6132-28	.0220-28	.3163-25	.3011-17					
5	.7000+04	.1753-24	.1437-24							
6	.8000+04									
7	.9000+04									
8	.1000+03	.1714-17	.2530-17	.1037-19	.2312-14	.1267-19	.2184-19	.7379-20	.6039-21	.3698-21
9	.1200+03			.1765-18	.4841-19	.2494-19	.2654-15	.2799-19	.1205-19	.1932-20
10	.1400+03			.2662-13	.1207-18	.5649-19	.6309-18	.8491-19	.3411-19	.1832-19
11	.1600+03			.2658-07	.5221-04	.1335-03	.1129-06	.1836-03	.1914-03	.2409-06
12	.1800+03			.3715-05	.6421-02	.2051-00	.6665-05	.2018-01	.2089-00	.1238-04
13	.2000+03			.4173-04	.1806+00	.2089-00	.7379-04	.2747-00	.2098-00	.1258-03
14	.2399+05			.2070-03	.4570-00	.2094-00	.3693-03	.7046-00	.2103-00	.8176-03
1	.3000+04			.7385-03	.7261-00	.2098-00	.2001-02	.7726-00	.2094-00	.6166-02
2	.4000+04			.3026-02	.7673-00	.2069-00	.9397-02	.7585-00	.2051-00	.2930-01
3	.5000+04			.3590-02	.7481-00	.2070-00	.3035-01	.6397-00	.1918-00	.1047-00
4	.6000+04			.2511-01	.7286-00	.1956-00	.3285-01	.4943-00	.1592-00	.2747-00
5	.7000+04			.1174-00	.5123-00	.1592-00	.3243-00	.2243-00	.8414-01	.6902-00
6	.8000+04			.3597-00	.2481-00	.9594-00	.6598-00	.6886-01	.2502-01	.8892-00
7	.9000+04			.5889-00	.8686-01	.4197-01	.8696-00	.1495-01	.5997-02	.9772-00
8	.1000+03			.7620-00	.2582-01	.1479-01	.9633-00	.2735-02	.1219-02	.1000+01
9	.1200+03			.8790-02	.1020-01	.5093-02	.9885-00	.1000-02	.2985-03	.1000+01
10	.1400+03			.9817-00	.2070-02	.8472-03	.1081+01	.1636-03	.5912-04	.1396+01

CASE = .1111111+31
 VELOCITY = .13240+02
 FREE STREAM PRESSURE = .03000
 FREE STREAM DENSITY = .13690-03
 FREE STREAM ENTHALPY = .03000
 FREE STREAM THERMAL RATIO = .25600+03
 AVERAGE DENSITY RATIO = .33030-01
 MODEL = 4

FCNIN = .10000+01
 FCNAD = .10000+01

L = .1 NS = 10 NSAS = 10

LINEOF = 3

ABS(AV INTEGRAND)*I.E-4 = .50000-04 ERK = .10000+00 FIRST NORMALIZED STEP = .50000-01

GROUP	IV	IV+	IV-	NLINE	TAUC	WALL	9SHOCK	TAUCT
1	.800	.800	.500	6	.39003-01	.18694+03	.38635+03	.33903-01
2	.900	.900	.800	6	.17577-01	.47563+02	.21563+03	.17577-01
3	1.050	1.050	.905	7	.12835-01	.16655+03	.34901+03	.12835-01
4	1.250	1.250	1.200	4	.69842-02	.14012+03	.27820+03	.89842-02
5	1.470	1.600	1.395	3	.68755-02	.10263+03	.22743+03	.68758-02
6	1.850	2.350	2.350	5	.39100-02	.19913+03	.48182+03	.39100-02
7	2.850	4.100	3.250	3	.17164-02	.13949+03	.19395+03	.39100-02
8	3.700	6.200	4.100	4	.37629-03	.12271+03	.13225+03	.17164-02
9	5.200	8.000	6.200	1	.91776-03	.91224+02	.91954+02	.91776-03
10	7.110	8.000	6.200	1	.70657-03	.12699+03	.17346+03	.91776-03
11	6.302	8.000	8.000	1	.68930-03	.12941+03	.20052+03	.70657-03
12	8.761	9.000	8.000	1	.69029-03	.31057+02	.49165+02	.69029-03
13	9.400	9.700	9.000	3	.13740-02	.51549+03	.16225+03	.69029-03
14	10.400	16.950	6.700	10	.16560-02	.51549+03	.84533+03	.13740-02
15	11.500	12.150	10.950	9	.28876-00	.53105+03	.10154+04	.16560-02
16	12.410	12.700	12.150	3	.23268+01	.11560+03	.45619+03	.28876-00
17	13.040	13.350	12.700	3	.23268+01	.83279+02	.38470+03	.23268+01
18	13.500	13.850	13.350	2	.23268+01	.36368+02	.23668+03	.23268+01
19	14.200	14.500	13.850	4	.29642+01	.24777+02	.23211+03	.29642+01
20	15.300	16.500	14.500	0	.75806+01	.26535+02	.33970+03	.29642+01
21	17.050	26.000	16.500	0	.75806+01	.61539+01	.11907+03	.75806+01
.65810+04								

(IF LINEOP=2, VALUES ARE NEGATIVE CORRECTION TO CONTINUUM MODEL; IF LINEOP=3, TOTAL)

STAGGRAS-ABLATION CALCULATION

NO ABLATION LAYER ATTENUATION, EMP = .31332-00

NCCOUL = 0	
.16923-00	
.48459+04	
.15295+04	
NCCOUL = 1	
1	.21721+01 .00000 .11718+01 .10003+01 .10861+01
2	.24928+01 .00000 .15154+01 .98341-00 .12623+01
3	.27937+01 .00000 .18390+01 .93668-00 .15491+01
4	.30743+01 .00000 .22028+01 .87177-00 .18355+01
5	.33361+01 .00000 .25462+01 .80991-00 .21213+01
6	.36081+01 .00000 .28897+01 .79833-00 .24081+01
7	.41012+01 .00000 .32333+01 .86760-00 .26944+01
8	.45762+01 .00000 .35764+01 .10000+01 .29808+01
9	.51009+01 .00000 .39263+01 .12104+01 .32671+01
10	.77679+01 .00000 .42041+01 .35033+01 .38839+01
NCCOUL = 2	
1	.11718+01 .10003+01 .10861+01 .10053+01 .10457+01
2	.15154+01 .98341-00 .12623+01 .10065+01 .10065+01
3	.18390+01 .93668-00 .15491+01 .10065+01 .10065+01
4	.22028+01 .87177-00 .18355+01 .10065+01 .10065+01
5	.25462+01 .80991-00 .21213+01 .10065+01 .10065+01
6	.28897+01 .79833-00 .24081+01 .10065+01 .10065+01
7	.32333+01 .86760-00 .26944+01 .10065+01 .10065+01
8	.35764+01 .10000+01 .29808+01 .10065+01 .10065+01
9	.39263+01 .12104+01 .32671+01 .10065+01 .10065+01
10	.42041+01 .35033+01 .38839+01 .10065+01 .10065+01

NCOURT =	16746+04	36215+01	33431+01	31769+01
NCOURT =	11	10078+01	10079+01	10073+01
1	10077+01	10078+01	10079+01	10073+01
2	10035+01	10237+01	10242+01	10240+01
3	10035+01	10397+01	10410+01	10403+01
4	10045+01	10551+01	10572+01	10561+01
5	10098+01	10729+01	10736+01	10719+01
6	10099+01	10897+01	10905+01	10891+01
7	11005+01	11019+01	11093+01	11056+01
8	11093+01	11359+01	11370+01	11313+01
9	11359+01	12006+01	12477+01	12354+01
10	30515+01	30768+01	30865+01	30816+01
NCWT =	U	NCOURT =	11	NCOURT =
NCWT =	10959+04	31101 =	16753+04	31102 =
NCOURT =	12	1176+01	11283+01	12365+01
10	30816+01	36607+01	36750+01	36861+01
NCWT =	16000-01	NCOURT =	14	NCOURT =

NCWT =	17606+04	NCWT =	17326+04	NCWT =	17333+04
1	10075+01	10074+01	10072+01	10072+01	10072+01
2	10028+01	10226+01	10217+01	10223+01	10223+01
3	10400+01	10372+01	10366+01	10367+01	10376+01
4	10555+01	10520+01	10537+01	10514+01	10526+01
5	10711+01	10608+01	10603+01	10662+01	10676+01
6	10671+01	10823+01	10817+01	10818+01	10832+01
7	11044+01	11092+01	11023+01	11010+01	11010+01
8	11362+01	11265+01	11253+01	11257+01	11270+01
9	12570+01	12356+01	12365+01	12312+01	12339+01
10	36790+01	38532+01	38661+01	37118+01	38685+01
DELTA	FO	VM	VM	VM	VM
VC	VC	VC	VC	VC	VC
21062+01	44147-00	63260-00	33100-00	32695+02	32695+02
VC	VC	VC	VC	VC	VC
1	30593+01	30654-02	10066+01	10072+01	33154-00
2	74007-01	27714-01	10121+01	10223+01	33273-00
3	13043-00	53696-01	99400-00	10376+01	33393-00
4	10681-00	79831-01	96269-00	10526+01	33639-00
5	24393-00	10658+00	96411-00	10676+01	33639-00
6	30187-00	13353-00	82652-00	10832+01	33748-00
7	30665-00	16022-00	75401-00	11010+01	33826-00
8	42057-00	16697-00	56996-00	11270+01	34060-00
9	49402-00	21908-00	47868-00	12339+01	34922-00
10	76650-00	45910-00	15538+01	33683+01	56554-00
NCOURT =	7	95403-00	95404-00	95408-00	95404-00
1	68200-00	68277-00	68279-00	68280-00	68280-00
2	68214-00	68309-00	68314-00	68336-00	68317-00
3	68152-00	68159-00	68159-00	68135-00	68149-00
4	76716-00	76705-00	76702-00	76702-00	76702-00
5	76705-00	76705-00	76702-00	76702-00	76702-00
6	76705-00	76705-00	76702-00	76702-00	76702-00

VC*	VC*	VC*	VC*	VC*	VC*
47794-03	47794-03	38550-00	17143+04	86063-01	420A9-04
32910+02	33362+02	33630+02	34292+02	34762+02	35259+02
26121+1A	26246+1A	26374+1A	26501+1A	26627+1A	26760+1A
42177+1A	41220+1A	40264+1A	39357+1A	38467+1A	37560+1A
44229+17	44022+17	43613+17	43357+17	43107+17	42959+17
19931+1A	19886+1A	19139+1A	19794+1A	19749+1A	19702+1A
37554+13	36830+13	40177+13	41532+13	42939+13	44456+13
NC+	NC+	NC+	NC+	NC+	NC+
42177+1A	41220+1A	40264+1A	39357+1A	38467+1A	37560+1A
44229+17	44022+17	43613+17	43357+17	43107+17	42959+17
19931+1A	19886+1A	19139+1A	19794+1A	19749+1A	19702+1A
37554+13	36830+13	40177+13	41532+13	42939+13	44456+13
NC+	NC+	NC+	NC+	NC+	NC+
42177+1A	41220+1A	40264+1A	39357+1A	38467+1A	37560+1A
44229+17	44022+17	43613+17	43357+17	43107+17	42959+17
19931+1A	19886+1A	19139+1A	19794+1A	19749+1A	19702+1A
37554+13	36830+13	40177+13	41532+13	42939+13	44456+13
NC+	NC+	NC+	NC+	NC+	NC+
42177+1A	41220+1A	40264+1A	39357+1A	38467+1A	37560+1A
44229+17	44022+17	43613+17	43357+17	43107+17	42959+17
19931+1A	19886+1A	19139+1A	19794+1A	19749+1A	19702+1A
37554+13	36830+13	40177+13	41532+13	42939+13	44456+13
NC+	NC+	NC+	NC+	NC+	NC+
42177+1A	41220+1A	40264+1A	39357+1A	38467+1A	37560+1A
44229+17	44022+17	43613+17	43357+17	43107+17	42959+17
19931+1A	19886+1A	19139+1A	19794+1A	19749+1A	19702+1A
37554+13	36830+13	40177+13	41532+13	42939+13	44456+13

N = 1 DELTA = .10000+02 CV .10000+02 CV
 TEMP(EV) = .1245+01 DYY= .10000+02 CV
 RHOSL/RHO = .3490+03

I NL/CC OI/CC E/CC
 1 .40099+17 .14751+17 .80591+17

ABS(AV INTEGRAND)*1.E-4 = .50000-04 ERR = .10000+00 FIPST NORMALIZED STEP = .50000-01

M	K	KM	JD	I	GAM(I)	SS(I)	SST(I+1)	SGAM(I,KM)	SGAMT(I+1)	TAUD(I)	TAUDT(I+1)	
1	1	1	6	1	.1507-02	.2331-02	.2331-02	.3514-05	.3514-05	.4924-00	.4924-00	
M	K	KM	JD	IP1	J	SS12	SGAM12	GAME12	ZETA12	WID12K	WID12(IP1,J)	TAU12
1	1	1	6	2	1	.2331-02	.3514-05	.1507-02	.2462-00	.2267-02	.2267-02	.4924-00
M	K	KM	JD	I	GAM(I)	SS(I)	SST(I+1)	SGAM(I,KM)	SGAMT(I+1)	TAUD(I) <td>TAUDT(I+1)</td>	TAUDT(I+1)	
1	2	2	6	1	.1507-02	.4754-02	.4754-02	.7165-05	.7165-05	.1004+01	.1004+01	
M	K	KM	JD	IP1	J	SS12	SGAM12	GAME12	ZETA12	WID12K	WID12(IP1,J)	TAU12
1	2	2	6	2	1	.4754-02	.7165-05	.1507-02	.5021-00	.3869-02	.6136-02	.1004+01
M	K	KM	JD	I	GAM(I)	SS(I)	SST(I+1)	SGAM(I,KM)	SGAMT(I+1)	TAUD(I) <td>TAUDT(I+1)</td>	TAUDT(I+1)	
1	3	3	6	1	.1507-02	.4754-02	.4754-02	.7165-05	.7165-05	.1004+01	.1004+01	

NCOUNT = 39 SMALLEST STEP = .39018-03 ERR = .10000+00 DMU = .30000-00 NORMALIZED SMALLEST STEP = .13006-02

NREJE = 10
 DAX(I) VALUES BELOW

.150-01	.667-02	.198-02	.878-03	.878-03	.878-03	.878-03	.878-03	.878-03	.878-03	.878-03	.878-03	.878-03
.878-03	.878-03	.878-03	.878-03	.878-03	.878-03	.878-03	.878-03	.878-03	.878-03	.878-03	.878-03	.878-03
.563-03	.878-03	.132-02	.132-02	.132-02	.132-02	.132-02	.132-02	.132-02	.132-02	.132-02	.132-02	.132-02
.198-02	.296-02	.198-02	.198-02	.198-02	.198-02	.198-02	.198-02	.198-02	.198-02	.198-02	.198-02	.198-02

M	IP1	I	ISO.WIDTH	ACT.WIDTH	DMU*TRN	ISO-ACT WIDTH						
1	2	1	.18113934-01	.17204014-01	.28279598-00	.90991985-03						
M	K	KM	JD	I	GAM(I)	SS(I)	SST(I+1)	SGAM(I,KM)	SGAMT(I+1)	TAUD(I)	TAUDT(I+1)	
2	7	1	5	1	.2353-03	.7494-03	.7494-03	.1763-06	.1763-06	.1014+01	.1014+01	
M	K	KM	JD	IP1	J	SS12	SGAM12	GAME12	ZETA12	WID12K	WID12(IP1,J)	TAU12
2	7	1	5	2	1	.7494-03	.1763-06	.2353-03	.5088-00	.6084-03	.6084-03	.1014+01